

IMPROVED MATHEMATICAL TECHNIQUES  
FOR SOLUTION OF  
ATMOSPHERIC DISPERSION MODELS

---

A Dissertation  
Presented to  
the Faculty of the Department of  
Chemical Engineering  
The University of Houston

---

In Partial Fulfillment  
of the Requirements for the Degree of  
Doctor of Philosophy in Chemical Engineering

---

by  
Miguel T. Fleischer  
March, 1978

To

My lovely wife, Jackie

and to

David and Ronnie

## ACKNOWLEDGMENTS

The author is indebted to Dr. Frank L. Worley, Jr., who supervised this dissertation and with whom it has been an honor to work, for his invaluable guidance, continuing advice and eternal optimism.

Sincere appreciation is expressed to Dr. John Villadsen for his priceless suggestions and increasing enthusiasm.

Special thanks are also due to the Department of Chemical Engineering for their financial support.

Finally, the author wishes to extend his hearty gratitude to his parents and the family for their love and admirable wisdom.

## TABLE OF CONTENTS

<u>Chapter</u>		<u>Page</u>
I	INTRODUCTION	1
II	FORMULATION OF MODELS AND THEIR SOLUTION TECHNIQUES	3
	Two Dimensional-Continuous Ground Level Line Source	3
	Two Dimensional-Continuous Elevated Line Source	15
	Two Dimensional Models with Chemical Reactions	19
	Three Dimensional-Continuous Point Source	21
	Constant Mean Wind Velocity and Turbulent Diffusivities	24
	Variable Mean Wind Velocity and Turbulent Diffusivities	32
	Three Dimensional Mean Wind Velocity	34
III	PARAMETERS ESTIMATION	39
	Mathematical Parameters	39
	Two Dimensional-Continuous Ground Level Line Source	39
	Two Dimensional-Continuous Elevated Line Source	49
	Three Dimensional-Continuous Point Source	52
	Meteorological Parameters	60
	Turbulent Diffusivities $K_y$ , $K_z$	60
	Velocity Profile	71

TABLE OF CONTENTS (Continued)

<u>Chapter</u>		<u>Page</u>
IV	PRESENTATION AND ANALYSIS OF RESULTS	77
	Two Dimensional Models	77
	Three Dimensional Models	79
V	SUMMARY OF RESULTS, CONCLUSIONS AND RECOMMENDATIONS	94
	BIBLIOGRAPHY	98
	APPENDICES	100
	A. Computer Program Listing	101
	B. Nomenclature	127

## LIST OF FIGURES

<u>Figure</u>		<u>Page</u>
2.1	Vertical Concentration Distribution at $x=0$ - Ground Level Line Source	8
2.2	Correct Vertical Concentration Distribution at any $\xi$ - Ground Level Line Source	11
2.3	Vertical Concentration Distribution at $x=0$ - Elevated Line Source	16
2.4	Correct Vertical Concentration Distribution at any $\xi$ - Elevated Line Source	18
3.1	Comparison of Downwind Concentration Distribution at Ground Level with Analytical Solution - Parametric Study on $N$	40
3.2	Comparison of Downwind Concentration Distribution at Ground Level with Analytical Solution - Parametric Study on $\beta$	43
3.3	Comparison of Downwind Concentration Distribution at Ground Level with Analytical Solution - Parametric Study on $r$	45
3.4	Comparison of Downwind Concentration Distribution at Ground Level with Analytical Solution - Parametric Study on $z_{\max}$	48
3.5	Comparison of Downwind Concentration Distribution at the Effective Emission Height with Analytical Solution - Parametric Study on $\beta$	50
3.6	Comparison of Downwind Concentration Distribution at the Effective Emission Height with Analytical Solution - Parametric Study on $z_{\max}$	53
3.7	Comparison of Downwind Concentration Distribution at the Effective Emission Height with Analytical Solution - Parametric Study on $\epsilon$	56
3.8	Comparison of Downwind Concentration Distribution at the Effective Emission Height with Analytical Solution - Parametric Study of $r$	59

LIST OF FIGURES (Continued)

<u>Figure</u>		<u>Page</u>
3.9	Comparison of Downwind Concentration Distribution at Ground Level with Analytical Solution and Gaussian Plume Equation - Stability Class A	62
3.10	Comparison of Downwind Concentration Distribution at Ground Level with Analytical Solution and Gaussian Plume Equation - Stability Class B	63
3.11	Comparison of Downwind Concentration Distribution at Ground Level with Analytical Solution and Gaussian Plume Equation - Stability Class C	64
3.12	Comparison of Downwind Concentration Distribution at Ground Level with Analytical Solution and Gaussian Plume Equation - Stability Class D	65
3.13	Comparison of Downwind Concentration Distribution at Ground Level with Analytical Solution and Gaussian Plume Equation - Stability Class E	66
3.14	Comparison of Downwind Concentration Distribution at Ground Level with Analytical Solution and Gaussian Plume Equation - Stability Class F	67
3.15	Vertical Diffusivity Profiles in the Present Work	70
4.1	Downwind Concentration Distribution at Ground Level - Two Dimensional Model with Chemical Reaction	78
4.2	Downwind Concentration Distribution at the Effective Emission Height - Two Dimensional Model with Inversion Layer	80
4.3	Downwind Concentration Distribution at Ground Level - Three Dimensional Models - Stability Class A	81
4.4	Downwind Concentration Distribution at Ground Level - Three Dimensional Models - Stability Class D	82
4.5	Downwind Concentration Distribution at Ground Level - Three Dimensional Models - Stability Class F	83
4.6	$\frac{xU}{Q}$ with Downwind Distance for Various Heights of Emission - Gaussian Plume Equation	85

LIST OF FIGURES (Continued)

<u>Figure</u>		<u>Page</u>
4.7	$\frac{Cu_1}{Q}$ with Travel Time for Various Heights of Emission - Present Work	87
4.8	Comparison of Downwind Concentration Distribution with Analytical Solution - Two Dimensional Wind Velocity	89
4.9	Isopleths at a Constant x - Three Dimensional Models	90
4.10	Downwind Concentration Distribution at Ground Level - Coriolis Effect vs Gaussian Plume Equation	91

## LIST OF TABLES

<u>Table</u>	<u>Page</u>	
3.1	Computer Time Requirements for Parametric Study on $N$ - Ground Level Line Source Model	41
3.2	Computer Time Requirements for Parametric Study on $\beta$ - Ground Level Line Source Model	42
3.3	Mass Flux vs $\delta_2$ at the First Integration Step - Ground Level Line Source Model	44
3.4	Computer Time Requirements for Parametric Study on $r$ - Ground Level Line Source Model	46
3.5	Computer Time Requirements for Parametric Study on $z_{\max}$ - Ground Level Line Source Model	47
3.6	Computer Time Requirements for Parametric Study on $\beta$ - Elevated Line Source Model	49
3.7	Mass Flux vs $\delta_1$ and $\delta_2$ at the First Integration Step - Elevated Line Source Model	51
3.8	Computer Time Requirements for Parametric Study on $z_{\max}$ - Elevated Line Source Model	52
3.9	Mass Flux vs $\delta_{2y}$ at the First Integration Step - Elevated Point Source Model	54
3.10	Computer Time Requirements for Parametric Study on $\epsilon$ - Elevated Point Source Model	55
3.11	Computer Time Requirements for Small Stepsize of Integration - Elevated Point Source Model	57
3.12	Constant Turbulent Diffusivities and Wind Speed used in the Present Method	69
3.13	Estimates for the Parameters in Equation (3.2)	71
3.14	Geostrophic Elevations used in the Present Work	74
3.15	Angle between Wind Velocity and Geostrophic Direction for the Surface Boundary Layer	75
4.1	Mass Rates at Several Downwind Positions - Coriolis Effect	93

## CHAPTER I

### INTRODUCTION

The increasing cost of controlling emissions from industrial sources has magnified the need to develop accurate mathematical models which can relate emission rate to air quality. In order to adequately describe the relationship between emissions and air quality, a model must be able to describe the variable (time and space) meteorological parameters and the chemical or physical processes which remove pollutants from the atmosphere.

During the past years, several models have been presented in the literature [8], ranging from very simple ones like the box model to more general cases solved by finite-difference techniques. The Eulerian formulation [8] has been the most common approach due to the availability of numerical techniques with which the equations can be solved.

A general model, one which includes temporal and spatial variations of meteorological parameters, should provide a good description of atmospheric diffusion processes. A dispersion model based on the K-theory and solved using orthogonal collocation was presented by Fleischer [8]. The atmospheric processes were described by the 3-dimensional, unsteady-state diffusion equation including chemical reactions. The work was validated with existing experimental data and shown to have several significant advantages over other available methods.

Understanding of the cause-effect relationship of pollutant emission and dispersion on the air quality may be difficult through a complex

general air pollution model. In addition, analytical solutions are available only for simplified diffusion equations. The disadvantages of solving simple cases using the same complex general method gave rise to the present work.

Dispersion models based on the K-theory and solved by improved mathematical techniques using spline orthogonal collocation are presented. All types of steady-state air pollution problems are simulated. These models extend from the simple ground level line source case to the complex 3-dimensional elevated point source model including the Coriolis effect. Spline orthogonal collocation, a weighted residual method, reduces the partial differential equation governing the mean concentration of pollutant species, within the plume generated by the source, to first-order ordinary differential equations. This system of equations is solved in a digital computer.

The present work was evaluated by comparing the results to available analytical solutions, e.g., two or three-dimensional cases with constant turbulent diffusivities and mean wind velocity, and no reaction. Mathematical parameters, inherent of the techniques developed, are determined through parametric studies. In addition, several hypothetical cases are simulated to explore the present method response to variations in atmospheric conditions.

CHAPTER II

FORMULATION OF MODELS AND THEIR SOLUTION TECHNIQUES

The basic mathematical statement for description of the temporal and spatial distribution of chemical species by the Eulerian approach is the mass balance or continuity equation. This equation, applied to a single species in the atmosphere, based on the K-theory is:

$$\frac{\partial C}{\partial t} + u \frac{\partial C}{\partial x} + v \frac{\partial C}{\partial y} + w \frac{\partial C}{\partial z} = \frac{\partial}{\partial x} \left( K_x \frac{\partial C}{\partial x} \right) + \frac{\partial}{\partial y} \left( K_y \frac{\partial C}{\partial y} \right) + \frac{\partial}{\partial z} \left( K_z \frac{\partial C}{\partial z} \right) + R \quad (2.1)$$

The main objective of the present work is to predict the concentration distribution with respect to time and space for various atmospheric dispersion cases. The diffusion equation (2.1) is the basis for all the models presented here. A description of these models and their methods of solution is given next, starting with the simplest one, the two dimensional continuous ground level line source.

Two Dimensional-Continuous Ground Level Line Source

A widely studied situation is the case of an infinite line source in the y-direction at ground level emitting at a constant rate. At steady state, equation (2.1) is simplified as

$$\frac{\partial C}{\partial t} = 0 \quad (2.2)$$

In addition, for an infinite crosswind (y) line source,

$$\frac{\partial}{\partial y} \left( K_y \frac{\partial C}{\partial y} \right) = 0 \quad (2.3)$$

Upon assuming that the mean flow is along the x-axis, i.e.,

$$v = w = 0 \quad (2.4)$$

and that the diffusion in the x-direction is negligible compared to the transport by the mean flow, i.e.,

$$\frac{\partial}{\partial x} \left( K_x \frac{\partial C}{\partial x} \right) \ll u \frac{\partial C}{\partial x} \quad (2.5)$$

equation (2.1) for the case when no chemical reactions are included, i.e.,  $R=0$  reduces to

$$u \frac{\partial C}{\partial x} = \frac{\partial}{\partial z} \left( K_z \frac{\partial C}{\partial z} \right) \quad (2.6)$$

with boundary conditions

$$C \rightarrow 0 \quad \text{as} \quad x, z \rightarrow \infty \quad (2.7a)$$

$$C \rightarrow \infty \quad \text{at} \quad x = z = 0 \quad (2.7b)$$

$$K_z \frac{\partial C}{\partial z} \rightarrow 0 \quad \text{as} \quad z \rightarrow 0, x > 0 \quad (2.7c)$$

The last boundary condition implies zero flux at the surface, i.e., the pollutant is completely reflected.

For the lower atmosphere, in adiabatic conditions, it has been seen that the wind velocity varies with the logarithm of the height. However, such a functional relationship proves intractable if an analytical solution of equation (2.6) is desired. When a power-law form is adopted for both the mean wind and turbulent diffusivity profiles, i.e.,

$$u = u_1 \left( \frac{z}{z_1} \right)^m \quad K_z = K_1 \left( \frac{z}{z_1} \right)^n \quad (2.8)$$

the analytical solution [2], valid for  $r = m-n+2 > 0$ , is

$$C(x, z) = \frac{Qr}{u_1 \Gamma(s)} \left[ \frac{u_1}{r^2 K_1 x} \right]^s \exp\left(-\frac{u_1 z^r}{r^2 K_1 x}\right) \quad (2.9)$$

where  $s = \frac{m+1}{r}$  and  $z_1$  is taken to be unity.

Continuity should be satisfied at any position in the x(downwind) direction:

$$\int_0^{\infty} u C(x, z) dz = Q \quad \text{for all } x > 0 \quad (2.10)$$

where Q is the constant emission rate per unit crosswind length.

The case which is solved in the present work considers  $m=n=0$ , i.e., the diffusion is Fickian. Equation (2.6) becomes

$$u \frac{\partial C}{\partial x} = K_z \frac{\partial^2 C}{\partial z^2} \quad (2.11)$$

and the analytical solution is reduced to

$$C(x, z) = \frac{2Q}{u\sqrt{\pi}} \left[ \frac{u}{4K_z x} \right]^{\frac{1}{2}} \exp\left[-\frac{uz^2}{4K_z x}\right] \quad (2.12)$$

The boundary condition  $C \rightarrow 0$  as  $z \rightarrow \infty$  is too restrictive because it cannot be applied to a case with an inversion layer at a certain height. This situation can be represented by

$$K_z \frac{\partial C}{\partial z} = 0 \quad \text{at } z = z_{\max} \quad (2.13)$$

Therefore, equation (2.13) is used as the second boundary condition in the vertical direction. If a comparison with the analytical solution is desired,  $z_{\max}$  can be given a sufficiently large value such that the pollutant never reaches the inversion layer. In addition, a solution

is usually needed up to a definite position in the x-direction. Equation (2.11) is solved numerically for

$$0 < x \leq x_{\max} \quad ; \quad 0 \leq z \leq z_{\max} \quad (2.14)$$

A transformation of the spatial coordinates to yield limits of 0 to 1 is performed by using

$$\xi = \frac{x}{x_{\max}} \quad z^* = \frac{z}{z_{\max}} \quad (2.15)$$

To complete the problem, a boundary condition in the x-direction must be specified, and the constant emission rate taken into account.

The model by Fleischer [8] defined the location of the source through a boundary condition in the x-direction as

$$C = \begin{cases} C_0 & \text{at } x = 0 \\ 0 & \text{elsewhere} \end{cases} \quad (2.16)$$

where  $C_0$  is an equivalent source concentration to be calculated from the emission rate using quadrature weights. Orthogonal collocation was the numerical technique used for solving the partial differential equation (2.1). One of the reasons as to why this was done is the attractive feature of being able to position the point source exactly as a collocation point with concentration  $C_0$  and the rest of the collocation points at  $x=0$  with zero concentration. However, this procedure gives rise to several problems:

1) Global collocation must be used, i.e., collocate points to reduce the partial differential equation to a system of ordinary differential equations throughout the entire region of interest. Since the

solution to a dispersion model should have approximately the shape of a conical plume, only a few points would be within this region. This means that at several positions in the x-direction, especially close to the source, only some points would have a certain concentration value and the rest would contain zero concentration. Accurate interpolation from such a concentration distribution is impossible;

2) One of the collocation points must match the location of the source; and

3) A ground level source cannot be placed at  $z=0$ , but at the position of the first collocation point, since only interior collocation points are used in the solution.

In spite of all these restrictions, which will be removed in the present work, it was proven that orthogonal collocation has better properties than other numerical techniques, and therefore will be used here again.

A point source, which usually represents a stack, can be considered as a very small area normal to  $u$  with a concentration  $C_0$  equivalent to the constant emission rate, as shown in Figure 2.1.

The present model then will have a discontinuous initial value profile expressed as

$$C^i = \begin{cases} C_0 & \text{at } \xi=0, & 0 \leq z^* \leq \beta \\ 0 & \text{at } \xi=0, & z^* > \beta \end{cases} \quad (2.17)$$

where  $C_0$  can be calculated using equation (2,10):

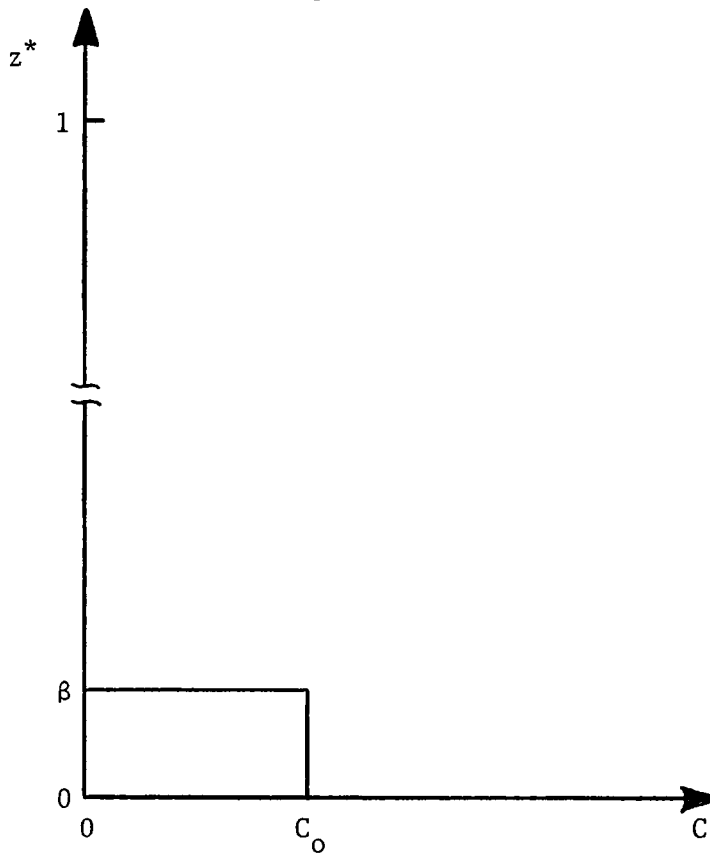


FIGURE 2.1 VERTICAL CONCENTRATION DISTRIBUTION  
AT  $x=0$  - GROUND LEVEL LINE SOURCE

$$Q = \int_0^{\beta} u C_0 z_{\max} dz^*$$

Solving for  $C_0$ ;

$$C_0 = \frac{Q}{u \beta z_{\max}} \quad (2.18)$$

Determination of the concentration distribution as a function of the spatial variables  $x$  and  $z$  requires then the solution of equation (2.11) with boundary conditions given by (2.7c) and (2.13), and the initial condition given by (2.17). The way this model is formulated overcomes

the restrictions, 2) and 3), previously discussed,

A suitable approach to this problem is immediately suggested by using spline orthogonal collocation in the vertical direction. A small interval  $[\beta-\delta_1, \beta+\delta_2]$  is considered and equation (2.11) is only solved in this interval. The required variable transformation is:

$$z^* = (\delta_1 + \delta_2)\zeta + \beta - \delta_1 \quad (2.19)$$

where  $0 \leq \zeta \leq 1$ . Equation (2.11) remains then as,

$$R_1 \frac{\partial C}{\partial \xi} = R_5 \frac{\partial^2 C}{\partial \zeta^2} \quad (2.20)$$

where

$$R_1 = \frac{u}{x_{\max}} \quad ; \quad R_5 = \frac{K_z}{z_{\max}^2 (\delta_1 + \delta_2)^2} \quad (2.21)$$

Global orthogonal collocation is applied to the  $\zeta$  domain such that a system of first order ordinary differential equations with respect to  $\xi$  is left to be solved. The zeros of the Jacobi polynomials  $P_{N_z}^{(0,0)}$  serve as collocation points.

The concentration distribution is obtained only within the  $[\beta-\delta_1, \beta+\delta_2]$  interval in the  $z^*$  domain, where the concentration is known to have a significant value, not just zero. Therefore, restriction 1) is eliminated from the method of solution. As  $x$  increases the penetration zone is broadened by choosing larger  $\delta_1$  and  $\delta_2$ . This implies that the technique considers moving boundary conditions in the vertical direction, and the edge of the plume is known at any position along the mean wind direction.

The calculational procedure is as follows; at any integration step, the concentrations at  $\zeta=0$  and  $\zeta=1$  are compared with  $C_0$  and zero, respectively. If the comparisons agree, as it is shown in Figure 2.2 the values for  $\delta_1$  and  $\delta_2$  are assumed correct and the integration continues to the next step.

Since the concentrations should approach  $C_0$  and 0 at  $\zeta=0$  and  $\zeta=1$ , respectively, the use of the following boundary conditions is valid:

$$\frac{\partial C}{\partial \zeta} = 0 \quad \text{at} \quad \zeta=0, \zeta=1 \quad (2.22)$$

If at any step, the concentration at  $\zeta=0$  is considerably smaller than  $C_0$ ,  $\delta_1$  is increased and the integration is performed for that same  $x$  with the previous good solution as initial condition. This comparison stops when  $\delta_1$  becomes  $\beta$ . When the concentration at  $\zeta=1$  is considerably larger than zero, the same previous procedure is applied to  $\delta_2$ . Finally, if an inversion layer is reached ( $\delta_2=1-\beta$ ) global collocation is used to continue the calculations until  $x=x_{\max}$ . In any problem  $\beta$  is usually small so that the condition  $\delta_1=\beta$  will always be obtained before  $\delta_2=1-\beta$ .

This technique gives rise to the question as to how close to zero, the "zero concentration" is. The present work assigns it as some fraction of the centerline concentration, as it is done for the Gaussian plume equation [18], where 10% of the centerline concentration is considered to be zero. Solutions for different ratios are compared in Chapter III.

The procedure to obtain the collocation matrix, used to integrate in the along wind direction, is presented next. Since orthogonal collocation is applied to the vertical direction with  $N_z$  number of collocation

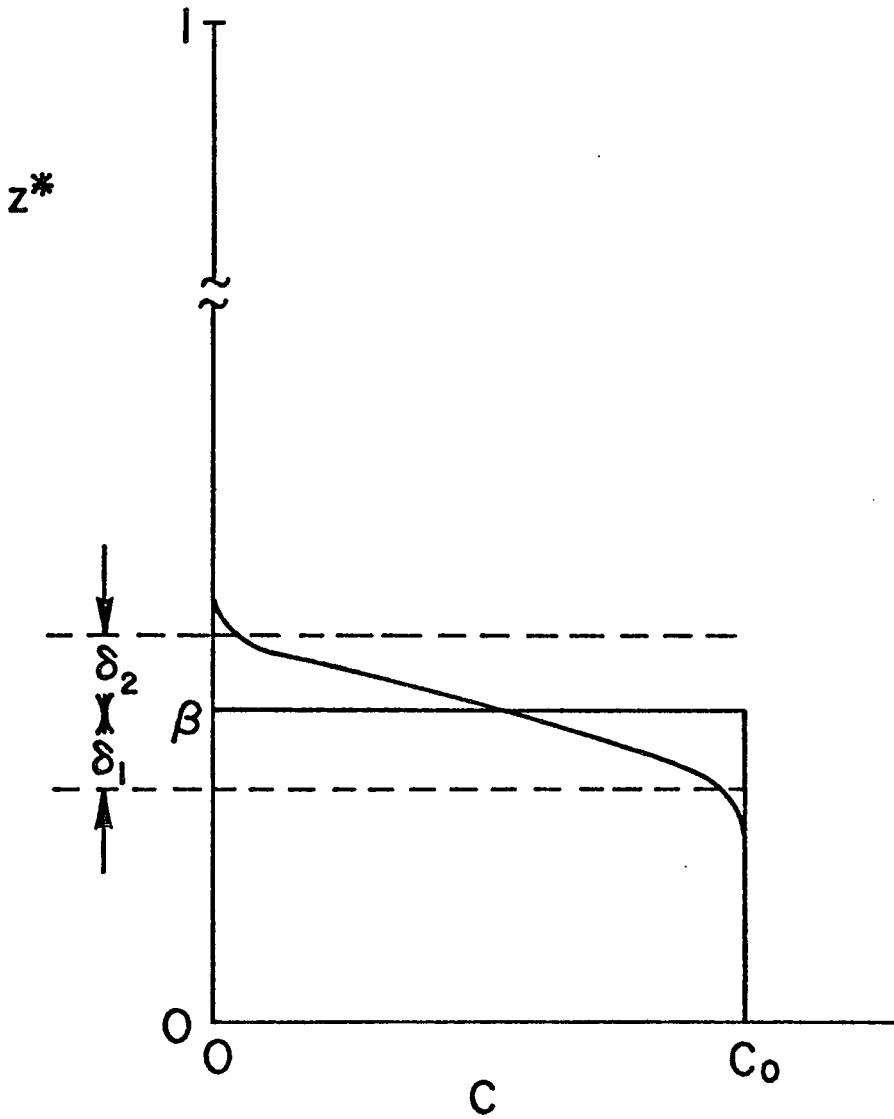


FIGURE 2.2 CORRECT VERTICAL CONCENTRATION DISTRIBUTION  
AT ANY  $\xi$  - GROUND LEVEL LINE SOURCE

points, equation (2.20) remains as

$$R_1 \frac{dC_\ell}{d\xi} = R_5 \sum_{i=1}^{N_z+2} B_{\ell i} C_i \quad , \text{ for } \ell=2, \dots, N_z+1 \quad (2.23)$$

The application of orthogonal collocation to the boundary conditions, equation (2.22), gives the following expressions:

$$\sum_{i=1}^{N_z+2} A_{1,i} C_i = 0 \quad \text{at } \zeta=0 \quad (2.24)$$

$$\sum_{i=1}^{N_z+2} A_{N_z+2,i} C_i = 0 \quad \text{at } \zeta=1$$

Solving for the concentration at the boundaries  $C_1$  and  $C_{N_z+2}$  as functions of the concentrations at the interior collocation points one obtains

$$C_1 = - \frac{\sum_{i=2}^{N_z+1} A1(i) C_i}{A_{1,1}} \quad (2.25)$$

$$C_{N_z+2} = \frac{\sum_{i=2}^{N_z+1} A2(i) C_i}{DEN} \quad (2.26)$$

where

$$A1(i) = A_{1,i} + \frac{A_{1,N_z+2} A2(i)}{DEN} \quad (2.27)$$

$$A2(i) = A_{1,1} A_{N_z+2,i} - A_{N_z+2,1} A_{1,i} \quad (2.28)$$

$$\text{DEN} = A_{N_z+2,1} A_{1,N_z+2} - A_{1,1} A_{N_z+2,N_z+2} \quad (2.29)$$

Finally, by substituting equations (2.25) and (2.26), equation (2.23) in matrix notation remains as follows:

$$\frac{d\underline{C}}{d\xi} = \underline{E} \underline{C} \quad (2.30)$$

where the elements of the matrix E are

$$E_{\ell i} = - \frac{R_5^{B_{\ell,1}} A_{1,1}^{A1(i)}}{R_1 A_{1,1}} + \frac{R_5^{B_{\ell i}}}{R_1} + \frac{R_5^{B_{\ell,N_z+2}} A_{N_z+2}^{A2(i)}}{R_1 \text{DEN}} \quad (2.31)$$

The solution of equation (2.30) is given by:

$$\underline{C}(\xi) = \underline{U} \exp(\underline{\Lambda} \xi) \underline{U}^{-1} \underline{C}^i(\xi - \Delta \xi) \quad (2.32)$$

where  $\underline{U}$ ,  $\underline{\Lambda}$ , and  $\underline{U}^{-1}$  are the eigenvectors, eigenvalues (diagonal), and eigenrows of the matrix E, respectively. The diagonalization of the collocation matrix E is performed by a subroutine called EISYS [12] such that  $\underline{U}$ ,  $\underline{\Lambda}$ , and  $\underline{U}^{-1}$  can be obtained. Since the collocation matrix depends on the parameters  $\delta_1$  and  $\delta_2$ , its eigenvalues, eigenvectors and eigenrows have to be recalculated any time  $\delta_1$  and/or  $\delta_2$  change.

The determination of the initial condition  $\underline{C}^i$  needed to solve equation (2.30) when  $\xi > 0$  uses the solution of  $\underline{C}$  for the previous integration step  $\Delta \xi$ . If neither  $\delta_1$  nor  $\delta_2$  are changed,  $\underline{C}^i(\xi - \Delta \xi)$  is equated to  $\underline{C}(\xi - \Delta \xi)$ . When the parameters  $\delta_1$  and/or  $\delta_2$  change, the initial condition is obtained through a Lagrangian interpolation of the previous good solution and the integration is repeated. This interpolation occurs only for the new position of the collocation points which lie within the previous region  $[\beta - \delta_1, \beta + \delta_2]$ . For points to the left of  $(\beta - \delta_1)$  and to the right

of  $(\beta+\delta_2)$  values of  $C_0$  and zero are assigned to the concentrations, respectively,

The flux at any position in the along wind direction is a useful piece of information that can be obtained from the results and provides a check for continuity. It can be expressed by the following equation:

$$Q_x = \int_0^{z_{\max}} u C(x,z) dz \quad (2.33)$$

Transformation of the spatial variables gives

$$Q_x = \int_0^1 u C(\xi, z^*) z_{\max} dz^* \quad (2.34)$$

By substituting equation (2.19) one obtains

$$Q_x = \int_0^{\beta-\delta_1} u C_0 z_{\max} d\zeta + \int_{\beta-\delta_1}^{\beta+\delta_2} u C(\xi, \zeta) z_{\max} d\zeta \quad (2.35)$$

Finally, using Gaussian quadrature weights, equation (2.35) can be transformed to

$$Q_x = Q_x^1 + u z_{\max} (\delta_1 + \delta_2) \sum_{i=1}^{N_z+2} W_i C_i \quad (2.36)$$

where

$$Q_x^1 = \begin{cases} u z_{\max} (\beta - \delta_1) C_0 & \text{for } \delta_1 < \beta \\ 0 & \text{for } \delta_1 = \beta \end{cases} \quad (2.37)$$

Two Dimensional-Continuous Elevated Line Source

Treatment of the two-dimensional diffusion equation (2.11) for the case of an elevated line source gives more generality to an air pollution model. The only variation with respect to the previous case takes place in the boundary condition (2.7b), which is transformed to:

$$C \rightarrow \infty \quad \text{at} \quad x = 0 \quad \text{and} \quad z = H \quad (2.38)$$

The analytical solution to this problem is given by

$$C(x,z) = \frac{Q}{2[\pi u K_z x]^{\frac{1}{2}}} \left( \exp\left(-\frac{u(z-H)^2}{4K_z x}\right) + \exp\left(-\frac{u(z+H)^2}{4K_z x}\right) \right) \quad (2.39)$$

The technique for solving this case is the same as the previous one, but with a different representation of the concentration distribution at  $x=0$ , as shown in Figure 2.3. This discontinuous initial value profile is expressed as:

$$C^i = \begin{cases} C_o & \text{at } \xi = 0, \quad h - \beta \leq z^* \leq h + \beta \\ 0 & \text{at } \xi = 0, \quad \text{elsewhere} \end{cases} \quad (2.40)$$

with

$$h = \frac{H}{z_{\max}} \quad (2.41)$$

and

$$C_o = \frac{Q}{2u\beta z_{\max}} \quad (2.42)$$

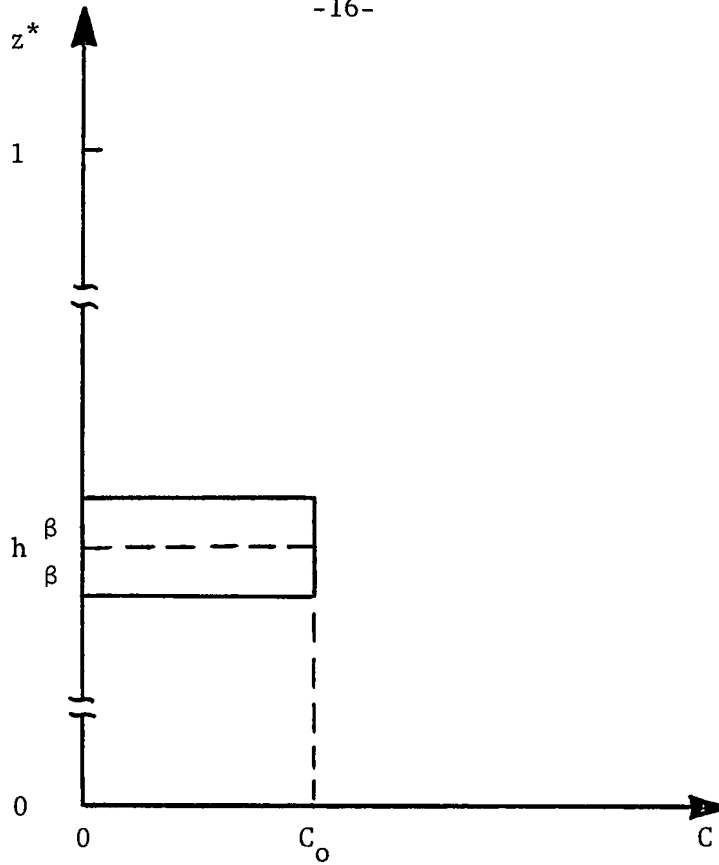


FIGURE 2.3 VERTICAL CONCENTRATION DISTRIBUTION  
AT  $x=0$  - ELEVATED LINE SOURCE

In order to apply orthogonal collocation to the entire region of interest in the  $z$  direction, and taking into account that  $\beta$  is very small compared to 1, the following variable transformation is performed:

$$z^* = (\delta_1 + \delta_2 + 2\beta)\zeta + h - (\beta + \delta_1) \quad (2.43)$$

where  $0 \leq \zeta \leq 1$ . The coefficients in equation (2.20) remain then as,

$$R_1 = \frac{u}{x_{\max}} \quad ; \quad R_5 = \frac{K_z}{z_{\max}^2 (\delta_1 + \delta_2 + 2\beta)^2} \quad (2.44)$$

The concentration distribution is now obtained only within the  $[h-\beta-\delta_1, h+\beta+\delta_2]$  interval in the  $z^*$  domain, as shown in Figure 2.4.

The check on the parameters  $\delta_1$  and  $\delta_2$  is done with the same previous criteria, but now the concentrations at  $\zeta=0$  and  $\zeta=1$  are both compared to zero (= some fraction of the centerline concentration). The comparison at  $\zeta=0$  stops when the plume has reached the ground, i.e.,  $\delta_1=h-\beta$ , and stops at  $\zeta=1$  when the plume reaches the inversion layer, i.e.,  $\delta_2=1-(h+\beta)$ .

The calculation of the collocation matrix and its diagonalization to obtain the eigenvalues, eigenvectors and eigenrows follows the same procedure as before, with its elements  $E_{li}$  given by equation (2.31). The solution to this problem is also determined by equation (2.32).

The initial condition  $\underline{C}^i$  at any integration step is calculated in the same way as previously discussed. Whenever an interpolation is needed for this purpose, zero concentration is assigned to every new collocation point that lies outside the region of interest  $[h-\beta-\delta_1, h+\beta+\delta_2]$  used for the previous step.

Equation (2.34) can be utilized to determine the flux at any position in the  $x$  direction. Substitution of equation (2.43) into (2.34) and the use of Gaussian quadrature weights gives the following expression:

$$Q_x = u z_{\max}^{N_z+2} (2\beta+\delta_1+\delta_2) \sum_{i=1}^{N_z+2} W_i C_i \quad (2.45)$$

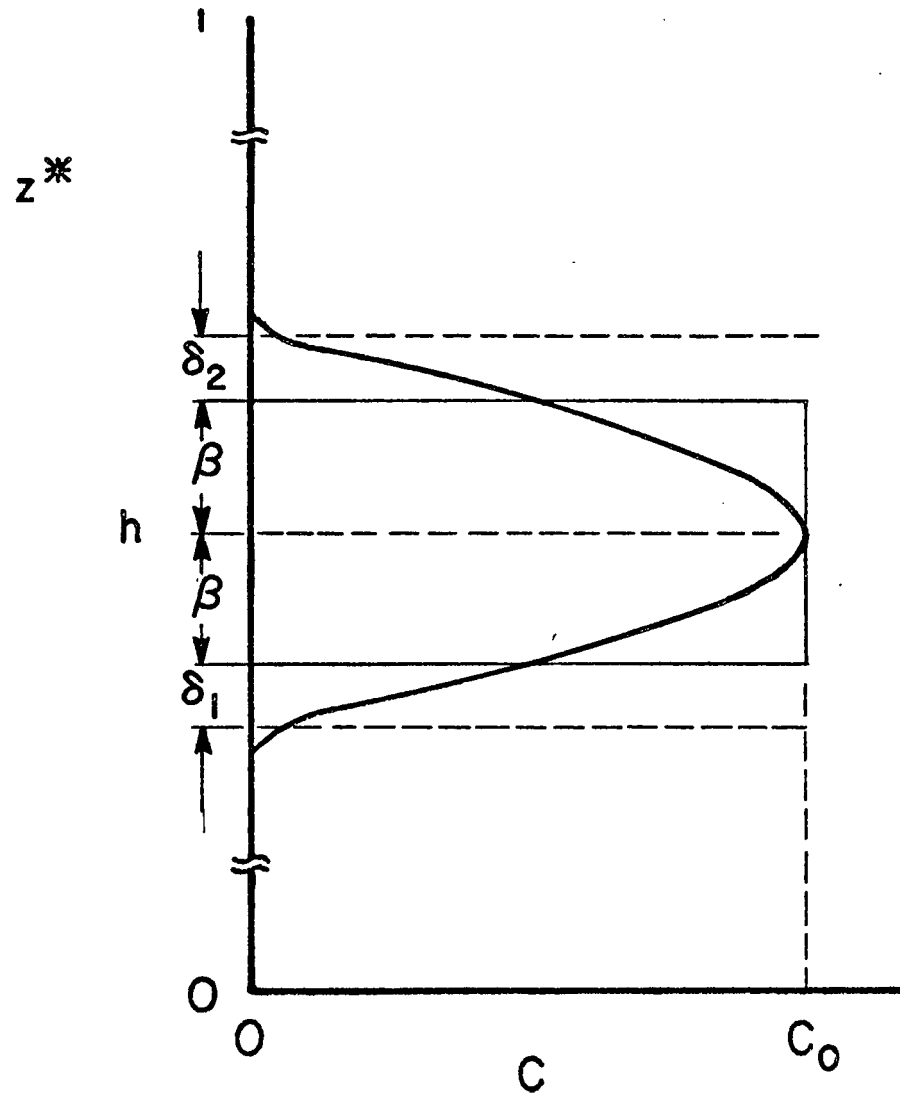


FIGURE 2.4 CORRECT VERTICAL CONCENTRATION DISTRIBUTION AT ANY  $\xi$  - ELEVATED LINE SOURCE

### Two Dimensional Models with Chemical Reactions

The next step in complexity of an air pollution model is to consider a line source case with a pollutant undergoing some kind of removal process, usually expressed as a chemical reaction. Steady-state models for reactive contaminants do not exist because conditions under which reactive pollutant concentrations are not changing with time are virtually non-existent. In spite of this, a solution to this problem is presented next since few modifications to the previous cases are required and its study will help to understand more complex models like the unsteady-state point source case.

The main difference between this case and the previous models occurs in equation (2.11). An additional term, which represents the chemical reaction, should be incorporated in the diffusion equation as

$$u \frac{\partial C}{\partial x} = K_z \frac{\partial^2 C}{\partial z^2} + R \quad (2.46)$$

The technique for solving the collocation equations that arise from equation (2.11), using the eigenvalues of the collocation matrix, is still valid for equation (2.46) if a first-order reaction model is utilized to represent pollutant removal from the atmosphere:

$$R = -k_1 C \quad (2.47)$$

The elements of the collocation matrix would now be given by

$$E_{\ell i} = - \frac{R_5 B_{\ell,1} A_1(i)}{R_1 A_{1,1}} + \frac{R_5 B_{\ell i}}{R_1} + \frac{R_5 B_{\ell, N_z+2} A_2(i)}{R_1 \text{DEN}} - \frac{k_1}{R_1} \delta_{\ell i} \quad (2.48)$$

where  $\delta_{\ell i}$  is the Kronecker delta function,

$$\delta_{\ell i} = \begin{cases} 1 & \text{for } \ell = i \\ 0 & \text{for } \ell \neq i \end{cases} \quad (2.49)$$

While this is the only modification that should be incorporated in the elevated line source model, two more changes should be considered in the ground line source case.

The check on the parameter  $\delta_1$  must be performed with another criteria, i.e., if  $\delta_1 < \beta$ , the calculated concentration at  $\zeta=0$  should be compared to  $C_o \exp(-\frac{k_1 x}{u})$ . The reason being the disappearance of contaminant due to the chemical reaction.

The other modification takes place in the calculation of the flux at any position in the x-direction. Equation (2.35) remains then as follows:

$$Q_x = \int_0^{\beta-\delta_1} u C_o e^{-\frac{k_1 \xi}{R_1}} z_{\max} d\zeta + \int_{\beta-\delta_1}^{\beta+\delta_1} u C(\xi, \zeta) z_{\max} d\zeta \quad (2.50)$$

Therefore, equation (2.36) would contain,

$$Q_x^1 = \begin{cases} uz_{\max}(\beta - \delta_1) C_0 e^{-\frac{k_1 \xi}{R_1}} & \text{for } \delta_1 < \beta \\ 0 & \text{for } \delta_1 = \beta \end{cases} \quad (2.51)$$

The procedure to follow for non-linear chemical reaction models would be to linearize the expression if the eigenvalue method is to be used. Another possibility, simpler and more effective, is to integrate the collocation equations with a technique that would not depend on the expression for the removal processes, e.g., a fourth-order Runge-Kutta method.

The concentration distribution for a continuous ground level line source for a case with a first-order chemical reaction model is presented in Chapter IV.

### Three Dimensional-Continuous Point Source

For a source which is continuously releasing material at a fixed point, the appropriate form of equation (2.1) (again with  $v$  and  $w$  zero, and neglecting the diffusion in the  $x$ -direction relative to convection) is

$$u \frac{\partial C}{\partial x} = \frac{\partial}{\partial y} (K_y \frac{\partial C}{\partial y}) + \frac{\partial}{\partial z} (K_z \frac{\partial C}{\partial z}) + R \quad (2.52)$$

At an early stage, observations of diffusion implied a dependence of  $K_y$  on the distance of travel [14]. On the grounds that it is physically irrational to regard  $K_y$  as a function of horizontal position, one approach

has been to seek solutions with  $K_y$ , as well as  $K_z$  and  $u$ , a function of height above the ground, i.e.,

$$u = u(z) \quad ; \quad K_y = K_y(z) \quad ; \quad K_z = K_z(z) \quad (2.53)$$

For this case, equation (2.52) remains as,

$$u(z) \frac{\partial C}{\partial x} - \frac{dK_z(z)}{dz} \frac{\partial C}{\partial z} = K_y(z) \frac{\partial^2 C}{\partial y^2} + K_z(z) \frac{\partial^2 C}{\partial z^2} + R \quad (2.54)$$

Consider an interval  $[0, y_{\max}]$  as the region of interest in the crosswind direction  $y$ , where a concentration distribution is to be obtained. For simplicity, the point source is located at  $y=0$ , such that no contaminant flows across the centerline  $y=0$ . The reason being symmetry, only the  $x$ -component of the wind velocity is taken into account. Therefore, the same approaches previously discussed can be used for this three-dimensional continuous point source model.

The crosswind dimension, a subset of the present case, can be considered as an analog of the two-dimensional continuous ground level line source. In addition, the two-dimensional continuous elevated line source can be used to represent the other subset, i.e., the vertical dimension. The reason for different approaches for each spatial dimension is that the concentration distribution in the crosswind direction is symmetric with respect to the centerline ( $y=0$ ), whereas the concentration distribution in the vertical direction is not symmetric with respect to the effective emission height ( $z=H$ ). The solution in the  $z$ -direction would

be symmetric if  $K_z$  and  $u$  were constant, and moreover only up to an x-position where the plume reaches the ground or the inversion layer.

Using the spline collocation approach, the following spatial variables transformations must be made:

$$\frac{y}{y_{\max}} = y^* = (\delta_{1y} + \delta_{2y})\eta + \beta_y - \delta_{1y} \quad (2.55)$$

$$\frac{z}{z_{\max}} = z^* = (\delta_{1z} + \delta_{2z} + 2\beta_z)\zeta + h - (\beta_z + \delta_{1z}) \quad (2.56)$$

where  $0 \leq \eta \leq 1$  and  $0 \leq \zeta \leq 1$ , and  $h$  is given by equation (2.41).

The dimensionless variable in the x-direction, presented in equation (2.15), is also introduced in the problem.

For completeness of the model, the following boundary conditions are used:

$$C^i = \begin{cases} C_o & \text{at point source, } \xi=0 ; y^*=0 ; z^*=h \\ 0 & \text{elsewhere, } \xi=0 \end{cases} \quad (2.57)$$

$$\frac{\partial C}{\partial \eta} = 0 \quad \text{at} \quad \eta=0,1 \quad (2.58)$$

$$\frac{\partial C}{\partial \zeta} = 0 \quad \text{at} \quad \zeta=0,1 \quad (2.59)$$

where the equivalent concentration at the point source can be calculated by continuity, as will be seen later.

This approach can be used to simulate any three-dimensional continuous point source model, e.g., few modifications must be done if the point source is located at the ground, i.e., equation (2.56) would be replaced by another equation (2.55) for the vertical direction; any type of removal process for the contaminant, e.g., sedimentation would be valid since equation (2.59) means no flux at  $\zeta=0,1$  and not at the effective emission height,  $h$ .

The use of spline collocation for this case again means that the solution is obtained with moving boundary conditions in the  $y$  and  $z$  directions. Since no changes in the technique were needed, as compared to the previous cases, the check and modifications on  $\delta_1$  and  $\delta_2$  for each direction at any integration step in the  $x$ -direction are performed as before.

The collocation equations for two different situations, constant  $u$ ,  $K_y$ , and  $K_z$ , and then as functions of elevation are presented next.

#### Constant Mean Wind Velocity and Turbulent Diffusivities

Substituting equations (2.15), (2.55) and (2.56) into equation (2.54) (with  $\frac{dK_z}{dz} = 0$ ) one obtains

$$R_1 \frac{\partial C}{\partial \xi} = R_5 \frac{\partial^2 C}{\partial \eta^2} + R_6 \frac{\partial^2 C}{\partial \zeta^2} + R(C) \quad (2.60)$$

where

$$R_1 = \frac{u}{x_{\max}} \quad (2.61)$$

$$R_5 = \frac{K_y}{y_{\max}^2 (\delta_{1y} + \delta_{2y})^2} \quad (2.62)$$

$$R_6 = \frac{K_z}{z_{\max}^2 (\delta_{1z} + \delta_{2z} + 2\beta_z)^2} \quad (2.63)$$

Application of orthogonal collocation to equation (2.60), with  $N_y$  and  $N_z$  as the number of interior collocation points in the  $y$  and  $z$  directions, respectively, gives

$$R_1 \frac{dC_{k\ell}}{d\xi} = R_5 \sum_{i=1}^{N_y+2} B_{ki}^{(2)} C_{i\ell} + R_6 \sum_{i=1}^{N_z+2} B_{\ell i}^{(3)} C_{ki} + R(C_{k\ell}) \quad (2.64)$$

$$\begin{aligned} \text{for } k &= 1, \dots, N_y + 2 \\ \ell &= 1, \dots, N_z + 2 \end{aligned}$$

where  $C_{k\ell}$  represents the mean concentration at the point  $(\eta_k, \zeta_\ell)$ . The superscripts of the discretizational matrix of second derivatives  $B$ , represent the direction and thus the way it is computed, i.e., (2) and (3) stand for the  $y$  and  $z$  directions, respectively.

The use of orthogonal collocation to the boundary conditions in the  $y$ -direction, equation (2.58) gives the following expressions:

$$\begin{aligned} \sum_{i=1}^{N_y+2} A_{1,i}^{(2)} C_{i\ell} &= 0 \quad \text{at } \eta=0 \\ \sum_{i=1}^{N_y+2} A_{N_y+2,i}^{(2)} C_{i\ell} &= 0 \quad \text{at } \eta=1 \end{aligned} \quad (2.65)$$

Solving for the concentration at the centerline and at the edge of the plume one obtains,

$$C_{1,\ell} = - \frac{\sum_{i=2}^{N_y+1} A1Y(i)C_{i\ell}}{A_{1,1}^{(2)}} \quad (2.66)$$

$$C_{N_y+2,\ell} = \frac{\sum_{i=2}^{N_y+1} A2Y(i)C_{i\ell}}{DENY} \quad (2.67)$$

where

$$A1Y(i) = A_{1,i}^{(2)} + \frac{A_{1,N_y+2}^{(2)} A2Y(i)}{DENY} \quad (2.68)$$

$$A2Y(i) = A_{1,1}^{(2)} A_{N_y+2,i}^{(2)} - A_{N_y+2,1}^{(2)} A_{1,i}^{(2)} \quad (2.69)$$

$$DENY = A_{N_y+2,1}^{(2)} A_{1,N_y+2}^{(2)} - A_{1,1}^{(2)} A_{N_y+2,N_y+2}^{(2)} \quad (2.70)$$

Application of orthogonal collocation to the boundary conditions in the z-direction, equation (2.59) gives:

$$\sum_{i=1}^{N_z+2} A_{1,i}^{(3)} C_{ki} = 0 \quad \text{at} \quad \zeta=0 \quad (2.71)$$

$$\sum_{i=1}^{N_z+2} A_{N_z+2,i}^{(3)} C_{ki} = 0 \quad \text{at} \quad \zeta=1$$

Following the same procedure as for the y-direction, the concentration at the edges of the plume in the z-domain is obtained from equation (2.71):

$$C_{k,1} = - \frac{\sum_{i=2}^{N_z+1} A_{1Z}(i) C_{ki}}{A_{1,1}^{(3)}} \quad (2.72)$$

$$C_{k,N_z+2} = \frac{\sum_{i=2}^{N_z+1} A_{2Z}(i) C_{ki}}{DENZ} \quad (2.73)$$

where

$$A_{1Z}(i) = A_{1,i}^{(3)} + \frac{A_{1,N_z+2}^{(3)} A_{2Z}(i)}{DENZ} \quad (2.74)$$

$$A_{2Z}(i) = A_{1,1}^{(3)} A_{N_z+2,i}^{(3)} - A_{N_z+2,1}^{(3)} A_{1,i}^{(3)} \quad (2.75)$$

$$DENZ = A_{N_z+2,1}^{(3)} A_{1,N_z+2}^{(3)} - A_{1,1}^{(3)} A_{N_z+2,N_z+2}^{(3)} \quad (2.76)$$

Substituting equations (2.66), (2.67), (2.72), and (2.73) into equation (2.64) one obtains,

$$\begin{aligned}
 R_1 \frac{dC_{k\ell}}{d\xi} = & R_5 \left( \sum_{i=2}^{N_y+1} \left( -B_{k,1}^{(2)} \frac{A1Y(i)}{A_{1,1}^{(2)}} + B_{ki}^{(2)} + B_{k,N_y+2}^{(2)} \frac{A2Y(i)}{DENY} \right) C_{i\ell} \right) + \\
 & R_6 \left( \sum_{i=2}^{N_z+1} \left( -B_{\ell,1}^{(3)} \frac{A1Z(i)}{A_{1,1}^{(3)}} + B_{\ell i}^{(3)} + B_{\ell,N_z+2}^{(3)} \frac{A2Z(i)}{DENZ} \right) C_{ki} \right) \\
 & + R(C_{k\ell}) \tag{2.77}
 \end{aligned}$$

or simplifying it:

$$\begin{aligned}
 \frac{dC_{k\ell}}{d\xi} = & \frac{R_5}{R_1} \left( \sum_{i=2}^{N_y+1} AKY(k,i) C_{i\ell} \right) + \frac{R_6}{R_1} \left( \sum_{i=2}^{N_z+1} AKZ(\ell,i) C_{ki} \right) + \\
 & + \frac{R(C_{k\ell})}{R_1} \tag{2.78}
 \end{aligned}$$

$$\begin{aligned}
 \text{for } & k=2, \dots, N_y+1 \\
 & \ell=2, \dots, N_z+1
 \end{aligned}$$

Equation (2.78) gives a set of  $(N_y)(N_z)$  first-order ordinary differential equations to solve for the concentration as a function of the along wind direction at the orthogonal collocation points in the crosswind and vertical directions. The initial condition for this system of equations is

$$C_{k\ell}^i = \begin{cases} C_o & \text{at } \xi=0, & 0 \leq y^* \leq \beta_y \\ & & h - \beta_z \leq z^* \leq h + \beta_z \\ 0 & \text{at } \xi=0, & y^* > \beta_y \end{cases} \quad (2.79)$$

elsewhere  $z^*$

Using continuity, the flux at the point source can be expressed as:

$$Q = 2 \int_0^{\beta_y} \int_{-\beta_z}^{\beta_z} u(h) C_o y_{\max} dy^* z_{\max} dz^* \quad (2.80)$$

Solving for  $C_o$ , the equivalent concentration at the source one obtains,

$$C_o = \frac{Q}{4u(h)\beta_z z_{\max} \beta_y y_{\max}} \quad (2.81)$$

For a ground level point source, the 4 in the denominator should be replaced by a 2.

The determination of the initial condition at any integration step follows the same procedure as before. If the concentration at the edges of the plume lies within the range specified by a fraction of the centerline concentration, the solution of the current step is used as the initial condition for the next step. For any boundary concentration outside this comparison, the corresponding  $\delta$  parameter must be changed. If this occurs, the new positions of the collocation

points have to be calculated by equations (2.55) and/or (2.56) and the concentration at these points determined through Lagrangian interpolation in two dimensions using the good solution of the previous step. This will be then the initial condition used at the current integration step. For simplicity,  $\delta_{1y}$  is equated to  $\beta_y$  such that the comparisons are performed strictly to the boundary concentrations at  $\eta=1$ ,  $\zeta=0$  and  $\zeta=1$ .

In order to apply the technique to any air pollution model, i.e., with any type of removal processes, the eigenvalue method for obtaining the solution was dropped. This method has the attractive feature that whenever the region of interest does not change, the same eigenvalues, eigenvectors and eigenrows for the previous step can be used for the current step. That is, the re-diagonalization of the collocation matrix must not be done at every integration step, which results in computational time savings. But in view of generality, other integration techniques were investigated.

A semi-implicit Runge-Kutta technique, based on the method proposed by Caillaud and Padmanabhan [3] was developed in the present work. This type of technique is applied to difficult stiff differential equations. As soon as the stiff component has faded away, at certain position from the point source, it becomes desirable to enlarge the stepsize. A stepsize adjustment algorithm, proposed by Villadsen [19] was used in the present work. This integration method appeared to be very stable and the calculated concentration distribution was the same as that determined by the eigenvalue technique. Unfortunately, the

complexity of the present air pollution model requires a large number of differential equations to be solved. The use of both methods involved a large computational time.

Finally DRKGS, a double precision subroutine furnished by IBM [11] which is a fourth-order Runge-Kutta method, was applied to the present problem. The use of this subroutine was discussed in details by Fleischer [8]. It was decided to keep it as the integration method for all three-dimensional models since the results were comparable to the ones obtained using the previous two methods, but with less than half of their computational time.

The present work for the case of no chemical reactions was validated by comparing the results to the Gaussian plume equation given by

$$C(x,y,z) = \frac{Q}{2\pi\sigma_y\sigma_z u} \exp\left(-\frac{1}{2}\left(\frac{y}{\sigma_y}\right)^2\right) \left( \exp\left(-\frac{1}{2}\left(\frac{z-H}{\sigma_z}\right)^2\right) + \exp\left(-\frac{1}{2}\left(\frac{z+H}{\sigma_z}\right)^2\right) \right) \quad (2.82)$$

and to the analytical solution of the diffusion equation with a reflecting plane at the ground  $z=0$ , given by

$$C(x,y,z) = \frac{Q}{4\pi x (K_y K_z)^{1/2}} \exp\left(-\frac{uy^2}{4K_y x}\right) \left( \exp\left(-\frac{u(z-H)^2}{4K_z x}\right) + \exp\left(-\frac{u(z+H)^2}{4K_z x}\right) \right) \quad (2.83)$$

The flux across any plane normal to the x axis is also calculated in the present work via

$$Q_x = 2 \int_0^{y_{\max}} \int_0^{z_{\max}} u C(x,y,z) dy dz \quad (2.84)$$

Substituting equations (2.55) and (2.56), and using Gaussian quadrature weights, equation (2.84) can be transformed to

$$Q_x = 2u(\delta_{1y} + \delta_{2y}) y_{\max} (\delta_{1z} + \delta_{2z} + 2\beta_z) z_{\max} \sum_{k=1}^{N_y+2} \sum_{\ell=1}^{N_z+2} W_k^{(2)} W_\ell^{(3)} C_{k\ell} \quad (2.85)$$

#### Variable Mean Wind Velocity and Turbulent Diffusivities

The governing equation for this case, equation (2.54), with the incorporation of the spatial variable transformations given by equations (2.15), (2.55) and (2.56) can be expressed as follows:

$$R_1(\zeta) \frac{\partial C}{\partial \xi} + R_3(\zeta) \frac{\partial C}{\partial \zeta} = R_5(\zeta) \frac{\partial^2 C}{\partial \eta^2} + R_6(\zeta) \frac{\partial^2 C}{\partial \zeta^2} + R(C) \quad (2.86)$$

where

$$R_1(\zeta) = \frac{u(\zeta)}{x_{\max}} \quad (2.87)$$

$$R_3(\zeta) = - \frac{\frac{dK_z}{dz}(\zeta)}{z_{\max}(\delta_{1z} + \delta_{2z} + 2\beta_z)} \quad (2.88)$$

$$R_5(\zeta) = \frac{K_y(\zeta)}{y_{\max}^2 (\delta_{1y} + \delta_{2y})^2} \quad (2.89)$$

$$R_6(\zeta) = \frac{K_z(\zeta)}{z_{\max}^2 (\delta_{1z} + \delta_{2z} + 2\beta_z)^2} \quad (2.90)$$

The procedure to obtain the collocation equations is exactly the same as the one previously done, with one extra term involving

$R_3(\zeta) \frac{\partial C}{\partial \zeta}$  in these equations. The final expression then is given by

$$\begin{aligned} \frac{dC_{k\ell}}{d\xi} = & -\frac{R_3(\ell)}{R_1(\ell)} \left( \sum_{i=2}^{N_z+1} \text{DAKZ}(\ell, i) C_{ki} \right) + \frac{R_5(\ell)}{R_1(\ell)} \left( \sum_{i=2}^{N_y+1} \text{AKY}(k, i) C_{i\ell} \right) + \\ & \frac{R_6(\ell)}{R_1(\ell)} \left( \sum_{i=2}^{N_z+1} \text{AKZ}(\ell, i) C_{ki} \right) + \frac{R(C_{k\ell})}{R_1(\ell)} \end{aligned} \quad (2.91)$$

for  $k=2, \dots, N_y+1$

$\ell=2, \dots, N_z+1$

where

$$\text{DAKZ}(\ell, i) = -A_{\ell,1}^{(3)} \frac{\text{ALZ}(i)}{A_{1,1}^{(3)}} + A_{\ell i}^{(3)} + A_{\ell, N_z+2}^{(3)} \frac{\text{A2Z}(i)}{\text{DENZ}} \quad (2.92)$$

and  $\text{AKY}(k, i)$ ,  $\text{AKZ}(\ell, i)$ ,  $\text{ALZ}(i)$ ,  $\text{A2Z}(i)$ , and  $\text{DENZ}$  are the same as before.

The flux across any plane normal to the along wind direction is calculated by an equation similar to (2.85), i.e.,

$$Q_x = 2(\delta_{1y} + \delta_{2y})y_{\max}(\delta_{1z} + \delta_{2z} + 2\beta_z)z_{\max} \sum_{k=1}^{N_y+2} \sum_{\ell=1}^{N_z+2} u^{(\ell)} W_k^{(2)} W_\ell^{(3)} C_{k\ell} \quad (2.93)$$

Analytical solutions for arbitrary source heights and unrestricted functions of  $u$ ,  $K_y$  and  $K_z$  with elevation have not yet been obtained. It should be pointed out that the present technique can be applied to any function of  $u$ ,  $K_y$  and  $K_z$  with respect to any spatial variable and meteorological parameter, as will be seen later. Few modifications must be done to the present model for cases involving functional relationship with respect to other spatial variables, besides elevation.

### Three Dimensional Mean Wind Velocity

Let us now consider a continuous point source emitting contaminants to a region where the axial and lateral components of the mean wind velocity are important. For this case, equation (2.1) is reduced to:

$$u \frac{\partial C}{\partial x} + v \frac{\partial C}{\partial y} = \frac{\partial}{\partial y} (K_y \frac{\partial C}{\partial y}) + \frac{\partial}{\partial z} (K_z \frac{\partial C}{\partial z}) + R \quad (2.94)$$

where the diffusion in the x-direction is again neglected compared to convection, and  $w$  is assumed to be zero. Using the same previous functional relationships for the velocities and diffusivities, i.e.,

$$u=u(z); \quad v=v(z); \quad K_y=K_y(z); \quad K_z=K_z(z) \quad (2.95)$$

equation (2.94) remains as

$$u(z) \frac{\partial C}{\partial x} + v(z) \frac{\partial C}{\partial y} - \frac{dK_z(z)}{dz} \frac{\partial C}{\partial z} = K_y(z) \frac{\partial^2 C}{\partial y^2} + K_z(z) \frac{\partial^2 C}{\partial z^2} + R \quad (2.96)$$

The previous approach used for the y-direction is not valid for the present model since the concentration distribution in this dimension is no longer symmetric with respect to the centerline (y=0). For an interval  $[-y_{\max}, y_{\max}]$  as the region of interest in the y-direction, the following variable transformations are performed:

$$y^* = \frac{\frac{y}{y_{\max}} + 1}{2} \quad (2.97)$$

$$z^* = \frac{z}{z_{\max}} \quad (2.98)$$

$$y^* = (\delta_{1y} + \delta_{2y} + 2\beta_y)\eta + \frac{1}{2} - (\beta_y + \delta_{1y}) \quad (2.99)$$

$$z^* = (\delta_{1z} + \delta_{2z} + 2\beta_z)\zeta + h - (\beta_z + \delta_{1z}) \quad (2.100)$$

where  $0 \leq \eta \leq 1$  ,  $0 \leq \zeta \leq 1$  .

The initial condition for this case can then be stated as

$$C^i = \begin{cases} C_o & \text{at point source, } \xi=0; y=0(y^*=\frac{1}{2}); z^*=h \\ 0 & \text{elsewhere, } \xi=0 \end{cases} \quad (2.101)$$

Substituting equations (2.97) through (2.100) and equation (2.15) into equation (2.96) one obtains

$$R_1(\zeta) \frac{\partial C}{\partial \xi} + R_2(\zeta) \frac{\partial C}{\partial \eta} + R_3(\zeta) \frac{\partial C}{\partial \zeta} = R_5(\zeta) \frac{\partial^2 C}{\partial \eta^2} + R_6(\zeta) \frac{\partial^2 C}{\partial \zeta^2} + R(C) \quad (2.102)$$

where  $R_1(\zeta) = \frac{u(\zeta)}{x_{\max}}$  (2.103)

$$R_2(\zeta) = \frac{v(\zeta)}{2y_{\max}(\delta_{1y} + \delta_{2y} + 2\beta_y)} \quad (2.104)$$

$$R_3(\zeta) = - \frac{\frac{dK_z}{dz}(\zeta)}{z_{\max}(\delta_{1z} + \delta_{2z} + 2\beta_z)} \quad (2.105)$$

$$R_5(\zeta) = \frac{K_y(\zeta)}{4y_{\max}^2(\delta_{1y} + \delta_{2y} + 2\beta_y)^2} \quad (2.106)$$

$$R_6(\zeta) = \frac{K_z(\zeta)}{z_{\max}^2(\delta_{1z} + \delta_{2z} + 2\beta_z)^2} \quad (2.107)$$

The boundary conditions in the y and z-directions are the same as before, given by equations (2.58) and (2.59). Therefore, application of orthogonal collocation to this model adds only one extra term to the right hand side of equation (2.91):

$$- \frac{R_2(\ell)}{R_1(\ell)} \left( \begin{array}{c} N_y + 1 \\ \Sigma \\ i=2 \end{array} AVY(k, i) C_{i\ell} \right) \quad (2.108)$$

with

$$AVY(k, i) = - A_{k,1}^{(2)} \frac{A1Y(i)}{A_{1,1}^{(2)}} + A_{ki}^{(2)} + A_{k, N_y + 2}^{(2)} \frac{A2Y(i)}{DENY} \quad (2.109)$$

The initial condition for this system of first-order ordinary differential equations, equation (2.101), can be expressed as,

$$C_{k\ell}^i = \begin{cases} C_o & \text{at } \xi=0, \frac{1}{2} - \beta_y \leq y^* \leq \frac{1}{2} + \beta_y \\ & h - \beta_z \leq z^* \leq h + \beta_z \\ 0 & \text{at } \xi=0, \text{ elsewhere } y^* \text{ and } z^* \end{cases} \quad (2.110)$$

The equivalent source concentration can again be obtained using continuity:

$$Q = \int_{-\beta_y}^{\beta_y} \int_{-\beta_z}^{\beta_z} u(h) C_o (2y_{\max} dy^*) z_{\max} dz^* \quad (2.111)$$

Solving for  $C_o$ , one obtains

$$C_o = \frac{Q}{8u(h)y_{\max}^{\beta_y} z_{\max}^{\beta_z}} \quad (2.112)$$

Finally, the flux at any position in the along wind direction can be calculated by

$$Q_x = \int_{-y_{\max}}^{y_{\max}} \int_0^{z_{\max}} u(z) C(x, y, z) dy dz \quad (2.113)$$

Using the same procedure as before, equation (2.113) can be reduced to:

$$Q_x = 2(\delta_{1y} + \delta_{2y} + 2\beta_y) y_{\max} (\delta_{1z} + \delta_{2z} + 2\beta_z) z_{\max} \sum_{k=1}^{N_y+2} \sum_{\ell=1}^{N_z+2} u^{(\ell)} W_k^{(2)} W_{\ell}^{(3)} C_{k\ell} \quad (2.114)$$

It should be pointed out that the incorporation of the third component of the mean wind velocity,  $w(z)$ , into the diffusion equation (2.94) modifies only one term. Equation (2.105) would have to be replaced by the following expression:

$$R_3(\zeta) = \frac{w(\zeta) - \frac{dK_z}{dz}(\zeta)}{z_{\max}(\delta_{1z} + \delta_{2z} + 2\beta_z)} \quad (2.115)$$

The procedure to find the edge of the plume in the lateral direction at any integration step is also modified with respect to the previous models. The centerline will not be at  $y=0$ , i.e., it might be to the right or left depending upon the direction of the horizontal mean wind velocity.

The concentration at the edges in the  $y$ -direction and at the effective emission height, i.e.,  $C(\eta=0, z^*=h)$  and  $C(\eta=1, z^*=h)$  are compared to a positive or negative value. A negative concentration means that the plume, at that downwind position, is wider than the actual plume, and therefore the parameter  $\delta_{1y}$  or  $\delta_{2y}$  is decreased until a positive concentration, at the same  $x$  position, is obtained. On the other hand, the same procedure used for the previous models is applied to positive concentrations at the crosswind direction boundaries. Both concentration values are compared to the centerline concentration multiplied by some ratio  $r$ , and if they/it are/is larger, the parameter(s)  $\delta_{1y}$  and/or  $\delta_{2y}$  are/is increased until the desired accuracy is reached.

CHAPTER III  
PARAMETERS ESTIMATION

Basic parameters are estimated for the simple models through parametric studies involving comparison of accuracy and computer time. As the complexity of the models increases, most of these parameters are kept, and others which are inherent of the model in question are estimated for the first time.

Accuracy tests are performed by comparing the calculated concentration values to the analytical solution. For this purpose, an error, which is used throughout this chapter is defined as,

$$e = \left( \frac{C_a - C_c}{C_a} \right) 100 \quad (\%) \quad (3.1)$$

where the subscripts a and c stand for analytical and calculated, respectively.

The calculations for the present work were done in a UNIVAC 1108 digital computer.

Mathematical Parameters

Two Dimensional-Continuous Ground Level Line Source

The first basic parameter which is estimated is the number of orthogonal collocation points that should be used in calculating the concentration distribution. This parametric study is shown in Figure 3.1. For this case, arbitrary values were assigned to the other

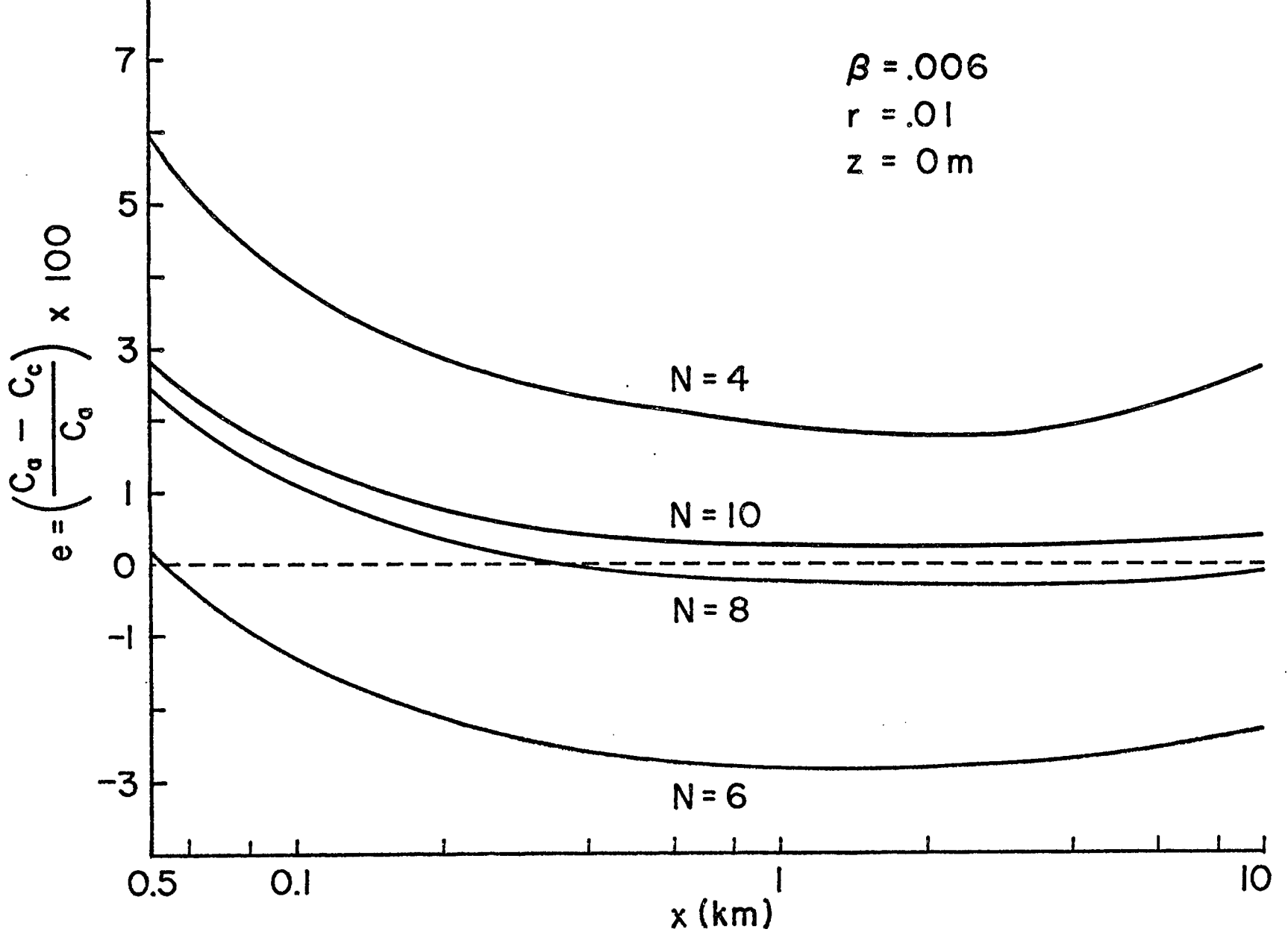


FIGURE 3.1 COMPARISON OF DOWNWIND CONCENTRATION DISTRIBUTION AT GROUND LEVEL WITH ANALYTICAL SOLUTION - PARAMETRIC STUDY ON N

parameters remaining, i.e.,  $\beta$  was equated to some small value .006, and the ratio of the concentration at the edge of the plume and the centerline concentration was assigned a value of 1%, i.e.,  $r = .01$ .

Concentration comparisons were performed for the effective emission height,  $z=0$ . The other key variable used to select the most convenient number of collocation points, the computer time requirement is shown for each case in Table 3.1.

Table 3.1 Computer Time Requirements for Parametric Study on N - Ground Level Line Source Model

N	Time (sec)
4	7
6	17
8	26
10	46

As it was expected, as N increases the error decreases and the computer time increases. The differences in the computer time spent are not very large with the exception of the last two cases, N=8 and N=10. In addition, the error is greatly minimized as N increases from 4 to 8 interior points, but the difference between the last two cases is negligible. Therefore, the number of interior orthogonal collocation points selected is 8.

The next parametric study done, on  $\beta$ , is shown in Figure 3.2. For this case,  $r$  was again given an arbitrary value of 0.01. Time requirements are given in Table 3.2.

Table 3.2 Computer Time Requirements for Parametric Study on  $\beta$  - Ground Level Line Source Model

$\beta$	Time (sec)
.003	31
.006	26
.018	32

An analysis for this case shows that as  $\beta$  increases, the error increases for downwind distances close to the emission source. This is exactly one of the objectives pursued in using spline collocation in problems with a discontinuous initial value profile. Since the parameters  $\delta$  will have a comparable value to  $\beta$ , small values mean that the concentration distribution is calculated only in a region where material exists, i.e., within the plume. This region of interest is very small close to the emission source. As the pollutant moves downwind the plume spreads, and therefore the region of interest is increased by means of the parameters  $\delta$ .

The computer time requirements for all cases was almost identical, so that a value of .005 was selected for  $\beta$ . Together with the estimation of  $\beta$ , the parameters  $\delta_1$  and  $\delta_2$  must be specified. The procedure is to

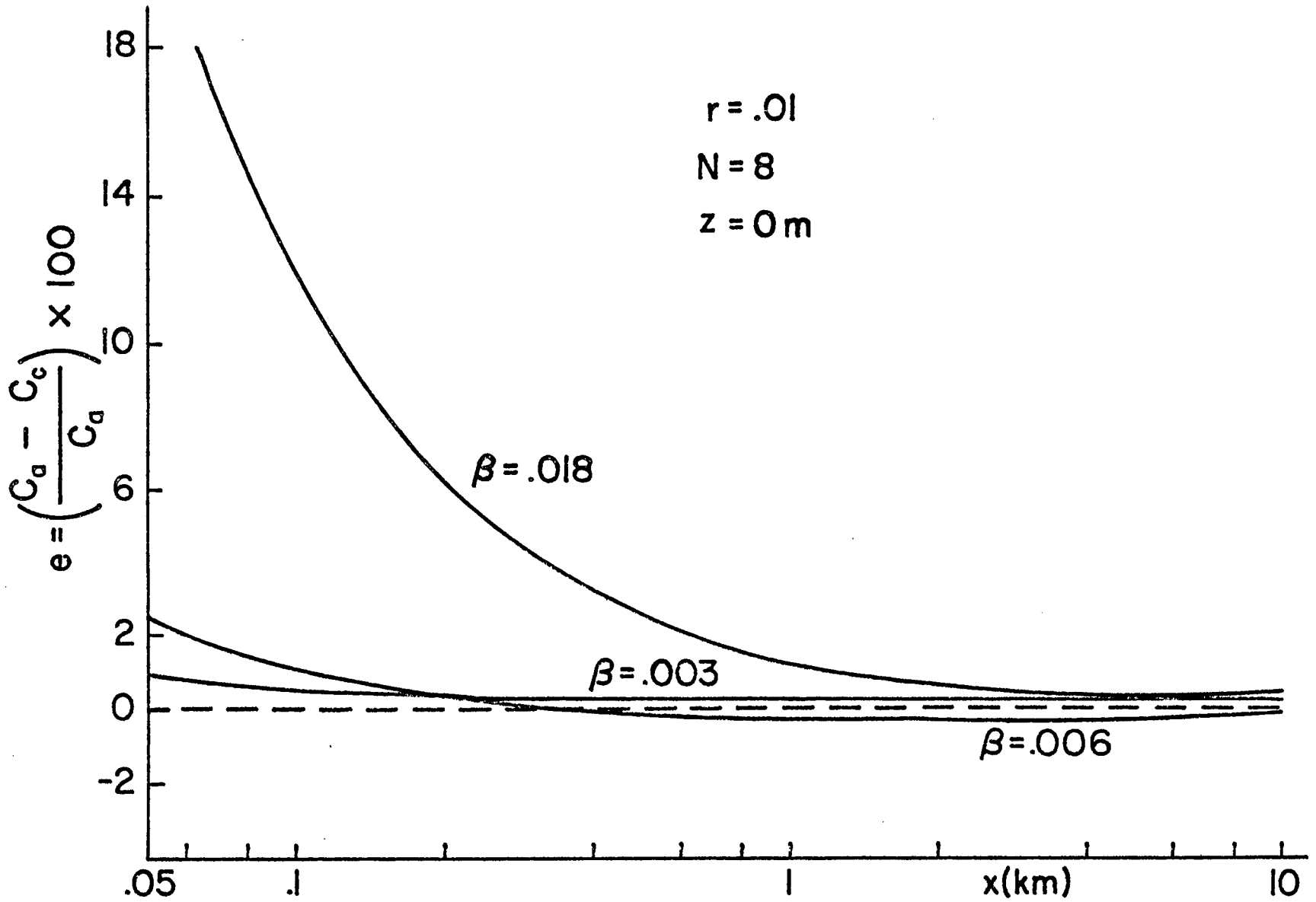


FIGURE 3.2 COMPARISON OF DOWNWIND CONCENTRATION DISTRIBUTION AT GROUND LEVEL WITH ANALYTICAL SOLUTION - PARAMETRIC STUDY ON  $\beta$

find the pair that will determine a region in space which will contain all the material emitted. Since  $\beta$  is very small compared to 1 which is the entire  $z^*$  domain, the same value of 0.005 was selected for  $\delta_1$ . In order to estimate  $\delta_2$ , two cases were simulated in the computer. The first case had a mass flux at the first integration step higher than the emission rate. The other case had  $Q_x$  smaller than  $Q$  such that a linear interpolation on both  $\delta_2$  gave the mass flux equal to the emission rate. The values for an emission rate of 1 gm/m s are shown in Table 3.3.

Table 3.3 Mass Flux vs  $\delta_2$  at the First Integration Step - Ground Level Line Source Model

$\delta_2$	$Q_x$ (gm/m s)
.004	.9
.006	1.1
.005	1.0

Everytime the concentration at the boundary is larger than zero, the region of interest is increased by adding .005 to the previous value for  $\delta_2$ . This "zero concentration" is assigned a certain fraction of the centerline concentration, as it is done in the Gaussian plume equation, where  $r = .10$  (10%). This is then the last basic parameter to be determined for this model, and the results of the parametric study are shown in Figure 3.3 and Table 3.4.

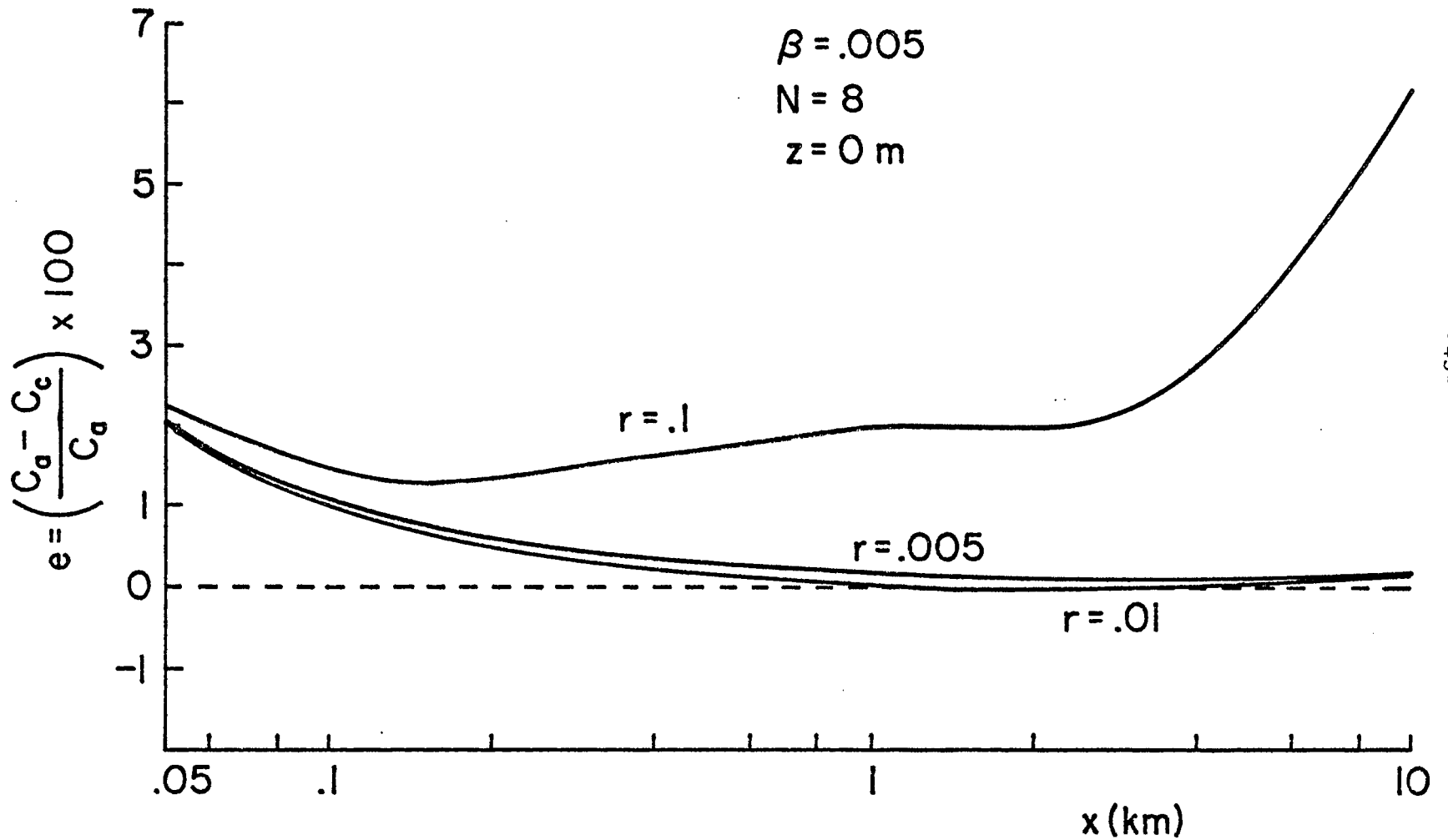


FIGURE 3.3 COMPARISON OF DOWNWIND CONCENTRATION DISTRIBUTION AT GROUND LEVEL WITH ANALYTICAL SOLUTION - PARAMETRIC STUDY ON  $r$

Table 3.4 Computer Time requirements for Parametric Study on  $r$  - Ground Level Line Source Model

$r$	Time (sec)
.005	31
.01	27
.1	20

As expected, the lower  $r$  the better is the description of the process, i.e., the boundary concentration is closer to zero. But there must be also a compromise in the computer time involved. Therefore,  $r$  is assigned a value of 0.01 for the rest of the present work.

There is one more variable in this model that should be analyzed,  $z_{\max}$ , the maximum elevation. If there is an inversion layer,  $z_{\max}$  must take on that value. On the other hand, if no inversion layer exists, any value for  $z_{\max}$  can be specified as input data as long as it does not create an artificial inversion layer. This could happen if  $x_{\max}$  is very large, e.g., 10 km, and  $z_{\max}$  very small, e.g., 50 m, such that the plume reaches the maximum elevation before  $x_{\max}$ .

An increase in the maximum elevation produces a similar effect as increasing  $\beta$ . The region of interest becomes wider such that the accuracy for downwind distances close to the emission source is aggravated. However, every time the parameter  $\delta_2$  is increased, a larger  $z_{\max}$  implies more separation from the ground. This results in fewer situations where the

boundary concentration is larger than zero, and thus fewer number of computations. In addition, the separations between interior collocation points in the z domain are larger so that the concentration gradients become smaller. Therefore, the computer time involved is reduced. This analysis is shown in Figure 3.4 and Table 3.5

Table 3.5 Computer Time Requirements for Parametric Study on  $z_{\max}$  - Ground Level Line Source Model

$z_{\max}$ (m)	Time (sec)
50	45
250	40
500	27
1000	16

Figure 3.4 shows incomplete curves for the cases with  $z_{\max}$  equal to 50 and 250 m. The reason being that at the corresponding downwind position the plume reached the maximum elevation and a comparison to the analytical solution is no longer valid.

The procedure to find the most convenient maximum elevation would be to simulate first a case with a large value for  $z_{\max}$ , and then by inspecting the results locate the maximum elevation the plume reaches. A value a little bit higher to the one obtained should be assigned to

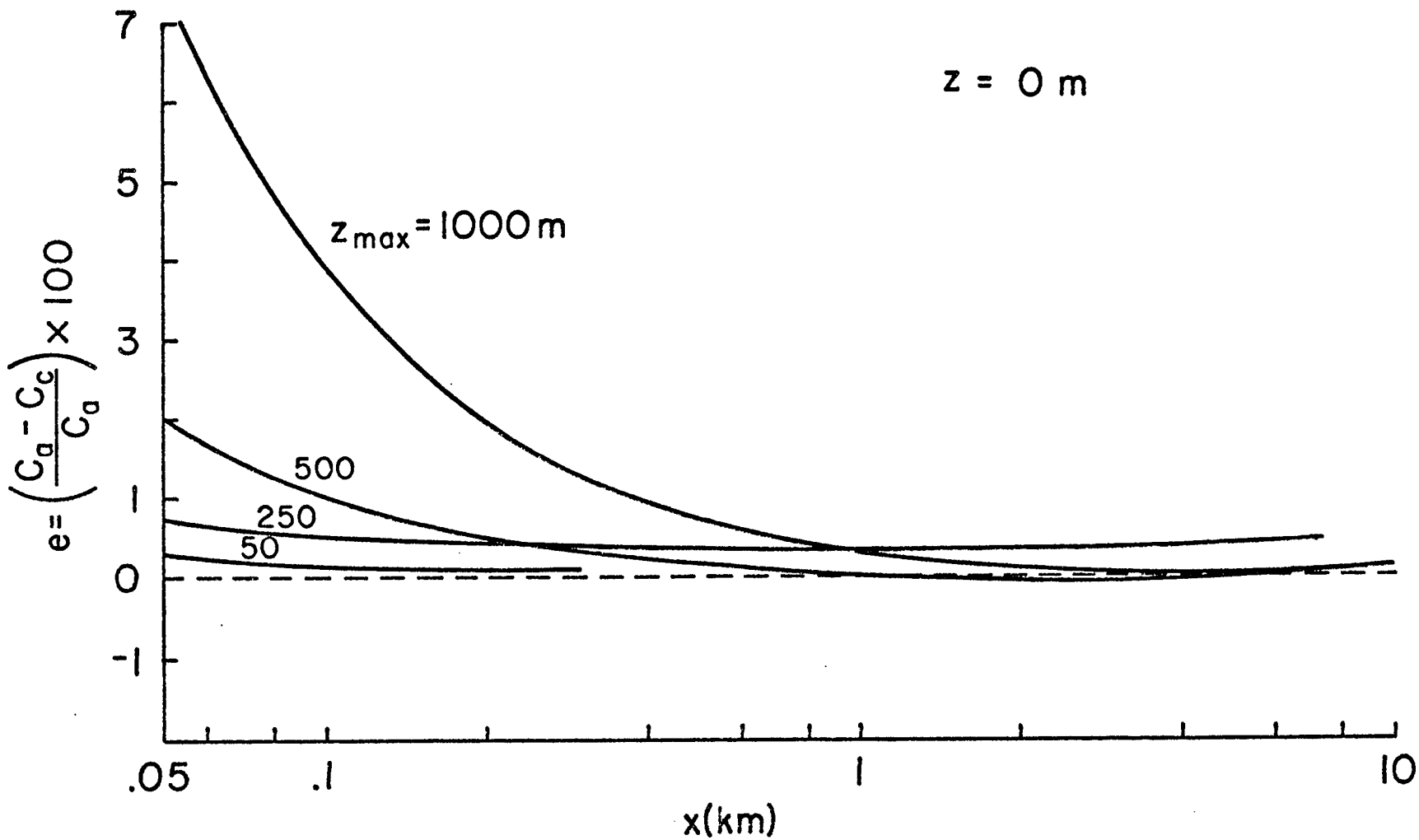


FIGURE 3.4 COMPARISON OF DOWNWIND CONCENTRATION DISTRIBUTION AT GROUND LEVEL WITH ANALYTICAL SOLUTION - PARAMETRIC STUDY ON  $z_{\text{max}}$

$z_{\max}$  if accuracy is the objective. For most cases,  $z_{\max} = 500$  m is reasonable enough, unless the problem involves a very unstable atmosphere and/or a very tall stack.

Two Dimensional - Continuous Elevated Line Source

The structure of the technique used to solve this model is different to the previous one in the sense that the parameter  $\beta$  is located to both sides of the effective emission height. For this reason the number of orthogonal collocation points is increased to  $N = 10$ .

There is no relation on  $\beta$  for this case and the ground level line source model, so that a parametric study was performed. This is shown in Figure 3.5 and Table 3.6.

Table 3.6 Computer Time Requirements for Parametric Study on  $\beta$  - Elevated Line Source Model

$\beta$	Time (sec)
.0010	84
.0012	83
.0013	83
.0014	92
.0015	98
.0020	100

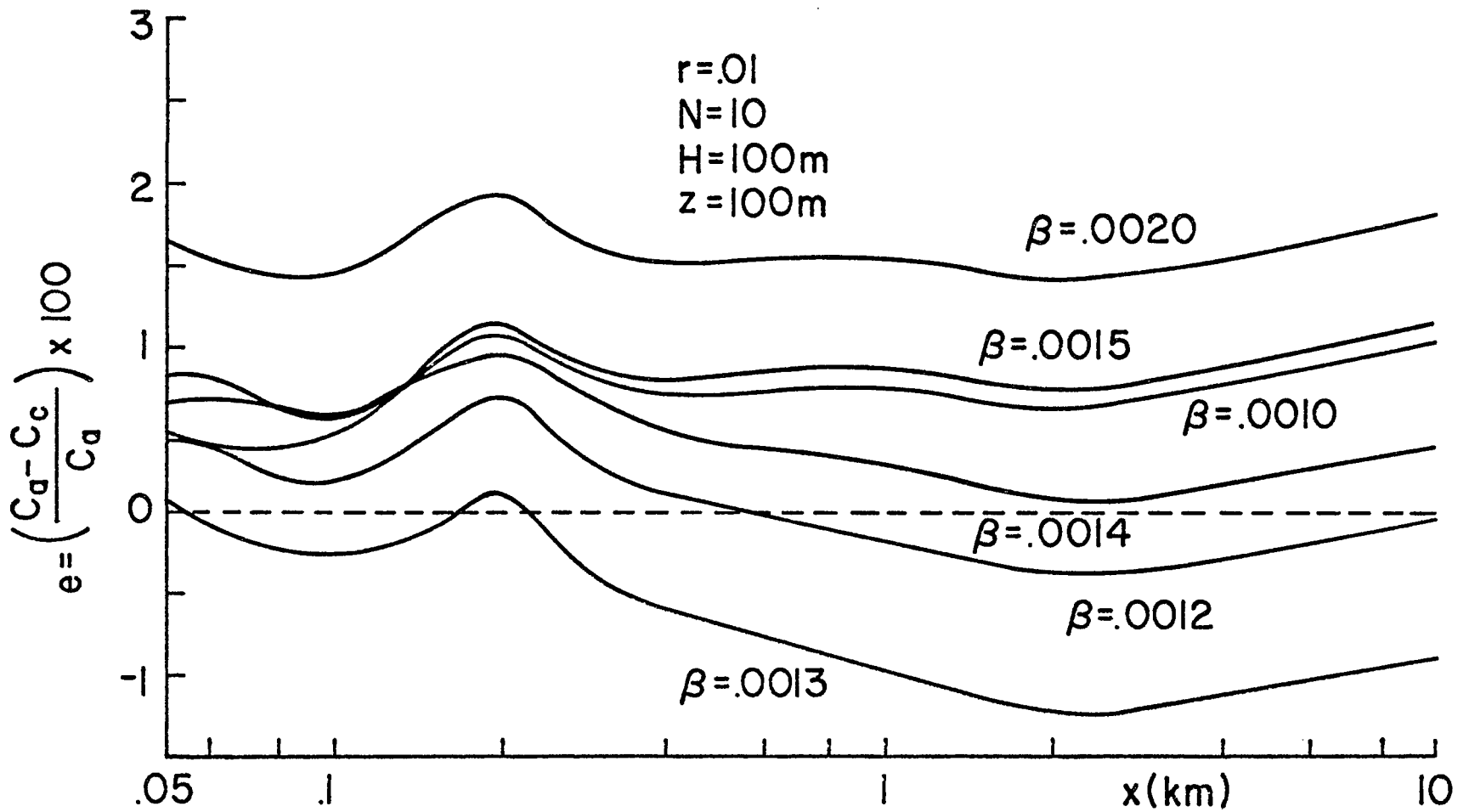


FIGURE 3.5 COMPARISON OF DOWNWIND CONCENTRATION DISTRIBUTION AT THE EFFECTIVE EMISSION HEIGHT WITH ANALYTICAL SOLUTION - PARAMETRIC STUDY ON  $\beta$

The computer time requirements were similar for all cases, so that the selection for  $\beta$  was made on grounds of accuracy. Something very peculiar happens for this approach in the sense that the errors oscillate between zero for the cases of  $\beta$  between .0010 and .0014. No explanation can be given to this, although it is a fact that as  $\beta$  is increased from .0014, the accuracy becomes worse, as it should be and was previously discussed. The errors were computed at the effective emission height, 100 m. It should be pointed out that it would be fortuitous if one of the interior collocation points coincided with the effective emission height. This is the reason why a one-dimensional Lagrangian interpolation was used to obtain the concentration at this elevation. This type of interpolation takes into account the concentration at all collocation points, so that the error calculated at H, besides  $Q_x$ , shows the overall error involved in the solution technique.

A value of 0.0012 was assigned for  $\beta$  in this model. The same procedure as before was used to estimate the parameters  $\delta_1$  and  $\delta_2$ . For an emission rate of 1 gm/s m, Table 3.7 shows the final values for  $\delta_1$  and  $\delta_2$  obtained.

Table 3.7 Mass Flux vs  $\delta_1$  and  $\delta_2$  at the First Integration  
Step - Elevated Line Source Model

$\delta_1$	$\delta_2$	$Q_x$ (gm/s)
.0030	.0030	1.0343
.0026	.0026	.9358
.002861	.002861	1.0001

The value by which these parameters are increased whenever the region of interest must be increased is given a similar value as  $\delta_1$ , i.e., .0025.

The same analysis for  $z_{\max}$  as previously discussed is presented in Figure 3.6 and Table 3.8. The conclusions are exactly the same, but since the main objective of the present work is accuracy,  $z_{\max} = 500$  m is used when possible throughout the entire research.

Table 3.8 Computer Time Requirements for Parametric Study  
on  $z_{\max}$  - Elevated Line Source Model

$z_{\max}$ (m)	Time (sec)
500	83
2000	27

### Three Dimensional Continuous Point Source

Estimation of parameters for this complex model proves that the analysis and understanding of the previous simple cases is valuable. Determination of a convenient set of parameters to get high accuracy would have been difficult without knowledge of the values specified for the previous models.

Let us first consider the case where only one component of the mean wind velocity is taken into account. In addition to  $u$ , both turbulent diffusivities,  $K_y$  and  $K_z$ , are assumed constant.

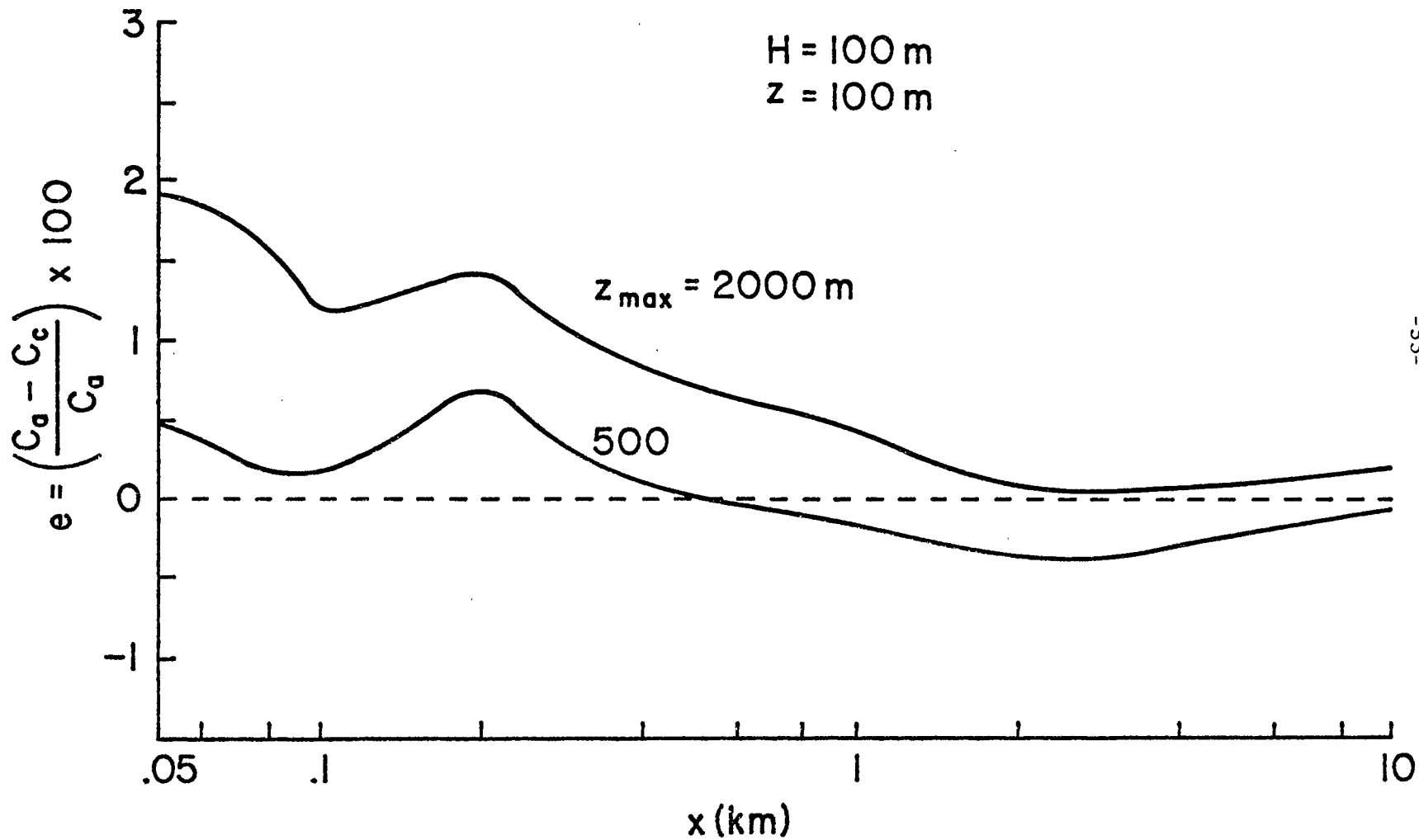


FIGURE 3.6 COMPARISON OF DOWNWIND CONCENTRATION DISTRIBUTION AT THE EFFECTIVE EMISSION HEIGHT WITH ANALYTICAL SOLUTION - PARAMETRIC STUDY ON  $z_{\max}$

Since the problem can be considered symmetric with respect to the centerline ( $y=0$ ), the technique utilized for the ground level line source can be used in the lateral direction. Therefore,  $N_y$  is equated to 8 and  $\beta_y$  to .005.

In many cases air pollution is due to elevated point sources, so that the approach used for the elevated line source model can be utilized for the z-direction. Therefore, ten interior orthogonal collocation points are used in the vertical dimension, i.e.,  $N_z = 10$ , and a value of 0.0012 is assigned to  $\beta_z$ .

The procedure to obtain the  $\delta$  parameters, now there are four, follows the one previously discussed. Three of these parameters were given the same value as before, i.e.,  $\delta_{1y}=.005$ ,  $\delta_{1z}=\delta_{2z}=.002861$  and the fourth parameter was obtained by comparing the mass flux at the first integration step with the emission rate. For this model,  $Q=1$  kg/s, and the parametric study is shown in Table 3.9. A value of .01069 was assigned to  $\delta_{2y}$ .

Table 3.9 Mass Flux vs  $\delta_{2y}$  at the First Integration

Step - Elevated Point Source Model

$\delta_{2y}$	$Q_x$ (kg/s)
.01	.95607
.011	1.01981
.01069	1.00005

The increments on these parameters, whenever the boundaries of the plume are changed, are the same as the ones used before with the exception of  $\delta_{2y}$  which now was changed. Again a comparable value is used for this purpose, i.e., 0.015. It should be pointed out that no matter what value is given for Q and H, all these parameters do not have to be changed again.

The use of a different method, DRKGS, for integrating the diffusion equation along the x direction, as compared to the eigenvalue technique utilized before, introduces one more parameter: the upper error bound,  $\epsilon$ , as discussed by Fleischer [8]. A parametric study was performed and is shown in Figure 3.7 and Table 3.10.

Table 3.10 Computer Time Requirements for Parametric Study on  $\epsilon$  - Elevated Point Source Model

$\epsilon$	Time (sec)
$1 \times 10^{-5}$	180
$1 \times 10^{-6}$	190
$1 \times 10^{-7}$	200
$1 \times 10^{-8}$	290

The cases simulated involved meteorological parameters that exist for very unstable conditions, which will be discussed in the next section. This was done in order to have large concentration gradients and the possibility of a difficult problem to solve. The error was calculated again at the effective emission height. A two-dimensional Lagrangian

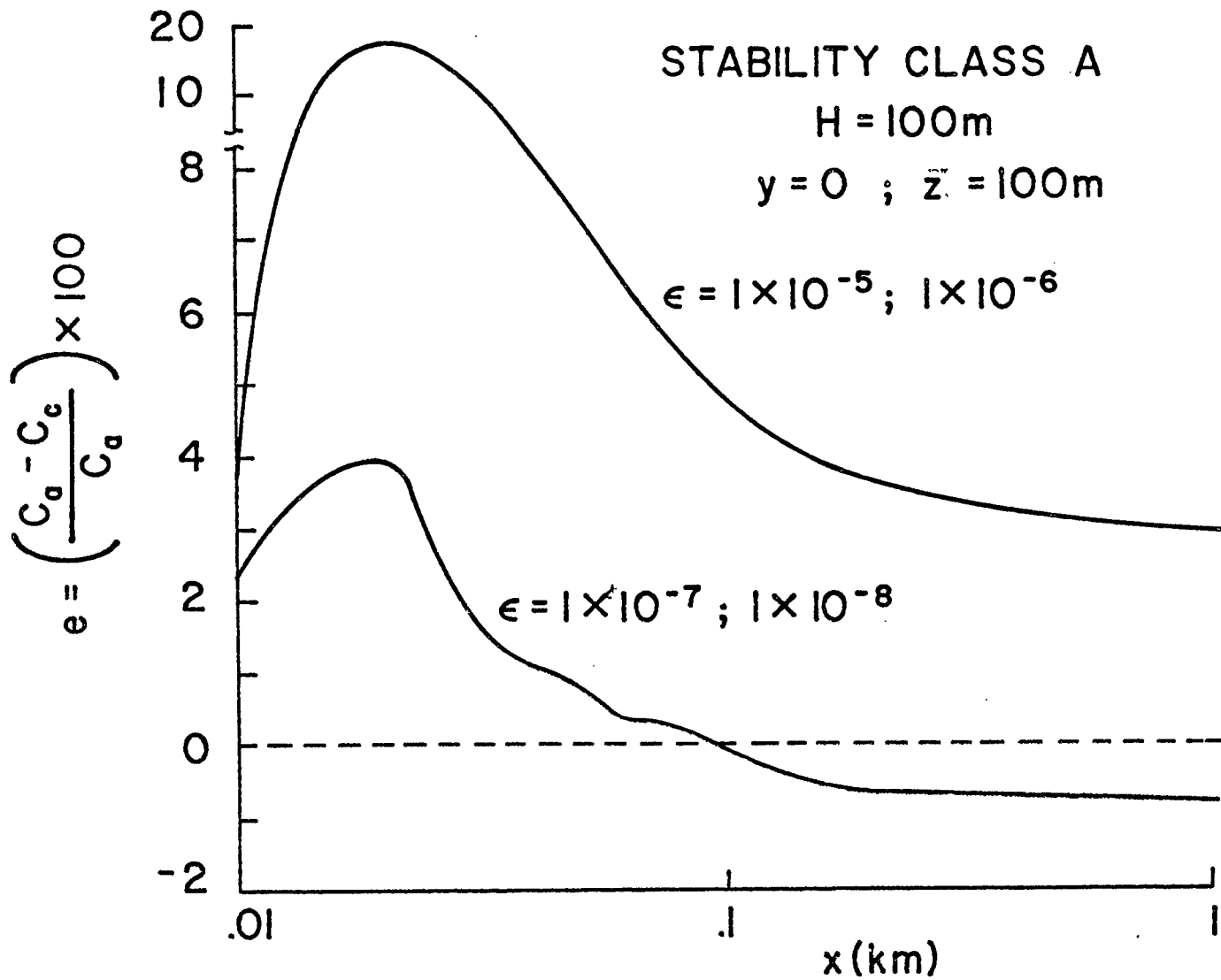


FIGURE 3.7 COMPARISON OF DOWNWIND CONCENTRATION DISTRIBUTION AT THE EFFECTIVE EMISSION HEIGHT WITH ANALYTICAL SOLUTION - PARAMETRIC STUDY ON  $\epsilon$

interpolation, which involves the solution at all collocation points, was used. The calculated error again gives an estimate of the overall error.

An analysis of Figure 3.7 shows that the accuracy is greatly improved by modifying the upper error bound from  $\epsilon = 1 \times 10^{-6}$  to  $\epsilon = 1 \times 10^{-7}$ , while the computer times involved are similar. The time requirements have increased very much compared to the two-dimensional cases because a system of 80 first-order ordinary differential equations is being solved for the present model.

A closer look at Figure 3.7 shows a peak in the error  $e$  at 20 m downwind from the source. For practical purposes this does not matter very much since the concentration distribution is usually desired from 50 to 100 m up downwind. Furthermore, this error is 4% which for these purposes is quite low. This peak occurs because of the large integration stepsize of 10 m at that location. A parametric study on  $\epsilon$  with a smaller stepsize of 2.5 m was simulated next. The absolute error  $e$  was identical for all previous  $\epsilon$  used, but not the computer time requirements which are presented in Table 3.11.

Table 3.11 Computer Time Requirements for Small Stepsize of Integration - Elevated Point Source Model

$\epsilon$	Time (sec)
$1 \times 10^{-5}$	250
$1 \times 10^{-6}$	260
$1 \times 10^{-7}$	270
$1 \times 10^{-8}$	310

Since there was no dependence of  $\epsilon$  in the error for this case, a parametric study to check  $r$  was performed again, and is shown in Figure 3.8. It can be seen that the absolute error is indeed decreased by using a smaller stepsize, and the peak is converted to a damped curve at downwind distances close to the point source. As expected and discussed before, as the ratio increased the error increased and the computer time decreased to 250 seconds ( $\epsilon = 1 \times 10^{-7}$ ). The main objective of the present work is to develop a highly accurate method of solution, so the small stepsize was adopted with an upper error bound of  $\epsilon = 1 \times 10^{-7}$ .

The analysis on  $z_{\max}$  discussed for the previous models still holds for the three dimensional case. It should be pointed out that an inversion layer in the lateral dimension is meaningless. Therefore,  $y_{\max}$  must always be specified by the user, and if the horizontal spread of the plume has reached that value, the solution from that downwind distance until  $x_{\max}$  would be erroneous. For such a case,  $y_{\max}$  should be increased.

Finally, the parameters for cases with two-dimensional mean wind velocities must be specified. These cases must be treated in a different way since the concentration distribution is not symmetric to the center-line ( $y=0$ ) anymore. The approach used for the vertical direction is then applied to the lateral dimension with  $y=0$  as the analog of the effective emission height. Therefore,  $N_y=N_z=10$ ,  $\beta_y=\beta_z=.0012$ , all  $\delta$  are equated to .002861 and their increments to .0025.

STABILITY CLASS A

H = 100m

y = 0; z = 100m

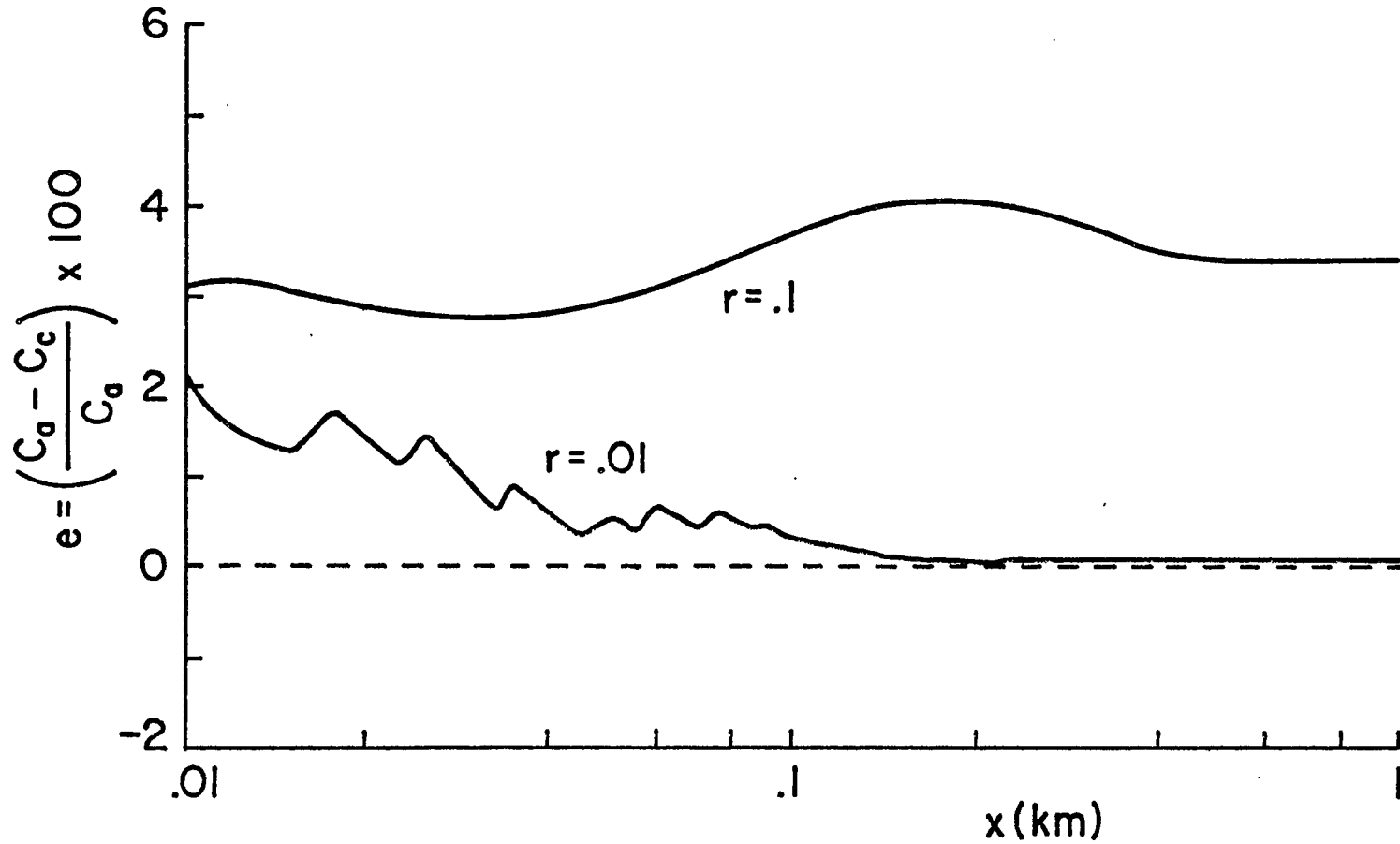


FIGURE 3.8 COMPARISON OF DOWNWIND CONCENTRATION DISTRIBUTION AT THE EFFECTIVE EMISSION HEIGHT WITH ANALYTICAL SOLUTION - PARAMETRIC STUDY OF  $r$

### Meteorological Parameters

General functional relationships and the corresponding parameters must be specified for the turbulent diffusivities and velocity profiles for completeness of the formulation of the present models. This is presented next.

### Turbulent Diffusivities $K_y$ , $K_z$

Any work related to air pollution modeling and dispersion processes in the atmosphere, which uses the K-theory, must include descriptions for the turbulent diffusivities in the lateral and vertical directions,  $K_y$  and  $K_z$ , respectively. Unfortunately, these descriptions vary from one work to another. Sometimes experimental data are available, but again they usually apply for the specific case in question.

Among the best of these works, Eschenroeder and Martinez [5] relate  $K_z$  to elevation and most importantly to stability classes, as defined by Pasquill and Gifford [18], a parameter that is widely used and known. The trapezoidal profile for  $K_z$ , discussed by Fleischer [8], and the values for the maximum constant vertical diffusivities from the knee height up to the inversion layer seem to describe fairly well  $K_z$ . Eschenroeder and Martinez, based on a Los Angeles tetron data, assigned a value of  $500 \text{ m}^2/\text{s}$  for the constant horizontal diffusivity. Unfortunately, this large value, when compared to others, is not appropriate to use as a typical measure for  $K_y$ . Therefore, their description for  $K_z$  is used in the present work, but with different absolute values for  $K_z$  and  $K_y$ .

The fact that the Gaussian plume equation, which uses dispersion parameters based on experimental data, is the most widely used method to determine the concentration distribution helped to develop a method for obtaining the turbulent diffusivities. Moreover, one of the most important questions in air quality is related to the position and magnitude of the maximum ground level concentration. Therefore, the three-dimensional continuous elevated point source solution, with constant wind speed and turbulent diffusivities, was matched to the Gaussian plume equation to give the same maximum ground level concentration at the same position. The vertical diffusivity was adjusted until the position of the maximum at some downwind distance from the source was equal to the one predicted by the Gaussian plume equation. Once  $K_z$  was determined, the horizontal diffusivity was obtained when the spread of the plume was enough such that the absolute value for the maximum concentration gave the same as the Gaussian plume equation prediction. Typical values for the wind speed, depending upon stability classes, were used. Since an analytical solution for this model is available, the present method was validated by their comparison.

The resulting concentration distributions are shown in Figures 3.9 through 3.14. All cases were simulated in approximately the same computational time, i.e., 270 seconds. Excellent agreement can be observed between the concentration profiles obtained by the present technique and the analytical solution. On the other hand, except for the maximum ground level concentration, the results do not agree with the Gaussian

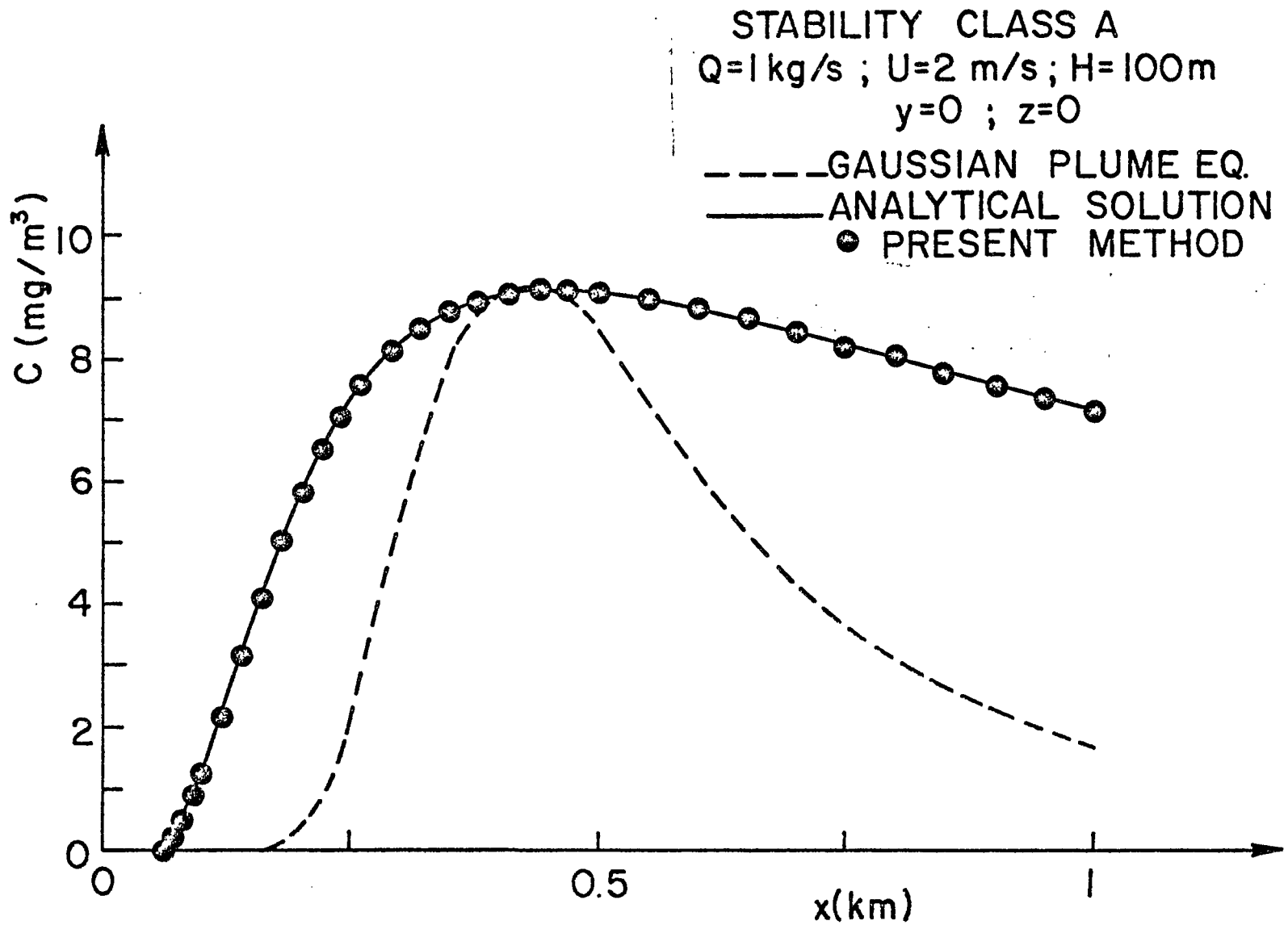


FIGURE 3.9 COMPARISON OF DOWNWIND CONCENTRATION DISTRIBUTION AT GROUND LEVEL WITH ANALYTICAL SOLUTION AND GAUSSIAN PLUME EQUATION - STABILITY CLASS A

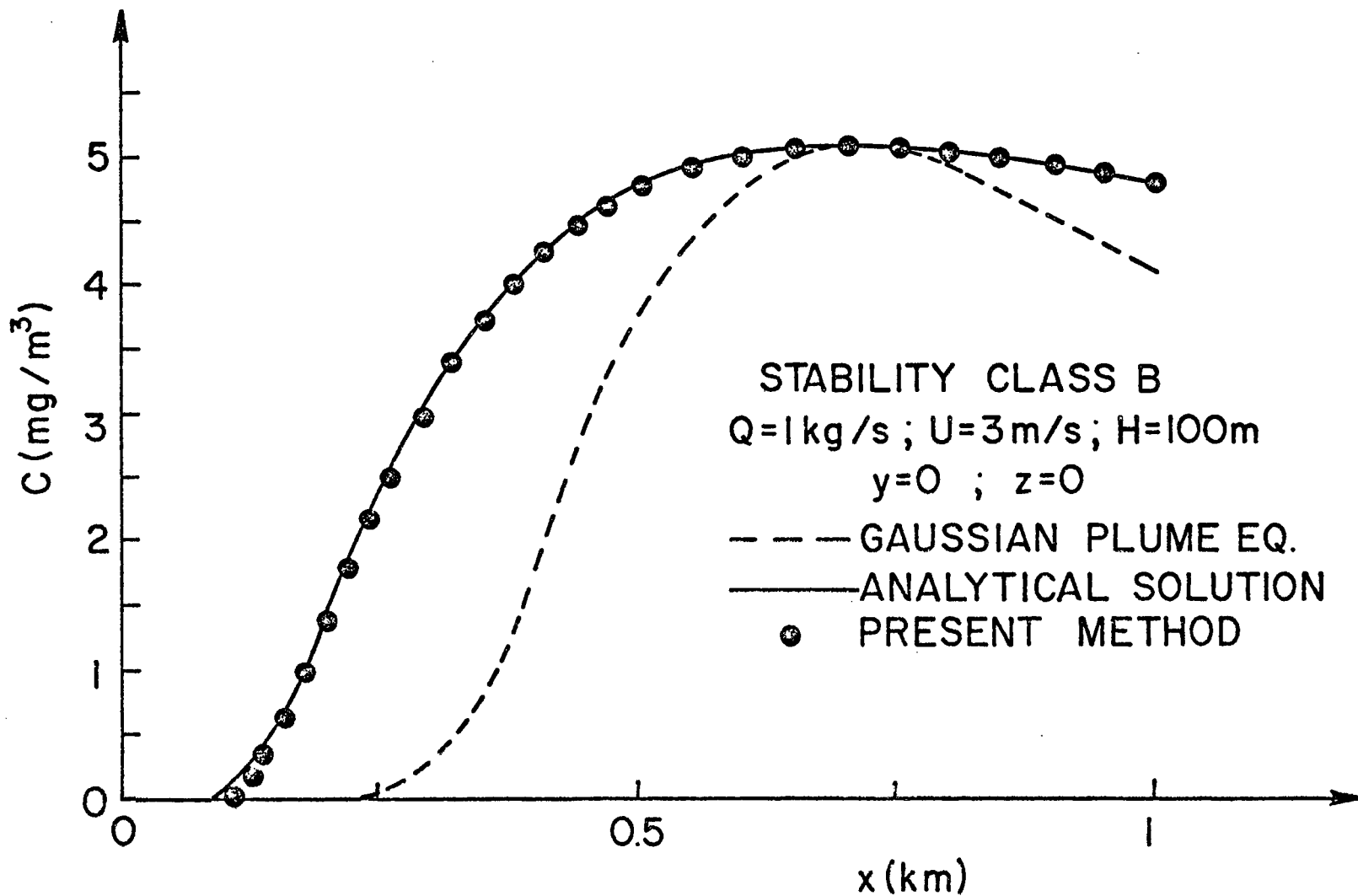


FIGURE 3.10 COMPARISON OF DOWNWIND CONCENTRATION DISTRIBUTION AT GROUND LEVEL WITH ANALYTICAL SOLUTION AND GAUSSIAN PLUME EQUATION - STABILITY CLASS B

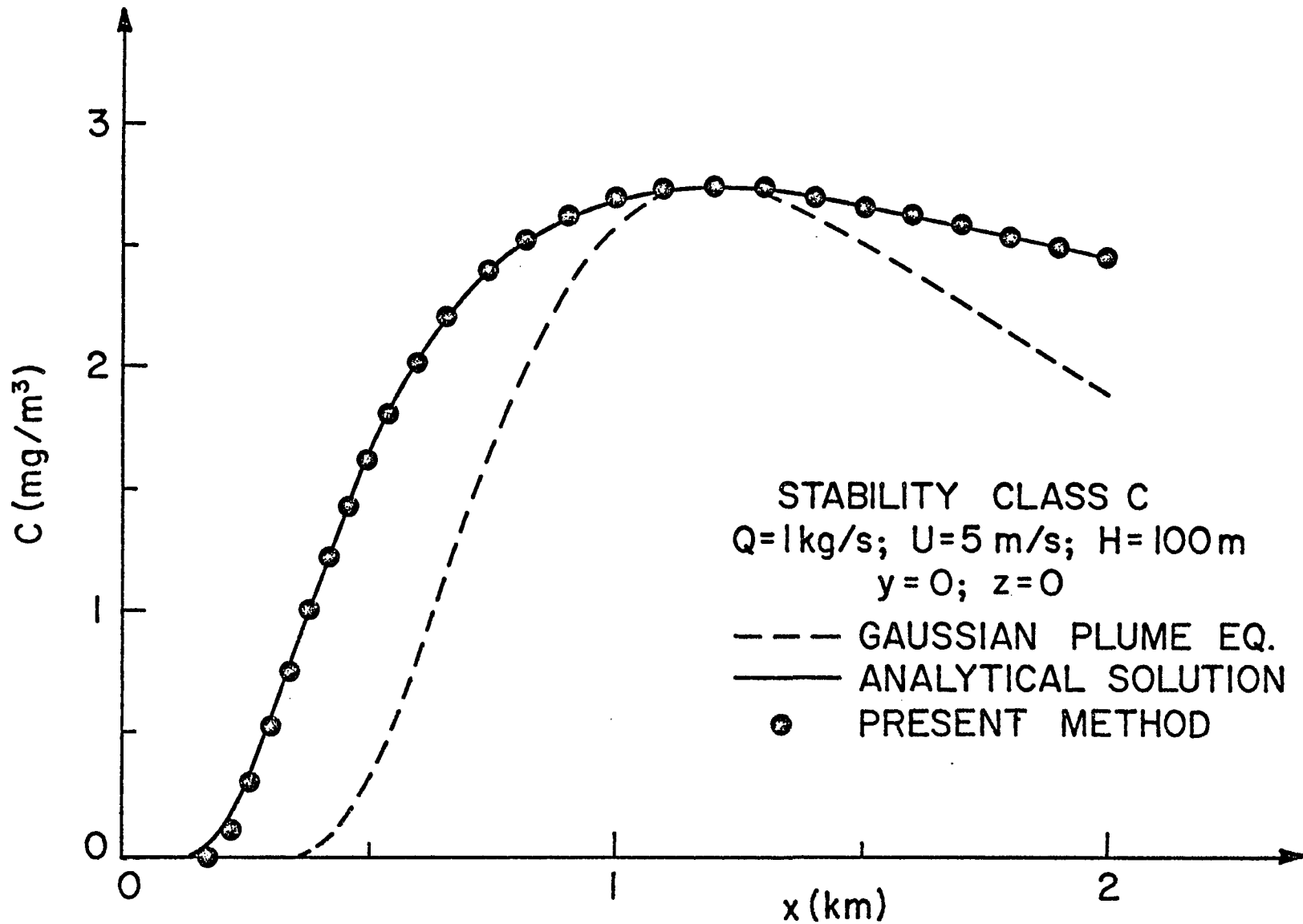


FIGURE 3.11 COMPARISON OF DOWNWIND CONCENTRATION DISTRIBUTION AT GROUND LEVEL WITH ANALYTICAL SOLUTION AND GAUSSIAN PLUME EQUATION - STABILITY CLASS C

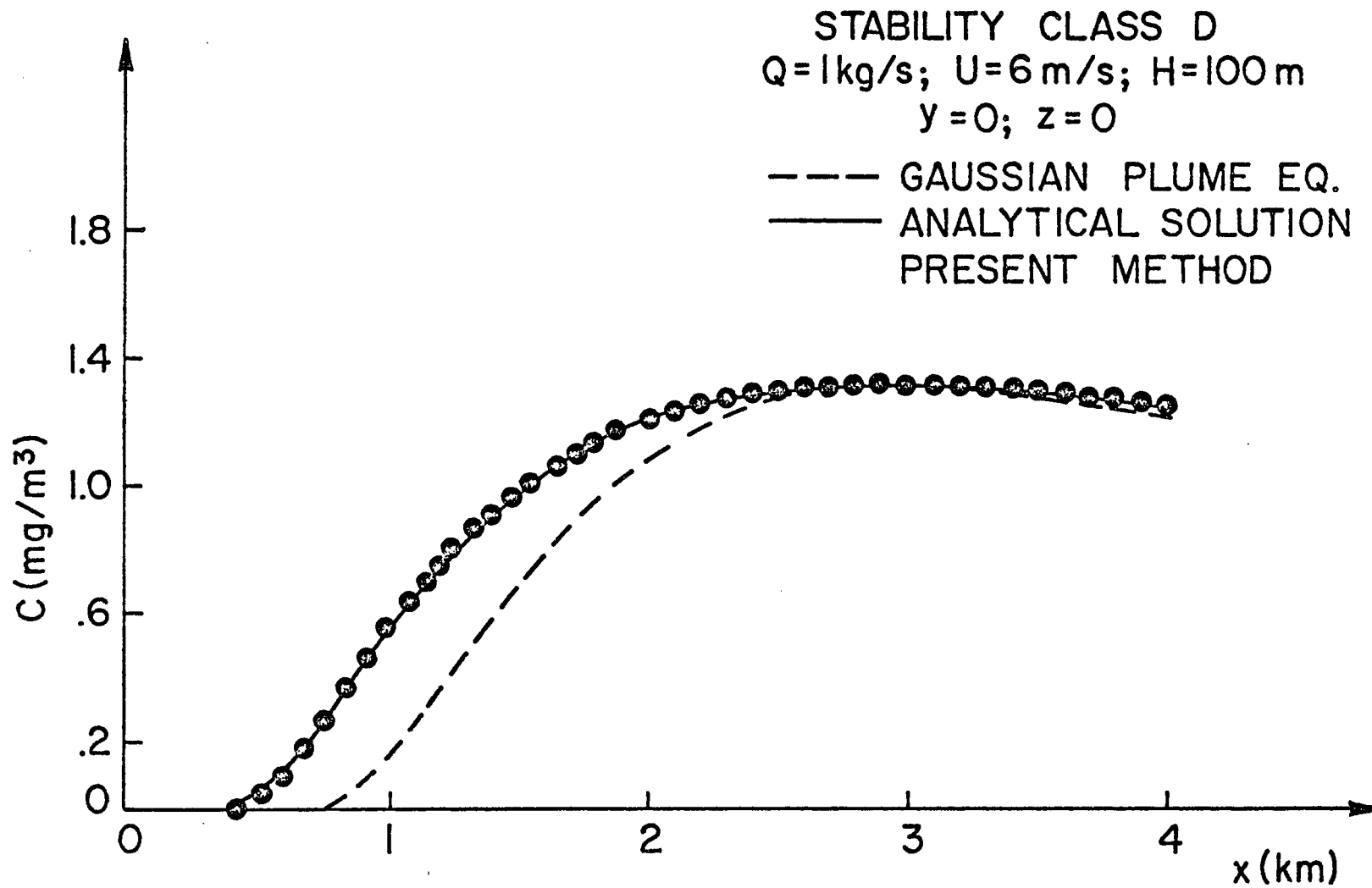


FIGURE 3.12 COMPARISON OF DOWNWIND CONCENTRATION DISTRIBUTION AT GROUND LEVEL WITH ANALYTICAL SOLUTION AND GAUSSIAN PLUME EQUATION - STABILITY CLASS D

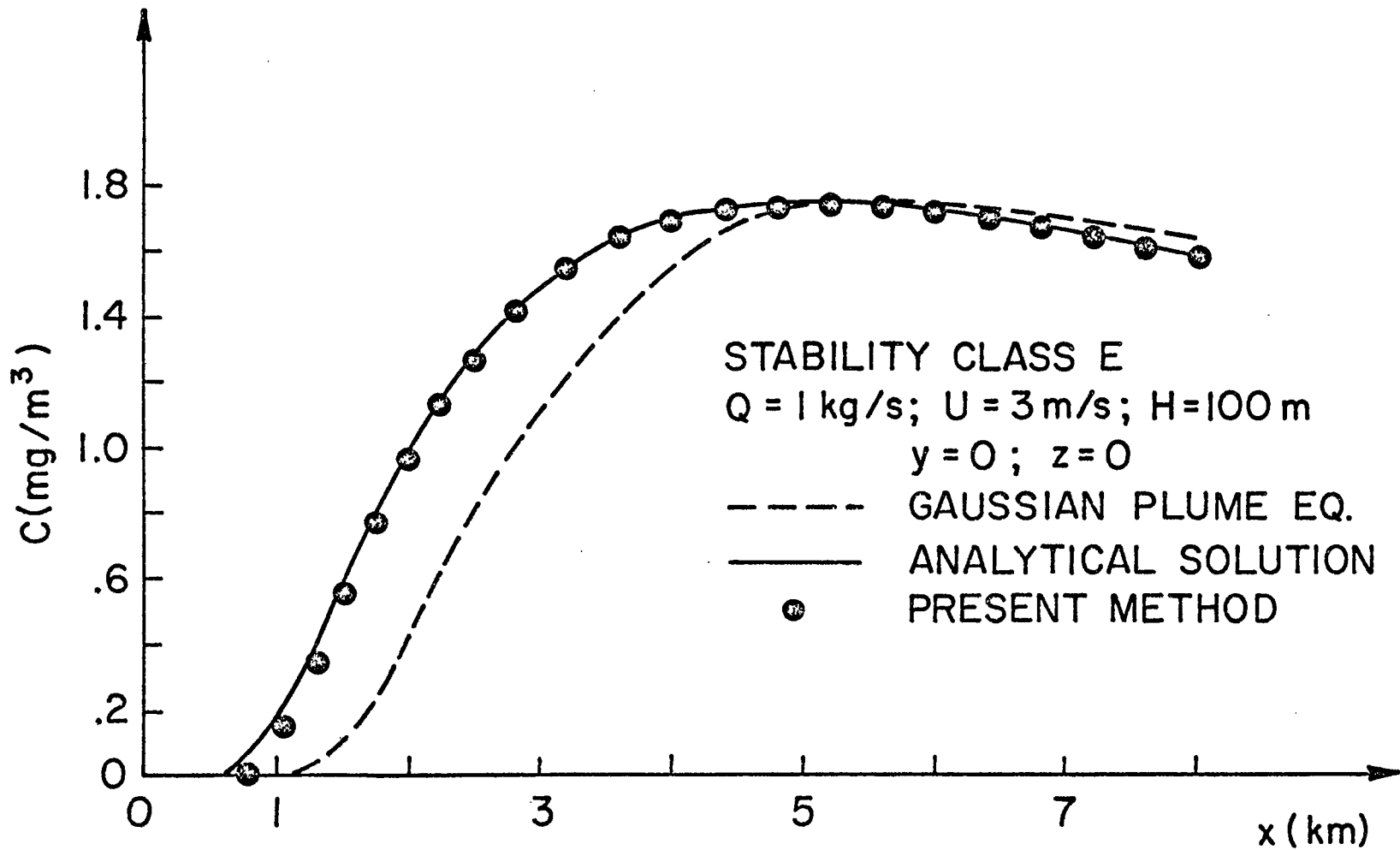


FIGURE 3.13 COMPARISON OF DOWNWIND CONCENTRATION DISTRIBUTION AT GROUND LEVEL WITH ANALYTICAL SOLUTION AND GAUSSIAN PLUME EQUATION - STABILITY CLASS E

STABILITY CLASS F  
 $Q=1\text{ kg/s}; U=2\text{ m/s}; H=100\text{ m}$   
 $y=0; z=0$

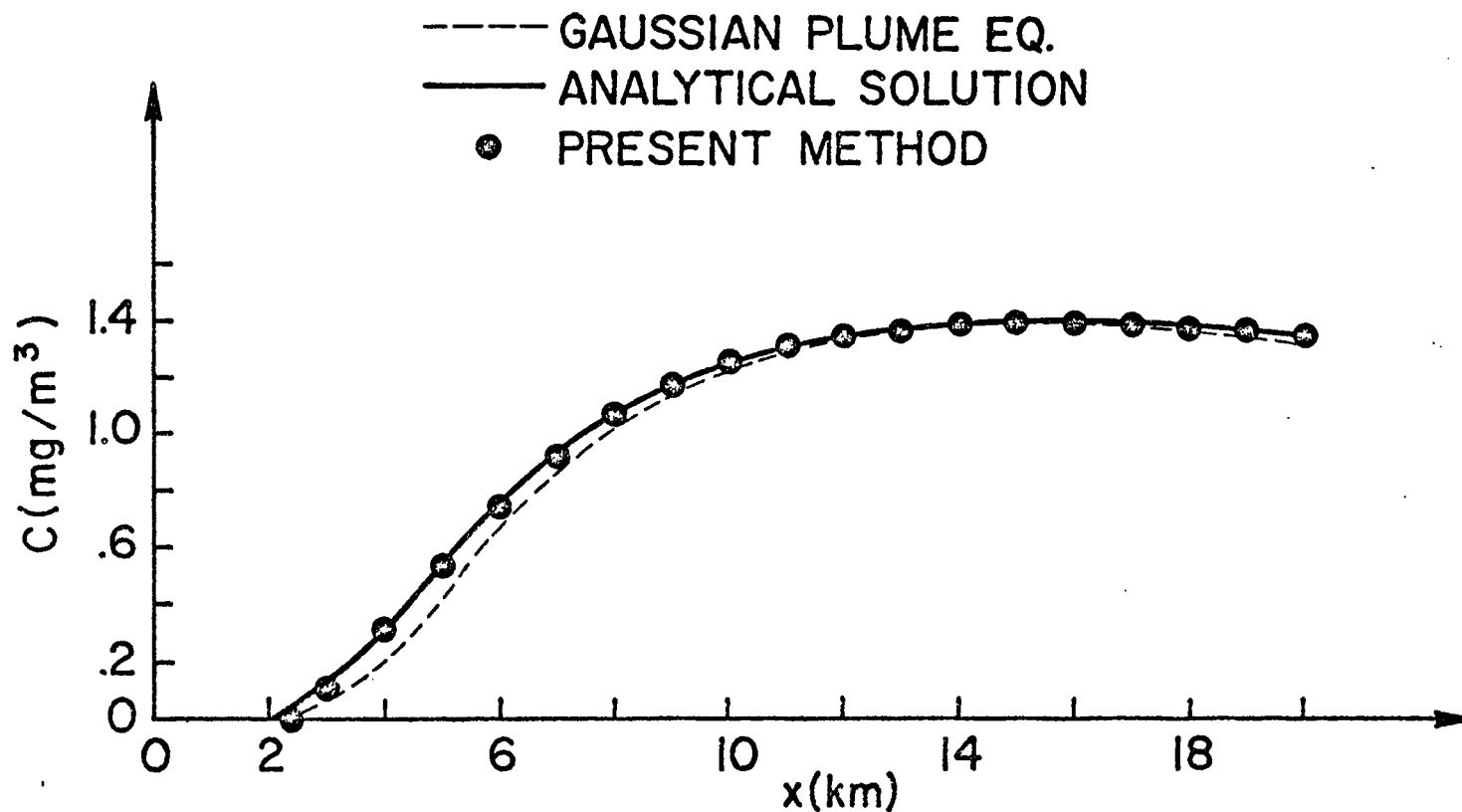


FIGURE 3.14 COMPARISON OF DOWNWIND CONCENTRATION DISTRIBUTION AT GROUND LEVEL WITH ANALYTICAL SOLUTION AND GAUSSIAN PLUME EQUATION - STABILITY CLASS F

plume equation predictions. This is due to several reasons. The Gaussian plume equation corresponds to the solution of a simplified continuity equation assuming Gaussian distribution for the plume spread. It is a statistical method that makes use of Taylor's theorem [17] for the standard deviation, a concept which is not applied to the present technique. Furthermore the Gaussian parameters  $\sigma_y$  and  $\sigma_z$ , made functions of travelled downwind distance, were obtained and adjusted from the Project Prairie Grass field data [1,2,10] which involved a small region of interest. The pollutant was emitted at 50 cm above the ground, and most samplers were placed at 1.5 m of elevation and along semicircular arcs from 50 to 800 meters from the source. The phenomena that occur in the lower layers of the atmosphere, such as wind shear, deposition, reflection, removal, etc., and the corresponding solution should be used with caution to represent most situations. Observation of Figures 3.9 through 3.14 confirms this analysis in the sense that the more unstable the atmosphere, the larger the difference between both methods.

It should be pointed out that the present mathematical technique is valid for any type of relationship between the turbulent diffusivities and meteorological and/or spatial variables. The more complicated models are compared to the Gaussian plume equation in Chapter IV. The selection of the present procedure to determine the turbulent diffusivities was done in order to present meaningful comparisons besides lack of a reasonable algorithm. The results for the constant vertical and horizontal diffusivities obtained are presented in Table 3.12.

Table 3.12 Constant Turbulent Diffusivities and  
Wind Speed used in the Present Method

Stability Class	Wind Speed (m/s)	$K_z$ ( $m^2/s$ )	$K_y$ ( $m^2/s$ )
A	2	11	18.15
B	3	10.75	25.26
C	5	10.5	30.76
D	6	5.2	46.28
E	3	1.5	30.00
F	2	.325	22.75

Some of the results for the vertical diffusivity are in agreement with the ones presented by Eschenroeder and Martinez [5].

The values for  $K_y$  presented in Table 3.12 are then used in the present work. The ones obtained for  $K_z$  are utilized in the constant portion of the trapezoidal profile, i.e., from the knee height up to an arbitrary elevation of  $(z_{\max} - 100)m$  if  $z_{\max} \geq 300m$  and there exists an inversion layer. If this is not the case, the constant value is used from the knee height all the way to the top. Eschenroeder and Martinez [5] use a knee height that varies from 25 to 75 meters. As suggested by Sutton [17], the surface boundary layer ends approximately at 50 meters, and therefore this is the elevation at which the knee height was put in the present work. The complete description for  $K_z$  as used in the present work, when applied as a variable with elevation, is shown in Figure 3.15.

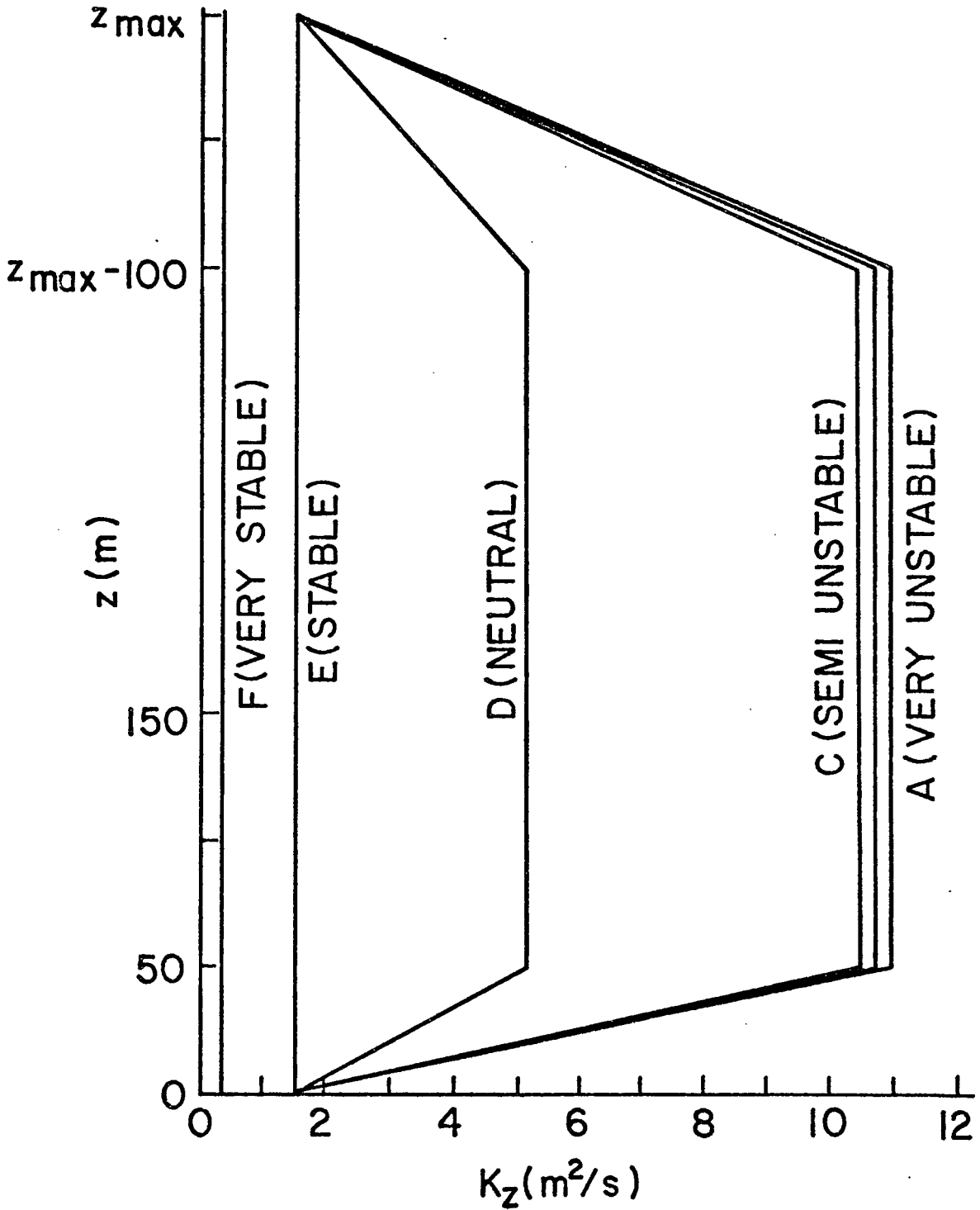


FIGURE 3.15 VERTICAL DIFFUSIVITY PROFILES IN THE PRESENT WORK

Velocity Profile

Several forms have been used to describe the one dimensional mean wind velocity [8]. They all relate  $u$  to elevation and roughness or stability classes. The power-law form is used in the present work as

$$u = u_1 \left(\frac{z}{z_1}\right)^m \tag{3.2}$$

The parameters  $u_1$ ,  $z_1$  and  $m$  should be supplied as input data by a user of the present method, although the values in Table 3.13 are given as default. Since in most cases the wind speed is known at 10 meters of elevation,  $z_1$  is equated to this value. Furthermore, the exponent of the power-law can be related to stability classes, as presented by Seinfeld [16] and shown in Table 3.13.

Table 3.13 Estimates for the Parameters  
in Equation (3.2)

Stability Class	$m$	$u_1(z_1=10m)$ (m/s)
A	.02	2
D	.14	6
F	.83	2

At some elevation  $z_G$  called the geostrophic elevation, which is determined in the following two-dimensional wind velocity description,

the mean wind velocity should become constant. Therefore, the complete specification for the one-dimensional mean wind velocity is given by

$$u = u_{10} \left(\frac{z}{10}\right)^m \quad 0 < z < z_G \quad (3.3)$$

$$u = u_{10} \left(\frac{z_G}{10}\right)^m \quad z \geq z_G \quad (3.4)$$

The value of the velocity at the ground ( $z=0$ ) is not needed in the present work since no interior collocation point will lie in a boundary, and the first and last Gaussian quadrature weights used to calculate the mass flux at any downwind position are zero.

To describe a two-dimensional wind velocity, one must analyze the phenomena that occur within the planetary boundary layer. That is, one should include the Coriolis force caused by rotation of the earth and use the basic equations of motion for two-dimensional steady mean flow, referred to axes fixed in the earth [9,13,17]:

$$f v - \frac{1}{\rho} \frac{\partial p}{\partial x} + \frac{1}{\rho} \frac{\partial}{\partial z} \tau_{zx} = 0 \quad (3.5)$$

$$-f u - \frac{1}{\rho} \frac{\partial p}{\partial y} + \frac{1}{\rho} \frac{\partial}{\partial z} \tau_{zy} = 0 \quad (3.6)$$

where  $f = 2w \sin \phi \approx 1.458 \times 10^{-4} \sin \phi \frac{1}{\text{sec}}$  and is called the Coriolis parameter,  $w$  being the angular velocity of rotation of the earth and  $\phi$  the geographical latitude.

By assuming that the eddy stresses are

$$\tau_{zx} = \rho K_z \frac{\partial u}{\partial z} \quad (3.7)$$

$$\tau_{zy} = \rho K_z \frac{\partial v}{\partial z} \quad (3.8)$$

equations (3.5) and (3.6) become

$$f v - \frac{1}{\rho} \frac{\partial p}{\partial x} + \frac{\partial}{\partial z} \left( K \frac{\partial u}{\partial z} \right) = 0 \quad (3.9)$$

$$-f u - \frac{1}{\rho} \frac{\partial p}{\partial y} + \frac{\partial}{\partial z} \left( K \frac{\partial v}{\partial z} \right) = 0 \quad (3.10)$$

If the x-direction is oriented parallel to the isobars, i.e.  $\frac{\partial p}{\partial x} = 0$  and knowing that the free-stream velocity, called geostrophic wind  $u_G$  blows along the isobars, the velocity component perpendicular to the isobars  $v$  vanishes at the height  $z_G$ . Therefore, from equation (3.10)

$$f u_G = - \frac{1}{\rho} \frac{\partial p}{\partial y} \quad (3.11)$$

and equations (3.9) and (3.10) have become independent of pressure.

The Coriolis effect can usually be neglected near the surface. If this is assumed to apply from the ground up to the knee height  $\Delta$ , equation (3.9) and (3.10) can be used to describe the velocity profile in the region where  $K_z$  is constant. The solution of the equations of motion is given by:

$$u = u_G (1 - e^{-az} \cos az) \quad (3.12)$$

$$v = u_G e^{-az} \sin az \tag{3.13}$$

where

$$a = \left(\frac{f}{2K_z}\right)^{\frac{1}{2}} \tag{3.14}$$

The geostrophic elevation, also used for one-dimensional velocity profiles as previously discussed, can be obtained by substituting  $v=0$  into equation (3.13), i.e.,

$$z_G = \frac{\pi}{a} \tag{3.15}$$

For a Coriolis parameter of  $f=10^{-4} \text{ sec}^{-1}$ , which corresponds to approximately a geographical latitude of  $40^\circ$  that occurs in the middle of the U.S., and the constant values of  $K_z$  given by Table 3.12, the resulting geostrophic elevations are presented in Table 3.14.

Table 3.14 Geostrophic Elevations used  
in the Present Work

Stability Class	$z_G$ (m)
A	1475
B	1455
C	1440
D	1015
E	545
F	255

For the surface boundary layer, between the ground and the knee height  $\Delta$ , the power-law form can be used for the component of the velocity in the x-direction. Since the Coriolis effect is neglected in this portion of the atmosphere, the direction of the velocity will be assumed constant and equal to the value that occurs at  $\Delta=50\text{m}$ , i.e., dependent on the stability class. These values are presented in Table 3.15.

Table 3.15 Angle between Wind Velocity and Geostrophic Direction for the Surface Boundary Layer

Stability Class	$\alpha(^{\circ})$
A	42
B	42
C	42
D	41
E	37
F	29

The results shown in Tables 3.14 and 3.15 are in agreement with the values suggested by Sutton [17].

The complete description for the two-dimensional wind velocity can be expressed then by the following algorithm:

$$u = u_{50}^c \left(\frac{z}{10}\right)^m \quad (3.16)$$

$$v = (\tan \alpha)u \quad (3.17)$$

$$u = u_G(1 - e^{-az} \cos az) \quad \text{for } z > \Delta \quad (3.18)$$

$$v = u_G e^{-az} \sin az \quad \text{for } \Delta < z < z_G \quad (3.19)$$

$$v = 0 \quad \text{for } z \geq z_G \quad (3.20)$$

where

$$u_{50}^c = u_G \left(\frac{10}{50}\right)^m (1 - e^{-50a} \cos 50a) \quad (3.21)$$

is required for a continuous velocity profile.

## CHAPTER IV

### PRESENTATION AND ANALYSIS OF RESULTS

The Eulerian approach was validated by Fleischer [8] through comparisons between calculated concentration distributions and the few available experimental data. The present models have been validated by comparing the calculated results with existing analytical solutions. Therefore, the main objective of the present work is to obtain concentration distributions for air pollution problems that are either difficult to simulate through conventional techniques, such as finite-differences, or which have never been solved or presented in the literature.

#### Two-Dimensional Models

The first problem that was simulated includes pollutant removal from the atmosphere, represented by a simplified first order chemical reaction model, and applied to the continuous ground level line source case. The value of  $1.67 \times 10^{-3}$  per minute or 10% loss per hour was used as the reaction rate constant. The results, obtained in 27 seconds of CPU time, are presented in Figure 4.1. They indeed show that there is no need to include chemical reactions to a steady state model since the concentration values can be calculated by multiplying the analytical solution to the factor  $\exp(-\frac{k_1 x}{u})$ . This factor is the result of the chemical reaction model when solved by itself.

The other two-dimensional model simulated included an inversion layer at 250 meters for a continuous elevated line source case, with an

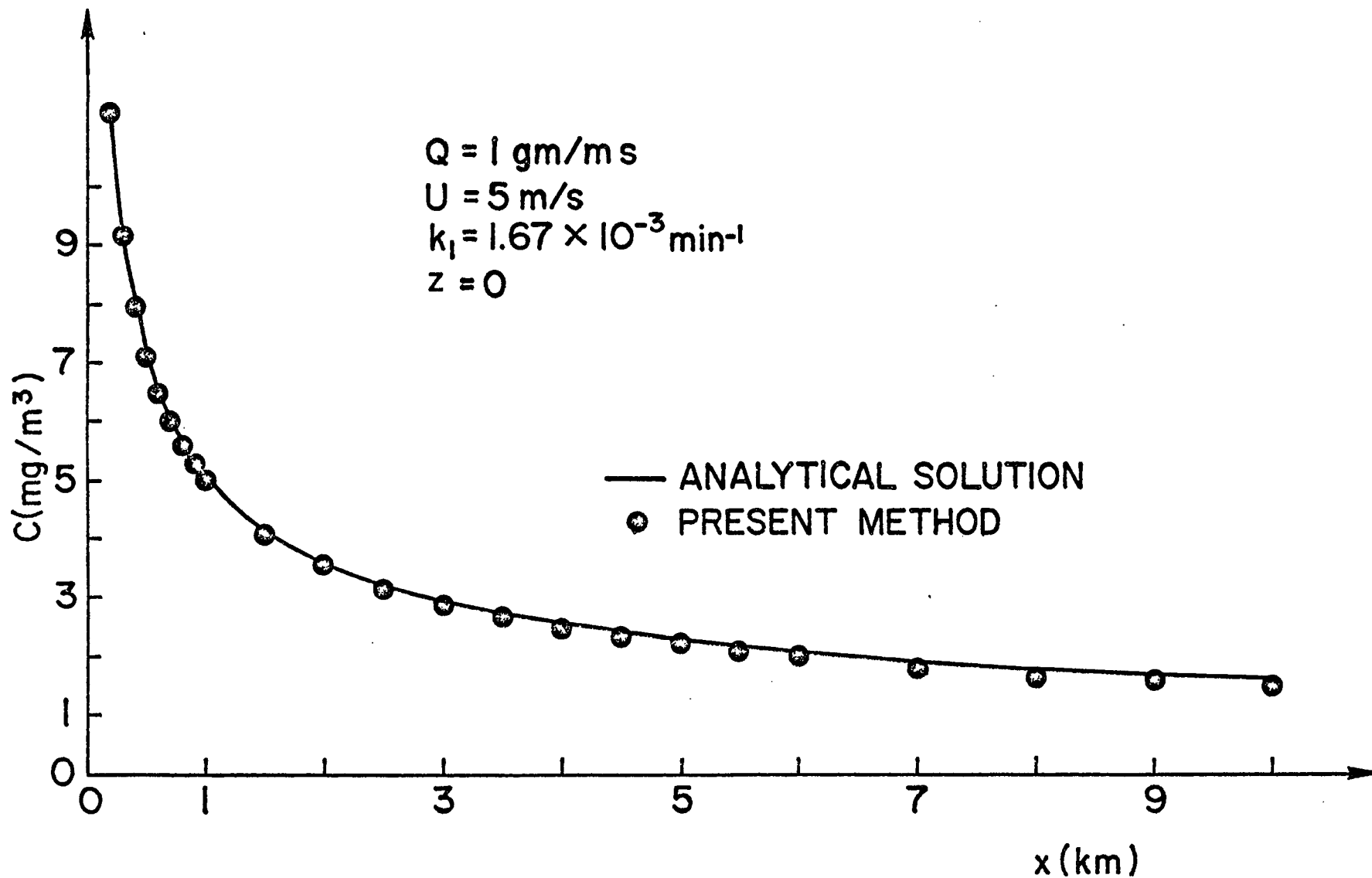


FIGURE 4.1 DOWNWIND CONCENTRATION DISTRIBUTION AT GROUND LEVEL - TWO DIMENSIONAL MODEL WITH CHEMICAL REACTION

effective emission height of 200 meters. The calculated and analytical concentration distributions are shown in Figure 4.2.

The results obtained from the present work in 117 seconds of CPU time predict that the plume reaches the inversion layer at a downwind distance of 300 m from the source. An inversion layer means that all the material reaching that elevation is reflected down. It can be observed that the inversion layer starts to affect the concentration at the effective emission height at about 1.5 km from the source. Since the analytical solution does not take into account the inversion layer, the calculated results are higher than the analytical solution for downwind distances over 1.5 km.

### Three-Dimensional Models

There are an infinite number of situations that could be simulated by the three-dimensional models. The most representative have been selected and are presented next.

The first interesting problem is to compare the effect of having a one-dimensional wind velocity profile as a function of elevation with respect to a constant wind speed. This comparison, together with the concentration distribution obtained for the case of wind velocity and vertical turbulent diffusivity variable with elevation is shown in Figures 4.3 through 4.5. The results were obtained for the three most important stability classes, A, D, and F in approximately 260, 240, and 220 seconds of CPU time, respectively.

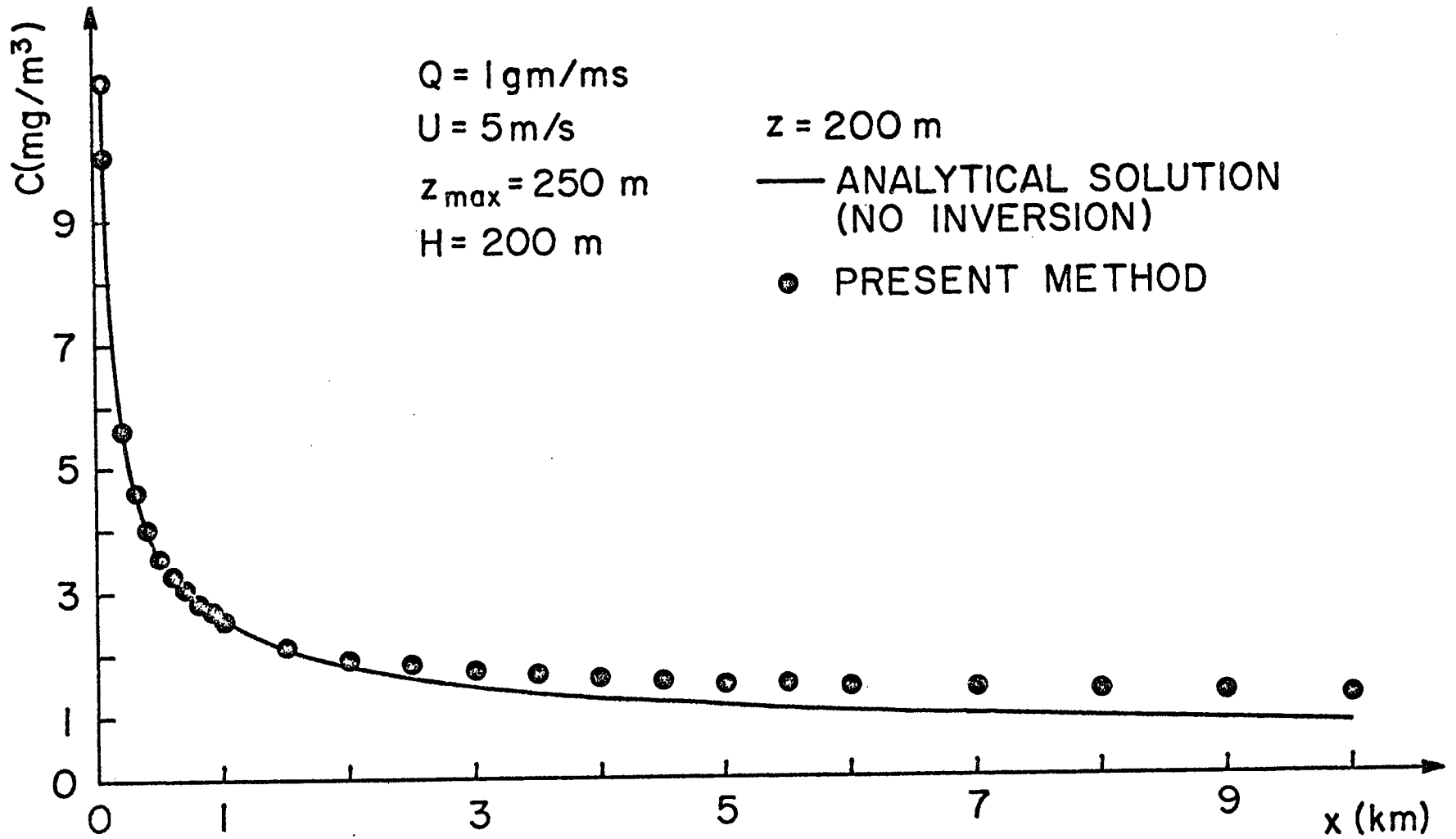


FIGURE 4.2 DOWNWIND CONCENTRATION DISTRIBUTION AT THE EFFECTIVE EMISSION HEIGHT - TWO DIMENSIONAL MODEL WITH INVERSION LAYER

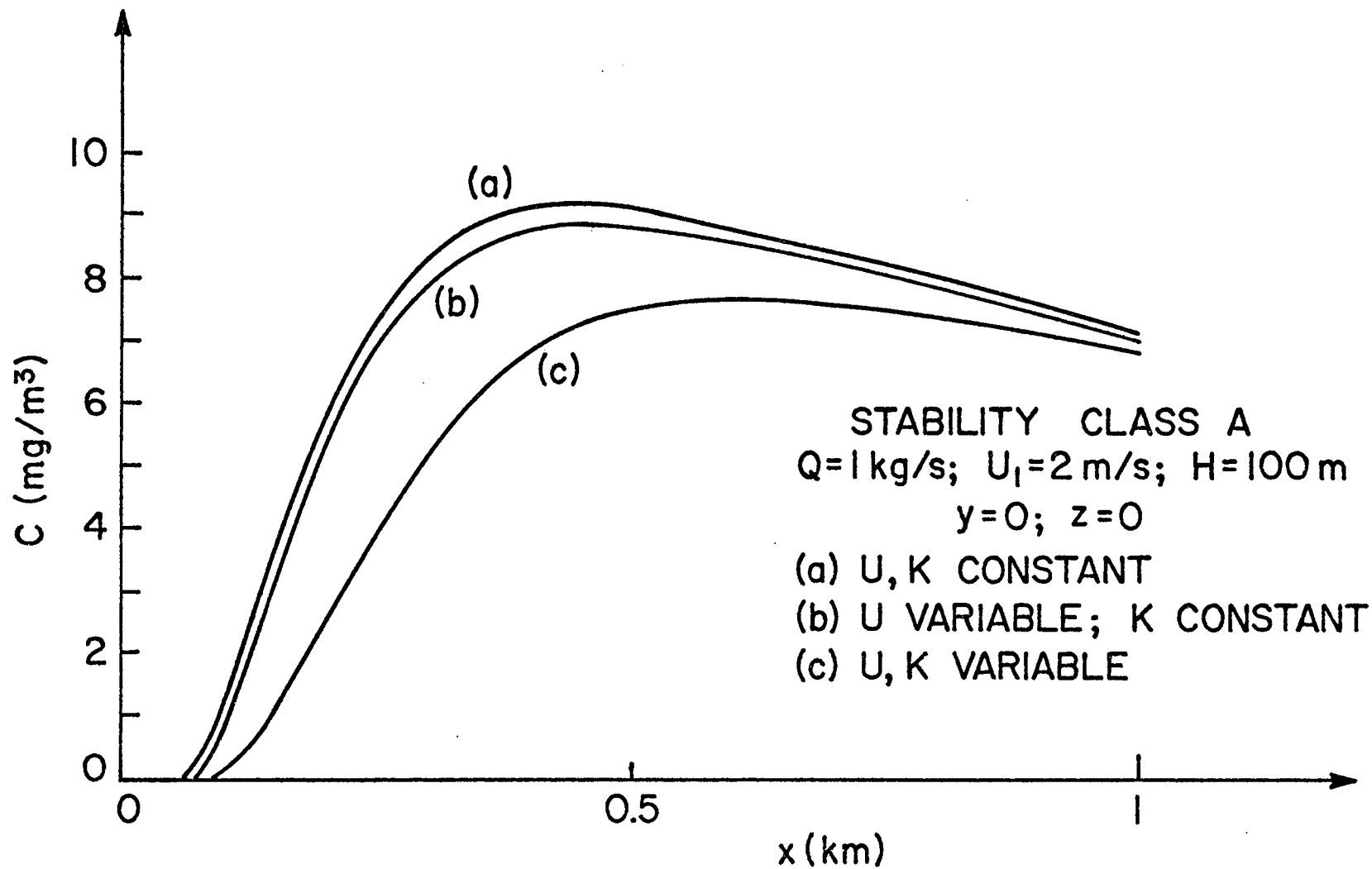


FIGURE 4.3 DOWNWIND CONCENTRATION DISTRIBUTION AT GROUND LEVEL - THREE DIMENSIONAL MODELS - STABILITY CLASS A.

STABILITY CLASS D  
 $Q=1 \text{ kg/s}; U_1=6 \text{ m/s}; H=100 \text{ m}$   
 $y=0; z=0$

(a) U, K CONSTANT  
(b) U VARIABLE; K CONSTANT  
(c) U, K VARIABLE

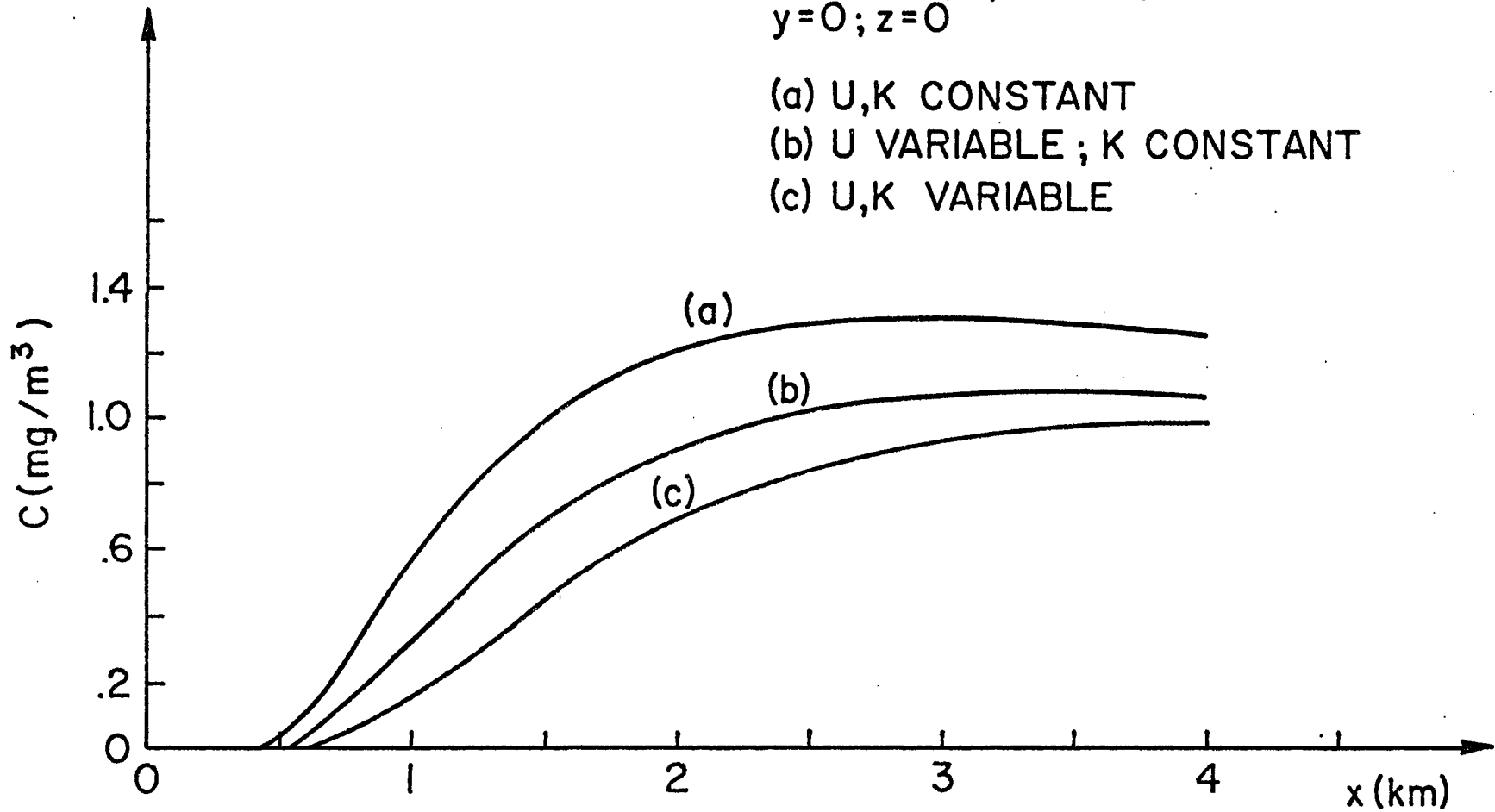


FIGURE 4.4 DOWNWIND CONCENTRATION DISTRIBUTION AT GROUND LEVEL - THREE DIMENSIONAL MODELS - STABILITY CLASS D

STABILITY CLASS F

$Q=1\text{kg/s}$ ;  $U_1=2\text{m/s}$ ;  $H=100\text{m}$

$y=0$ ;  $z=0$

(a) U, K CONSTANT

(b) U VARIABLE; K CONSTANT

(c) U, K VARIABLE

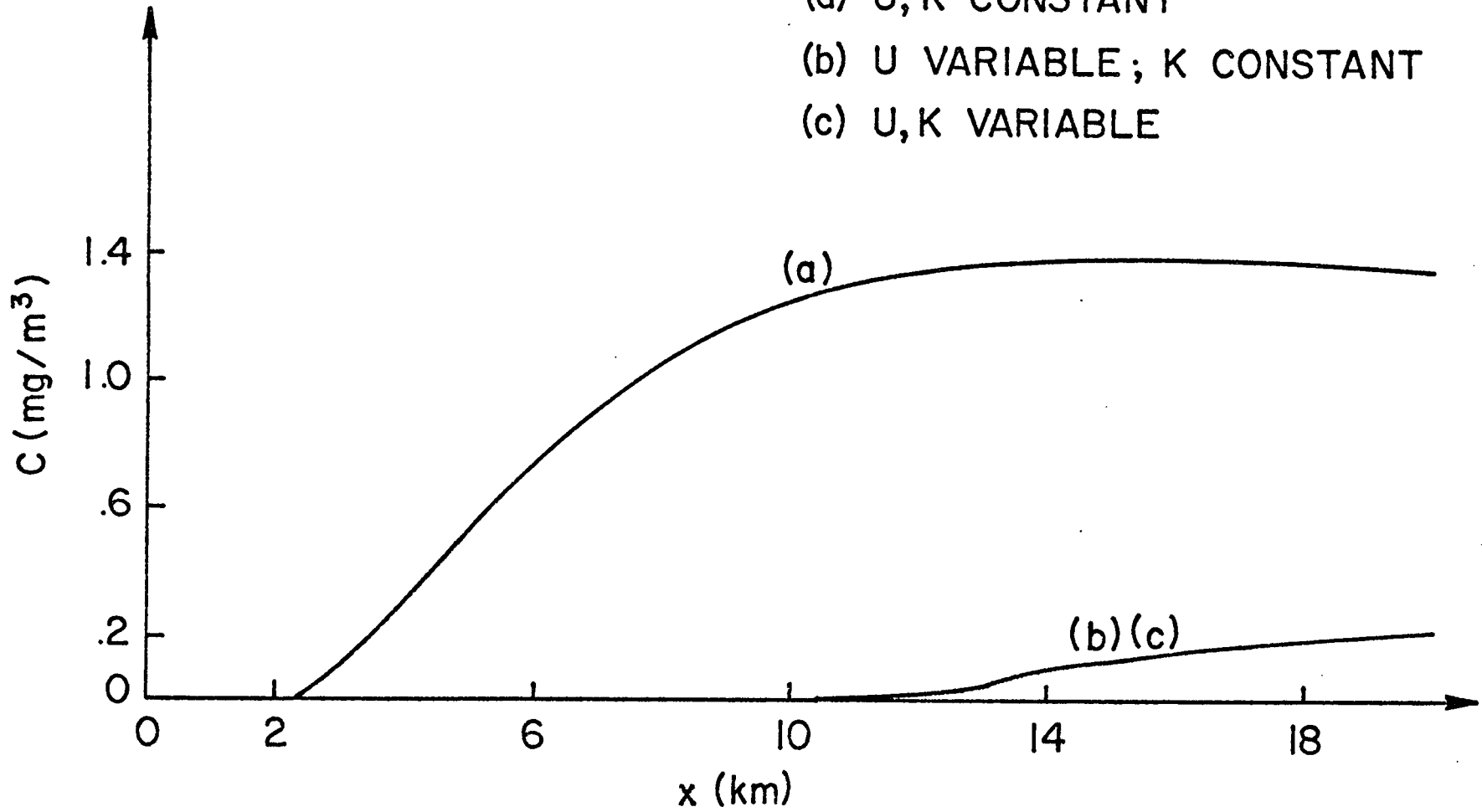


FIGURE 4.5 DOWNWIND CONCENTRATION DISTRIBUTION AT GROUND LEVEL - THREE DIMENSIONAL MODELS - STABILITY CLASS F

The wind speed at 10 meters,  $u_1$  in equation (3.2), was equated to the wind speed for the constant velocity case. This means that the velocity below 10 m is lower than the constant wind speed, and that above this elevation is higher than  $u_1$ . The results, as expected, show a maximum ground level concentration lower than for the constant  $u$  and  $K_z$  model, and therefore at a larger distance downwind from the source.

The results also show the influence of the power-law exponent and the description of the variable vertical turbulent diffusivity in the ground level concentration distribution. A small value for  $m$  means that the deviation of the variable mean wind velocity with respect to the constant profile is negligible as shown by cases (a) and (b) in Figure 4.3. As  $m$  increases, the deviation from case (a) increases such that for the extreme case (very stable atmosphere, Figure 4.5) where  $m=.83$  (Table 3.13) the concentration distribution is significantly different.

The description for the variable vertical turbulent diffusivity involves a smaller  $K_z$ , from the ground up to the knee height, when compared to the corresponding constant value. As the instability of the atmosphere increases, this constant  $K_z$  increases and the difference between cases (b) and (c) in Figures 4.3 and 4.4 is magnified. An extreme case is again a stability class F (Figure 4.5), where no difference exists between variable and constant turbulent diffusivity, and therefore cases (b) and (c) lie in the same curve,

The Gaussian plume equation is the most widely used model in air pollution since the concentration can be obtained in a very simple way. Figure 4.6, extracted from Turner [18], shows the ease with which the ground

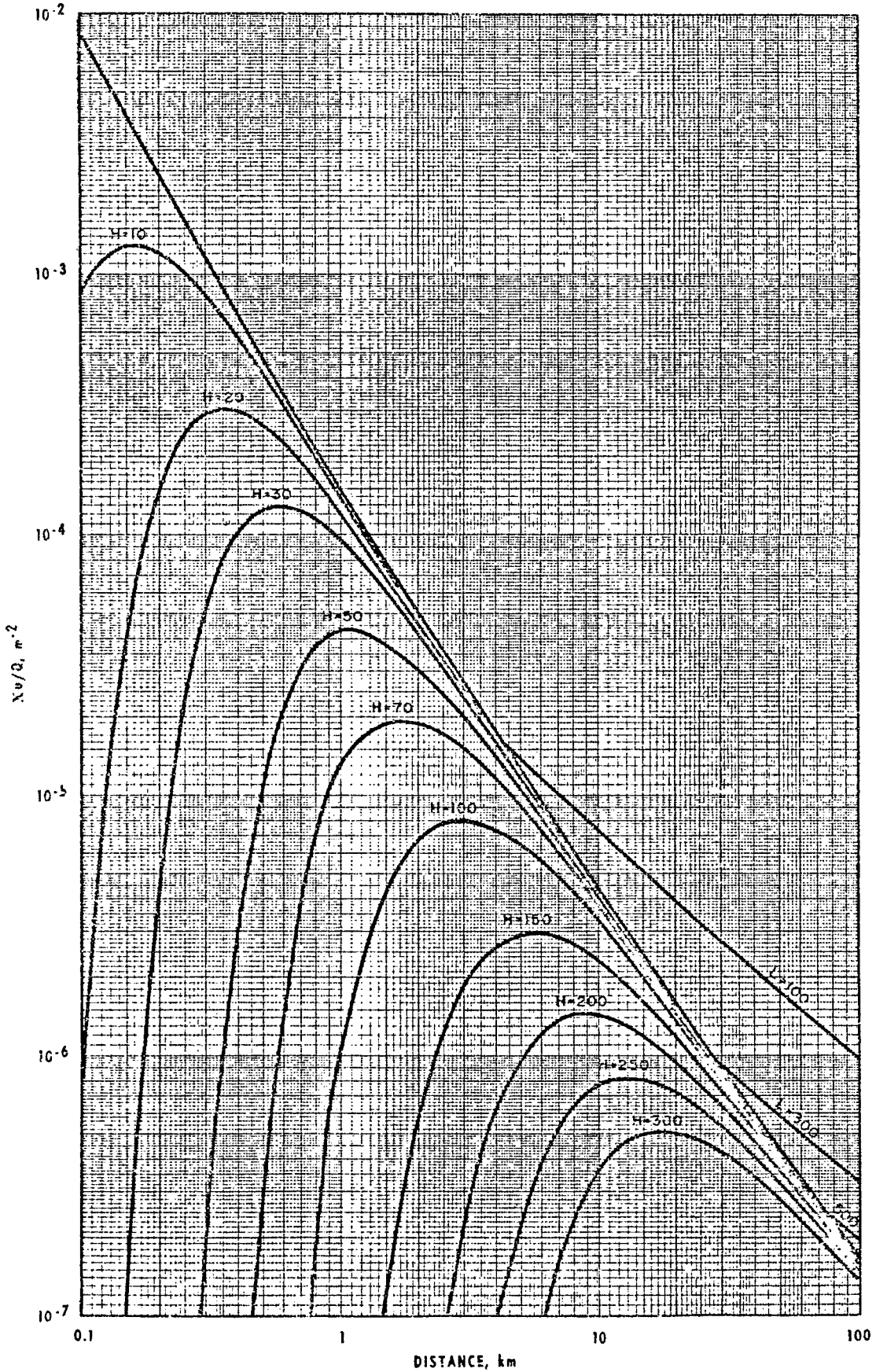


FIGURE 4.6  $\frac{XU}{Q}$  WITH DOWNWIND DISTANCE FOR VARIOUS HEIGHTS OF EMISSION - GAUSSIAN PLUME EQUATION

level concentration can be obtained for any emission rate  $Q$ , wind speed  $U$ , effective emission height  $H$ , and stability class. Unfortunately, this model should be used only for homogeneous and stationary conditions, with all the restrictions discussed in Chapter III.

A graphical method, similar to the one discussed above, is developed in the present work for estimation of ground level concentration for the several Pasquill-Gifford stability classes. The present computed results were obtained for a wind velocity profile which obeys equations (3.3) and (3.4), a vertical turbulent diffusivity represented by Figure 3.15, and  $K_y$  given by Table 3.12.

The main difference of the present model and the Gaussian plume equation is that the position of the maximum ground level concentration depends on the wind speed, as it should. Therefore, the variable plotted in the abscissa is the time of flight  $\frac{x}{u_1}$  and not  $x$ .

The results, for stability class D, are shown in Figure 4.7.

The next more complex three-dimensional model which is solved in the present work incorporates a two-dimensional wind velocity profile. In order to validate the present results, a constant wind direction case was solved first, such that an analytical solution could be available.

A continuous point source emitting 1 kg/s of material at an effective emission height of 100 m into a neutral atmosphere (constant diffusivities) with a constant axial velocity of 6 m/s and a lateral wind speed of 3 m/s in the negative  $y$ -direction was simulated using the present technique. The results are compared to the analytical solution with a constant wind speed of the resultant velocity, i.e., 6.71 m/s. The concentration

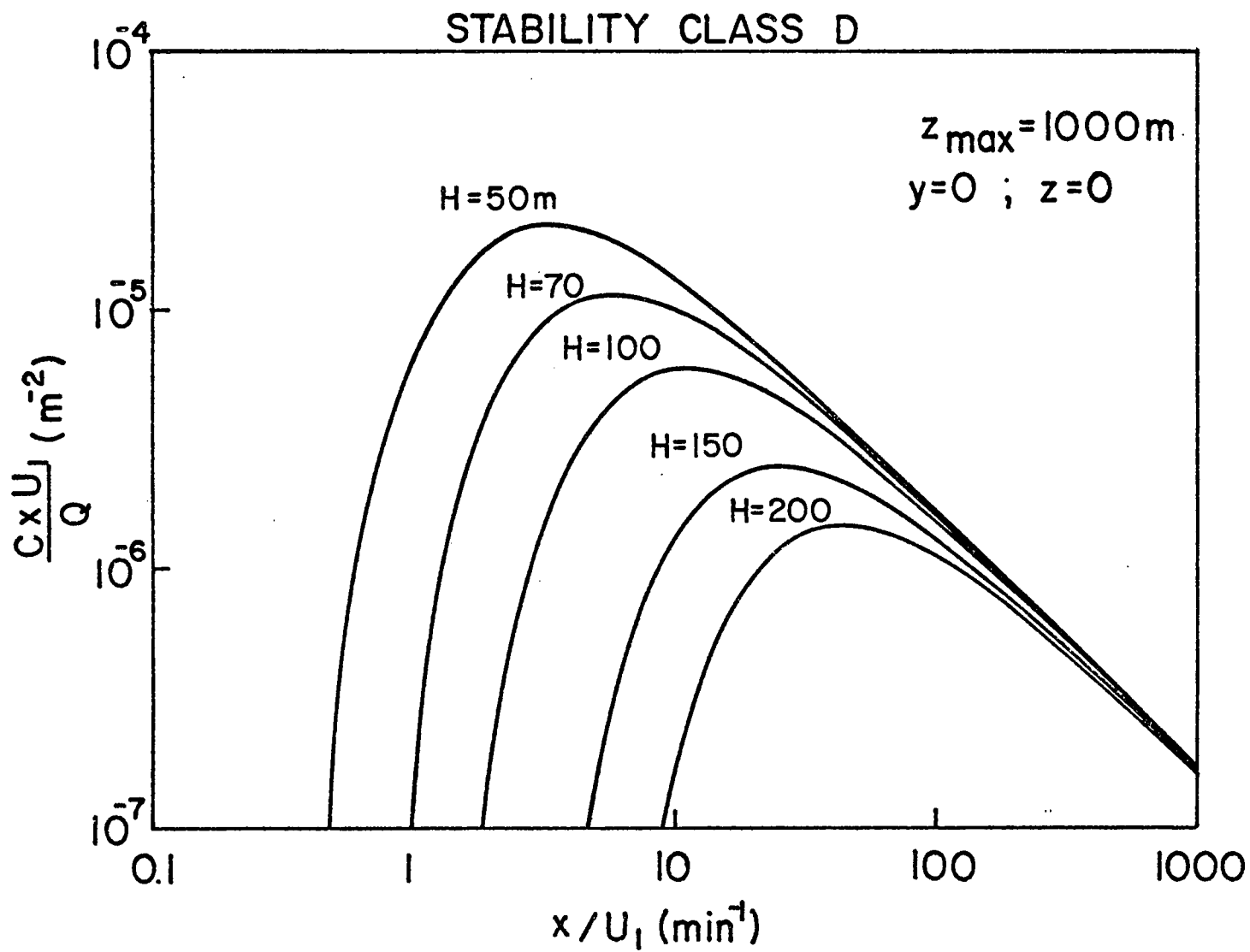


FIGURE 4.7  $\frac{C_{u_1}}{Q}$  WITH TRAVEL TIME FOR VARIOUS HEIGHTS OF EMISSION - PRESENT WORK

distribution at ground level and at the effective emission height are presented in Figure 4.8. The agreement is excellent. It should be pointed out that again the concentration at  $z=100$  m is obtained through two-dimensional Lagrangian interpolation, and therefore shows the overall error involved in the computed results. The computer time was 800 seconds.

With the present work validated for the case of a two-dimensional wind velocity profile, the next step was to solve the problem with the Coriolis effect. The wind velocity was represented by equations (3.16) through (3.21) and the vertical diffusivity profile by Figure 3.15. The constant horizontal diffusivity was given by Table 3.12. The geostrophic velocity was taken to be the same as  $u_G$  given by the power-law equation, with  $u_1$  for a stability class D assumed to be equal to 6 m/s. A value of  $u_G = 11.45$  m/s was calculated for these conditions.

Isopleths of  $3 \text{ mg/m}^3$  for the present model and the constant wind speed and turbulent diffusivity are shown in Figure 4.9. Both cases are quite different, as expected. The centerline for case (a) occurs at  $y=0$  while for case (b) is skewed to the left. Furthermore, the areas are different but the mass flux is the same, i.e., 1 kg/s. The reason being that in general, the concentrations for the constant case are higher than for the Coriolis model, e.g., the maximum concentrations found were .  $5.36 \text{ mg/m}^3$  and  $5.00 \text{ mg/m}^3$ , respectively. The peculiar form of the curve at the left, i.e., more voluminous is due to the effect that the isopleth has reached the ground and the material is being reflected upwards.

Figure 4.10 shows the comparison of the Coriolis model to the Gaussian plume equation for the ground level concentration at both

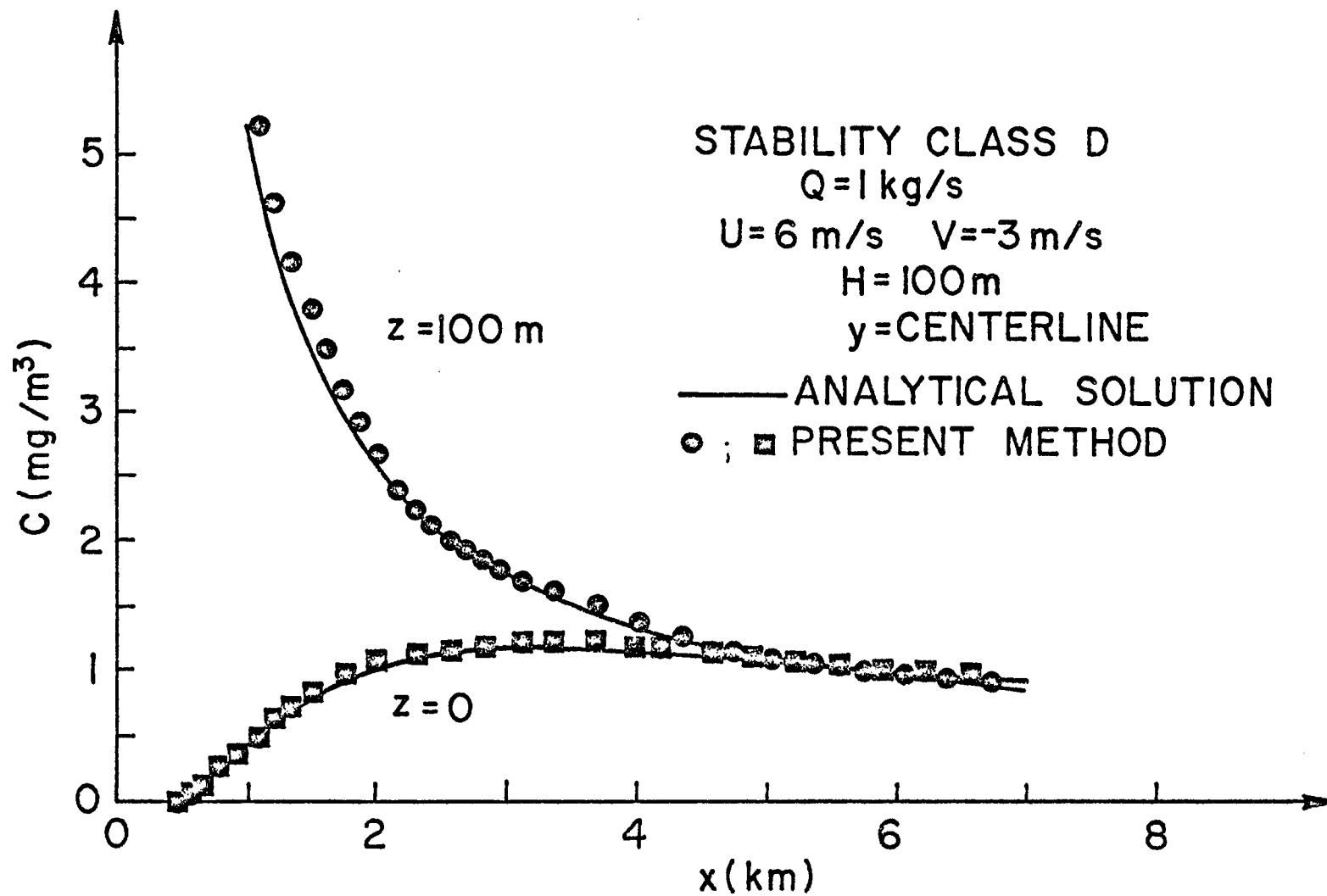


FIGURE 4.8 COMPARISON OF DOWNWIND CONCENTRATION DISTRIBUTION WITH ANALYTICAL SOLUTION - TWO DIMENSIONAL WIND VELOCITY

STABILITY CLASS D

$Q=1 \text{ kg/s}$ ;  $H=100 \text{ m}$

$x=960 \text{ m}$ ;  $C=3 \text{ mg/m}^3$

(a) U, K CONSTANT

(b) PRESENT METHOD-CORIOLIS

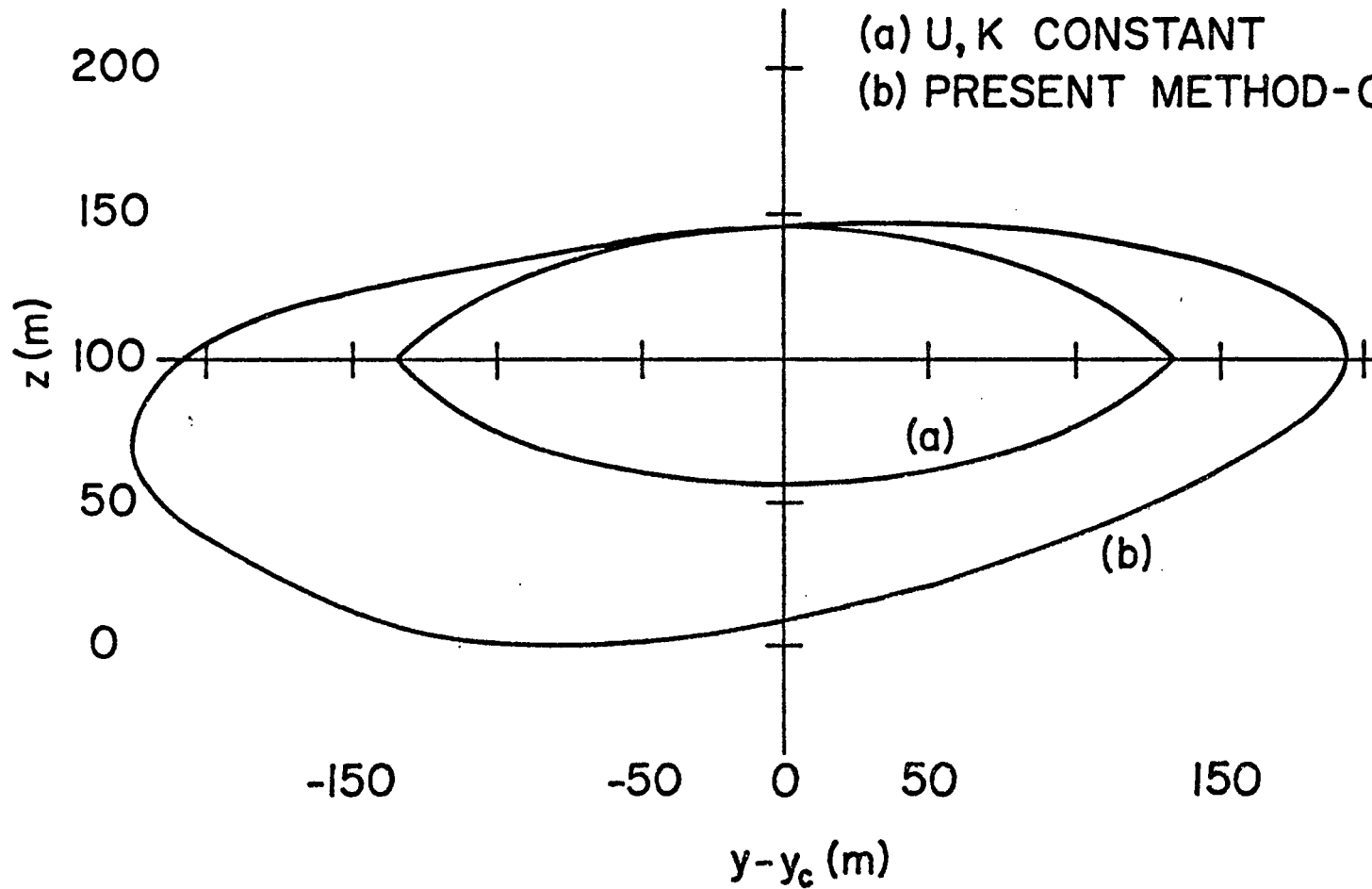


FIGURE 4.9 ISOPLETHS AT A CONSTANT  $x$  - THREE DIMENSIONAL MODELS

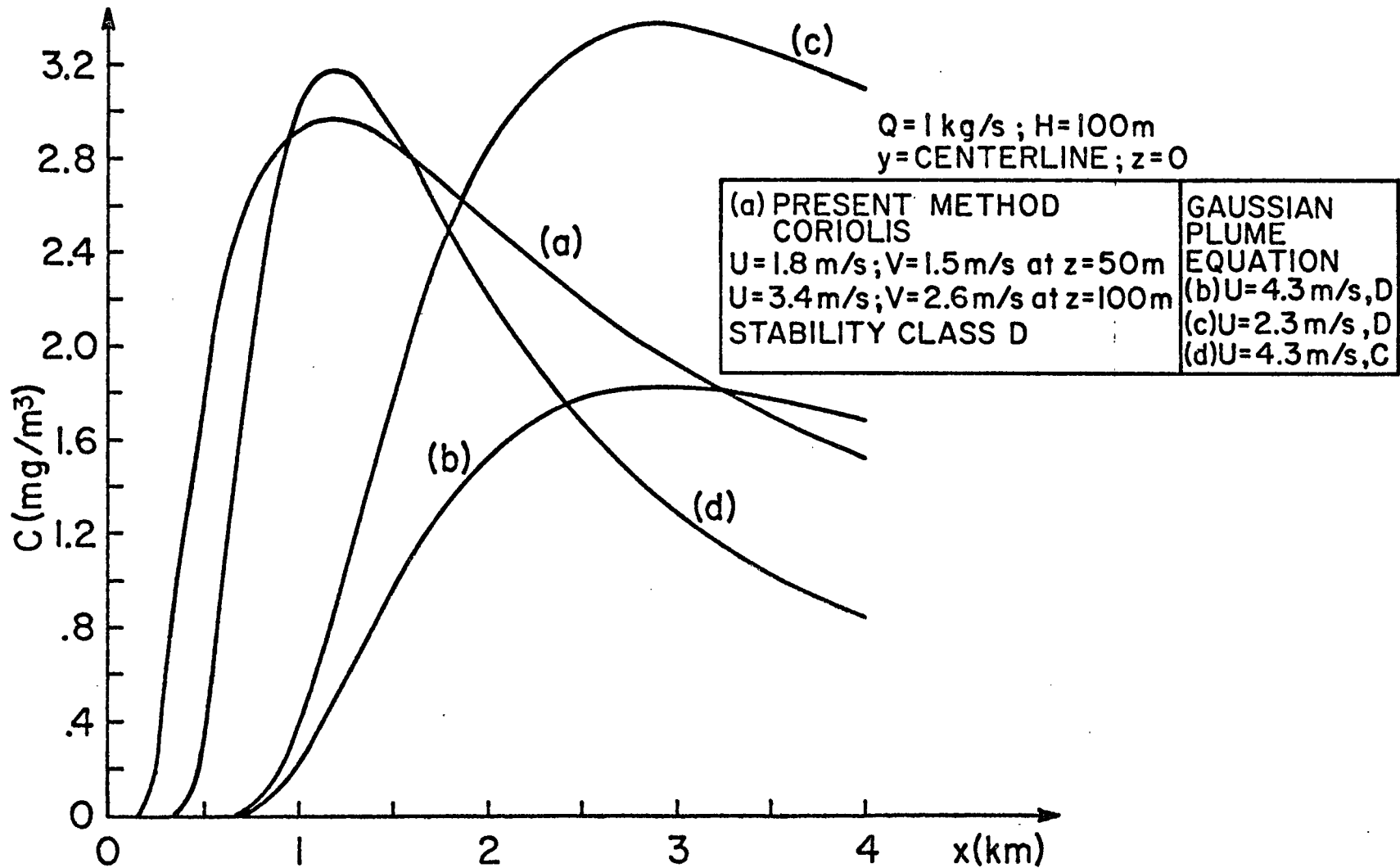


FIGURE 4.10 DOWNWIND CONCENTRATION DISTRIBUTION AT GROUND LEVEL - CORIOLIS EFFECT VS GAUSSIAN PLUME EQUATION

centerlines. Cases (b) and (c) were obtained for a wind speed equal to the resultant of the velocity for the present model at the effective emission height, 100 m, and at an elevation of 50 meters, respectively. The three cases were obtained for neutral stability, and the results are quite different.

Since the wind speed used for case (b) is 4.3 m/s, it would be more appropriate to obtain the solution using the Gaussian plume equation for a stability class C. This concentration distribution is also shown in Figure 4.10 as case (d), and the comparison to the present model is closer, at least in the downwind position and the value of the maximum ground level concentration. For the wind speed of 2.3 m/s no stability class was found that would give a Gaussian plume equation solution closer to the present model.

It should be noted, as has extensively been done before, that less rigorous mathematical parameters can provide a decrease in the computational time. The Coriolis model case (a) was obtained in 880 seconds of CPU time. A similar problem was simulated next, but the mathematical parameter  $r$  was changed to 0.1. A comparison of the mass fluxes at several downwind positions is shown in Table 4.1.

Table 4.1 Mass Rates at Several  
Downwind Positions - Coriolis Effect

x(m)	$Q_x$ (kg/s)	
	r = .01	r = .1
10	1.0026	1.0031
20	1.0011	1.0108
50	1.0003	.9990
100	1.0067	.9759
200	1.0054	.9881
500	.9976	.9902
960	.9992	1.0348
2000	.9874	.9973
4000	.9846	.9768

It can be observed that the results for the case with  $r = 0.1$  ( $Q=1$  kg/s) are still adequate as compared to the simulation using  $r = 0.01$ , but the main difference lies in the computer time involved of 580 seconds.

## CHAPTER V

### SUMMARY OF RESULTS, CONCLUSIONS AND RECOMMENDATIONS

Turbulent diffusion from single ground level or elevated line or point sources in the atmosphere was successfully simulated using the K-theory and solved by spline orthogonal collocation. Improved mathematical techniques were used to describe the plume, which is generated at the source, by means of moving boundary conditions. This implies that the edges of the plume are known at any downwind distance from the source, and the concentration distribution is obtained only within the region of interest, i.e., in the plume. Although the solution was calculated at the orthogonal collocation points, accurate two-dimensional Lagrangian interpolation was used to obtain the concentration at other desired positions such as the effective emission height.

Several techniques for solving the resulting system of first-order ordinary differential equations with respect to the along wind direction were tested in the present work. An eigenvalue method was selected for the two-dimensional models, and the three-dimensional models were solved by a fourth-order Runge-Kutta method.

The present work was used to simulate steady state air pollution models. Mathematical parameters, inherent of the techniques developed, were determined through parametric studies. The values assigned for these mathematical parameters should remain unchanged if the present work is used for other problem specifications.

Empirical equations were used to describe the mean wind velocity

and the turbulent diffusivities. Several meteorological parameters were included in these equations so that many atmospheric conditions can be simulated by the present technique. A two-dimensional wind velocity profile, including the Coriolis effect, obtained by solving the equations of motion analytically, was incorporated in the three-dimensional air pollution model.

Excellent agreement was observed between the calculated concentration distribution and the analytical solution for cases where the latter exists. The present model had also an excellent response to variations in atmospheric conditions. This was obtained by simulating hypothetical cases. In addition to the concentration distribution, the flux across any plane normal to the along wind direction was calculated. Its comparison to the constant emission rate (steady-state models, no removal processes) was excellent. All the results were obtained with a very reasonable amount of computer time. This computational time could have been decreased by changing some mathematical parameters, but it was decided not to do so in order to obtain very accurate results. A graphical method for presenting computed results was developed to permit estimation of ground level concentration for any source emission rate, wind velocity and effective emission height for neutral stability.

Several extensions to the present technique should be investigated and are recommended next. They cover a wide spectrum of air pollution problems and do not involve significant changes to the present method.

1) Solution of pollutant dispersion from multiple sources in the atmosphere can be obtained by superposition of the effects of the individual plumes [4]. This involves only bookkeeping of the solutions in the computer. The present method required approximately 20 and 30K of storage for the two and three-dimensional models, respectively, leaving enough room for solving this type of problem. It should be pointed out that the CPU time would be the one used in the present work multiplied by the number of sources involved. If the number of sources is very large it might be more convenient, timewise, to treat them as area sources and use finite-difference as the numerical technique.

2) There is sometimes a need for solving air pollution models involving complex terrain such as buildings, hills, etc. The idea of a vertical moving boundary, similar to the one used in the present work, but fixed to the description of the terrain could be used to solve this type of problem.

3) Finally, unsteady-state models are of some interest in air pollution modeling. Sources with emission rates as functions of time, problems involving complex removal processes and/or meteorological parameters variable with respect to time are typical examples of situations that are represented by unsteady-state models.

An unsteady-state model was tried using the present technique. It required the solution of 800 first-order ordinary differential equations at each time-step of integration. The method was abandoned because it involved an excessive amount of CPU time.

Experimental data for time-changing emissions and also meteorological conditions are usually given in time intervals of one hour or higher. This suggests then to utilize a "quasi-steady-state" assumption. A solution using the present model could be obtained and applied to some interval of time, comparable to  $x_{\max}/u$ . Each interval could be assumed sufficiently long to permit full development of the concentration distribution at all locations. This could be a poor approximation at low wind speeds. The extreme case studied in the present work, the very stable atmosphere, involved a time interval of approximately 2 hours for the maximum downwind distance considered significant. The general unsteady-state situation could then be obtained through a sequence of steady-state intervals. In general, both the pollutant emission and the meteorological conditions could then be varied between the consecutive time periods.

Finally, air pollution models involving complex removal processes could be treated in a similar way. The chemical kinetic terms generally require smaller time steps for stability when compared to advection time steps. This suggests then to separate the solution of the removal processes from the diffusion equation for any advection time step. The present method could be used to obtain the concentration distribution for a time step equivalent to  $\Delta x/u$ ,  $\Delta x$  being the integration step in the downwind direction. The chemistry would then be calculated until the chemical time equals the advection time. The process of first calculating advection and then incorporating the chemistry solution could be repeated as long as desired. This splitting technique has been used by Eskridge and Demerjian [6,7] and by Rizzi and Bailey [15].

BIBLIOGRAPHY

1. Barad, M.L., "Project Prairie Grass, A Field Program in Diffusion", Vol. I, Geophysical Research Papers No. 59, AFCRC Report TR-58-235 (i) (1958).
2. Barad, M.L., "Project Prairie Grass, A Field Program in Diffusion", Vol. II, Geophysical Research Papers No. 59, AFCRC Report TR-58-235 (ii) (1959).
3. Caillaud, J.B. and L. Padmanabhan, "An Improved Semi-Implicit Runge-Kutta Method for Stiff Systems", Chem. Eng. Journal, 2, 227 (1971).
4. Calder, K.L., "Multiple-Source Plume Models of Urban Air Pollution-Their General Structure", Atmospheric Environment, 11, 403 (1977).
5. Eschenroeder, A.Q., J.R. Martinez and R.A. Nordsieck, "Evaluation of a Diffusion Model for Photochemical Smog Simulation", General Research Corporation, EPA-R4-73-012a, October (1972).
6. Eskridge, R.E. and K.L. Demerjian, "Evaluation of a Numerical Scheme for Solving a Conservation of Species Equation", Proc. 1976 Summer Computer Simulation Conf., Washington, D.C., 394 (1976).
7. Eskridge, R.E. and K.L. Demerjian, "Evaluation of Numerical Schemes for Solving a Conservation of Species Equation with Chemical Terms", Atmospheric Environment, 11, 1029 (1977).
8. Fleischer, M.T., "Solution of a Generalized Air Pollution Model by Orthogonal Collocation", M.S. Thesis, Dept. of Chemical Engineering, University of Houston (1975).
9. Gifford, F.A., Jr., "An Outline of Theories of Diffusion in the Lower Layers of the Atmosphere", in Slade, D.H., Editor, Meteorology and Atomic Energy, USAEC, Div. Tech. Inf., Oak Ridge, Tenn. (1968).
10. Haugen, D.A., "Project Prairie Grass, A Field Program in Diffusion", Vol. III, Geophysical Research Papers No. 59, AFCRC Report TR-58-235 (iii) (1959).
11. IBM Application Program, "System/360 Scientific Subroutine Package", H20-0166-5, IBM Co., 6th Ed., 333 (1970).
12. Michelsen, M.L., "Algorithms for Collocation Solution of Ordinary and Partial Differential Equations", Instituttet for Kemiteknik (1973).

13. Monin, A.S. and A.M. Yaglom, Statistical Fluid Mechanics: Mechanics of Turbulence, Vol. I, the M.I.T. Press, Cambridge, Mass. (1971) (English translation).
14. Pasquill, F., Atmospheric Diffusion, 2nd Ed., John Wiley and Sons, New York (1974).
15. Rizzi, A.W. and H.E. Bailey, "Split Space-Marching Finite-Volume Method for Chemically Reacting Supersonic Flow", AIAA J., 14, 621 (1976).
16. Seinfeld, J.H., Air Pollution, McGraw-Hill Book Co., New York (1975).
17. Sutton, O.G., Micrometeorology, McGraw-Hill Book Co., New York (1953).
18. Turner, D.B., Workbook of Atmospheric Dispersion Estimates, PHS Publ. No. 999-AP-26 (1969).
19. Villadsen, J.V. and M.L. Michelsen, Solution of Differential Equation Models by Polynomial Approximation, Inst. for Kemiteknik Numer. Inst. Danmarks Tekniske Højskole, Copenhagen (1976).

A P P E N D I C E S

APPENDIX A

COMPUTER PROGRAM LISTING

Part of the computer program used for the three-dimensional - Coriolis effect model is shown next. The main programs for the other models and the subroutines common to all of them can be obtained from the Chemical Engineering Department at the University of Houston. All statements are written in Fortran IV. These programs have been executed in IBM 360/44 and UNIVAC 1108 digital computers.

1:	C	*****MAIN	10
2:	C		MAIN 20
3:	C	THREE DIMENSIONAL MODEL WITH CURVILIS EFFECT	MAIN 30
4:	C		MAIN 40
5:	C	DEVELOPED BY MIGUEL T. FLEISCHER	MAIN 50
6:	C		MAIN 60
7:	C	*****MAIN	70
8:	C		MAIN 80
9:	C		MAIN 90
10:	C	NOMENCLATURE	MAIN 100
11:	C		MAIN 110
12:	C	AKYR,AKZB - TURBULENT DIFFUSIVITIES	MAIN 120
13:	C	ALPHA - CONSTANT TO DETERMINE THE HORIZONTAL DIFFUSIVITY	MAIN 130
14:	C	AM,AMM - CONSTANTS USED IN THE VELOCITY PROFILES	MAIN 140
15:	C	BETAY,BETAZ - MATHEMATICAL PARAMETERS IN MODEL	MAIN 150
16:	C	CRX - EQUIVALENT SOURCE CONCENTRATION	MAIN 160
17:	C	C(Y,Z) - MEAN CONCENTRATION AT Y AND Z	MAIN 170
18:	C	DKN(ISTB) - KNEE HEIGHT FOR AKZB	MAIN 180
19:	C	DUN(ISTB) - REFERENCE HEIGHT FOR POWER-LAW VELOCITY PROFILE	MAIN 190
20:	C	D1Y,.,.,D2Z - MATHEMATICAL PARAMETERS IN MODEL	MAIN 200
21:	C	DD1Y,.,DD2Z - INCREMENTS OF THE PREVIOUS PARAMETERS	MAIN 210
22:	C	HGEO(ISTB) - GEOSTROPHIC ELEVATION	MAIN 220
23:	C	HSKN - IF GT H, NO SECOND KNEE HEIGHT FOR AKZB	MAIN 230
24:	C	ISTB - STABILITY CLASS (1 VERY UNSTABLE, 6 VERY STABLE)	MAIN 240
25:	C	NY,NZ - NUMBER OF COLLOCATION POINTS IN Y,Z DIRECTIONS	MAIN 250
26:	C	QS - SOURCE STRENGTH	MAIN 260
27:	C	RATIO - RATIO OF BOUNDARY TO CENTERLINE CONCENTRATION	MAIN 270
28:	C	SEL - EFFECTIVE EMISSION HEIGHT (LIMITS 0 TO 1)	MAIN 280
29:	C	U,V - WIND VELOCITY IN X,Y DIRECTIONS	MAIN 290
30:	C	UCR - VELOCITY AT GROUND LEVEL	MAIN 300
31:	C	US - VELOCITY AT THE EFFECTIVE EMISSION HEIGHT	MAIN 310
32:	C	UST - GEOSTROPHIC VELOCITY	MAIN 320
33:	C	WY,WZ - QUADRATURE WEIGHTS	MAIN 330
34:	C	X,X0,DX - DOWNWIND DIRECTION, INITIAL VALUE, INCREMENT	MAIN 340
35:	C	XMAX,YMAX,H - MAXIMUM DISTANCES IN X,Y,Z DIRECTIONS	MAIN 350

36:	C	Y,Z	- LATERAL AND VERTICAL DIRECTIONS	MAIN	350
37:	C			MAIN	370
38:		IMPLICIT REAL*3(A-H,C-Z)		MAIN	380
39:		EXTERNAL FCT		MAIN	390
40:		DIMENSION FAY(12),FAZ(12),FB(12),FC(12),RTY(12),RTZ(12),		MAIN	400
41:		1AY(12,12),EY(12,12),AZ(12,12),BZ(12,12),WY(12),WZ(12),		MAIN	410
42:		2VEC(12),A1Y(12),A2Y(12),A1Z(12),A2Z(12),AVY(12,12),		MAIN	420
43:		2Y(12),Z(12),AKY(12,12),AKZ(12,12),DAKZ(12,12),ACTY(12),ACTZ(12),		MAIN	430
44:		4YINTP(12),ZINTP(12),P(100),CECO(12),EHCO(12),CECCY(12),		MAIN	440
45:		5C(12,12),CC(12,12),PW(100,100),		MAIN	450
46:		6PRMT(5),DY(100),AUX(8,100),DKN(6),DUN(6),FGFC(6),		MAIN	460
47:		7R1(12),R2(12),R3(12),R5(12),R6(12),AKYR(12),AKZB(12),DAKZP(12),		MAIN	470
48:		BL(12),V(12)		MAIN	480
49:	C			MAIN	490
50:	C	READ AND WRITE INPUT DATA		MAIN	500
51:	C			MAIN	510
52:		HEAD(5,100) NY,NZ,ISTR		MAIN	520
53:	100	FORMAT(3I5)		MAIN	530
54:		READ(5,101) XMAX,H,YMAX,ALPHA,AK		MAIN	540
55:	101	FORMAT(5D15.4)		MAIN	550
56:		READ(5,106) UST,AM,UGR,QS,SEL		MAIN	560
57:	106	FORMAT(5D15.4)		MAIN	570
58:		READ(5,98) (DKN(I), I=1,6)		MAIN	580
59:	98	FORMAT(6D10.1)		MAIN	590
60:		READ(5,99) (DUN(I), I=1,6)		MAIN	600
61:		READ(5,99) (FGEC(I), I=1,6)		MAIN	610
62:	99	FORMAT(6D10.1)		MAIN	620
63:		READ(5,104) (PRMT(I), I=1,4)		MAIN	630
64:	1 4	FORMAT(4D15.4)		MAIN	640
65:		READ(5,102) D1Y,D2Y,PATIC,BETAY		MAIN	650
66:		READ(5,1020) D1Z,D2Z,BETAZ		MAIN	660
67:	102	FORMAT(4D15.4)		MAIN	670
68:	1020	FORMAT(3D15.4)		MAIN	680
69:		READ(5,103) XC,PX,DD1Y,DD2Y		MAIN	690
70:		READ(5,102) DD1Z,DD2Z,FSKN,AMM		MAIN	700
71:	1 3	FORMAT(4D15.4)		MAIN	710

```

72:      WRITE(6,105) (PRMT(I), I=1,4)          MAIN 720
73: 105  FORMAT(10(/),20X,'PRMTS =',4(E15.4,10X))  MAIN 730
74:      WRITE(6,400) XMAX,YMAX,H,SEL,UST,UGR,AM,AMM,QS,ALPHA,AK,X0,DX,  MAIN 740
75:      1RATIO,BETAY,BETAZ,D1Y,D2Y,D1Z,D2Z,DD1Y,DD2Y,DD1Z,DD2Z,NY,NZ,ISTB,  MAIN 750
76:      2DKN(ISTB),DUN(ISTR),H$KN,HGED(ISTR)    MAIN 760
77: 400  FORMAT(2(/),20X,'XMAX =',F15.4,10X,'YMAX =',F15.4,10X,  MAIN 770
78:      1'H =',F15.4,10X,'SFL =',F15.4,2(/),20X,'UST =',F15.4,10X,  MAIN 780
79:      2'UCR =',F15.4,10X,'AM =',F15.4,2(/),20X,'AMM =',F15.4,10X,  MAIN 790
80:      3'QS =',F15.4,10X,'ALPHA =',F15.4,10X,'AK =',E15.4,2(/),  MAIN 800
81:      420X,'X0 =',E15.4,10X,'DX =',E15.4,10X,'RATIO =',E15.4,10X,  MAIN 810
82:      52(/),20X,'BETAY =',E15.4,10X,'BETAZ =',E15.4,  MAIN 820
83:      62(/),20X,'D1Y =',E15.4,  MAIN 830
84:      710X,'D2Y =',E15.4,10X,'D1Z =',E15.4,10X,'D2Z =',E15.4,2(/),  MAIN 840
85:      820X,'DD1Y =',E15.4,5X,'DD2Y =',E15.4,10X,'DD1Z =',E15.4,5X,  MAIN 850
86:      9'DD2Z =',E15.4,2(/),20X,'NY =',I3,9X,'NZ =',I3,9X,'ISTB =',I3,2(/)  MAIN 860
87:      *,20X,'DKN =',F15.4,10X,'DUN =',F15.4,10X,'H$KN =',F15.4,10X,  MAIN 870
88:      *'HGED =',F15.4,/)  MAIN 880
89: C      MAIN 890
90: C      INITIALIZATION  MAIN 900
91: C      MAIN 910
92:      IOKYP=0  MAIN 920
93:      ICKYM=0  MAIN 930
94:      IIOKY=0  MAIN 940
95:      IST=J  MAIN 950
96:      FSEL=SEL*F  MAIN 960
97:      DMULY=1.00  MAIN 970
98:      DMULZ=1.00  MAIN 980
99:      D10Y=D1Y  MAIN 990
100:     D10Z=D1Z  MAIN1000
101:     D20Y=D2Y  MAIN1010
102:     D20Z=D2Z  MAIN1020
103:     NTY=NY+2  MAIN1030
104:     N1Y=NY+1  MAIN1040
105:     N1YH=NTY/2  MAIN1050
106:     N1YH1=NTYH+1  MAIN1060
107:     NTZ=NZ+2  MAIN1070

```

108:	N1Z=NZ+1	MAIN1080
109:	NDIM=NY*NZ	MAIN1090
110:	C	MAIN1100
111:	C CALCULATION OF ORTHOGONAL POINTS, QUADRATURE WEIGHTS,	MAIN1110
112:	C AND MATRICES A AND B	MAIN1120
113:	C	MAIN1130
114:	CALL JCBI(12,NY,1,1,C.ODD,C.CDC,FAY,FB,FC,RTY)	MAIN1140
115:	CALL DFCPR(12,NY,1,1,I,3,FAY,FB,FC,RTY,WY)	MAIN1150
116:	DO 457 I=1,NTY	MAIN1160
117:	CALL DFOPR(12,NY,1,1,I,1,FAY,FB,FC,RTY,VEC)	MAIN1170
118:	DO 2 K=1,NTY	MAIN1180
119:	2 AY(I,K)=VEC(K)	MAIN1190
120:	CALL DFOPR(12,NY,1,1,I,2,FAY,FB,FC,RTY,VEC)	MAIN1200
121:	DO 3 K=1,NTY	MAIN1210
122:	3 BY(I,K)=VEC(K)	MAIN1220
123:	457 CONTINUE	MAIN1230
124:	CALL JCBI(12,NZ,1,1,C.ODD,C.CDC,FAZ,FB,FC,RTZ)	MAIN1240
125:	CALL DFCPR(12,NZ,1,1,I,3,FAZ,FB,FC,RTZ,WZ)	MAIN1250
126:	DO 458 I=1,NTZ	MAIN1260
127:	CALL DFOPR(12,NZ,1,1,I,1,FAZ,FB,FC,RTZ,VEC)	MAIN1270
128:	DO 222 K=1,NTZ	MAIN1280
129:	222 AZ(I,K)=VEC(K)	MAIN1290
130:	CALL DFOPR(12,NZ,1,1,I,2,FAZ,FB,FC,RTZ,VEC)	MAIN1300
131:	DO 333 K=1,NTZ	MAIN1310
132:	333 BZ(I,K)=VEC(K)	MAIN1320
133:	458 CONTINUE	MAIN1330
134:	NS=NY*NZ	MAIN1340
135:	X=XI	MAIN1350
136:	C	MAIN1360
137:	C INITIAL CONDITION DETERMINATION	MAIN1370
138:	C	MAIN1380
139:	CALL VELDIF(Z,H,UGR,UST,AM,U,V,ISTB,ALPHA,NTZ,AKYB,AKZB,DAKZB,	MAIN1390
140:	ISEL,C,US,CKN,DUN,HSKN,HGEC,AMM)	MAIN1400
141:	PV=-UST*DEXP(-SEL*H/AM)*DSIN(SEL*H/AM)/US	MAIN1410
142:	CRX=QS/8.00/US/YMAX/H/BETAY/BETAZ	MAIN1420
143:	DO 26 J=1,NZ	MAIN1430

144:	DO 26 I=1,NY	MAIN1440
145:	JJ=I+(J-1)*NY	MAIN1450
146:	PP=1.000	MAIN1460
147:	IF((D1Y+D2Y+2.00*BETAY)*RTY(I+1)-D1Y) 29,28,27	MAIN1470
148:	29 P(JJ)=0.000	MAIN1480
149:	GO TO 26	MAIN1490
150:	28 PP=0.500	MAIN1500
151:	GO TO 299	MAIN1510
152:	27 IF((D1Y+D2Y+2.00*BETAY)*RTY(I+1)-D1Y-2.00*BETAY) 299,298,297	MAIN1520
153:	297 P(JJ)=0.000	MAIN1530
154:	GO TO 26	MAIN1540
155:	298 PP=C.500	MAIN1550
156:	GO TO 299	MAIN1560
157:	299 IF((D1Z+D2Z+2.00*BETAZ)*RTZ(J+1)-D1Z) 39,38,37	MAIN1570
158:	39 P(JJ)=0.000	MAIN1580
159:	GO TO 26	MAIN1590
160:	38 P(JJ)=0.500*CBX	MAIN1600
161:	GO TO 26	MAIN1610
162:	37 IF((D1Z+D2Z+2.00*BETAZ)*RTZ(J+1)-D1Z-2.00*BETAZ) 35,35,34	MAIN1620
163:	34 P(JJ)=0.000	MAIN1630
164:	GO TO 26	MAIN1640
165:	35 P(JJ)=0.500*CBX	MAIN1650
166:	GO TO 26	MAIN1660
167:	36 P(JJ)=CBX*FP	MAIN1670
168:	26 CONTINUE	MAIN1680
169:	C	MAIN1690
170:	C CALCULATION OF EXPRESSIONS USED IN MODEL (DEPENDENT	MAIN1700
171:	C OF THE NUMBER OF COLLLOCATION POINTS ONLY)	MAIN1710
172:	C	MAIN1720
173:	DENY=AY(NTY,1)*AY(1,NTY)-AY(1,1)*AY(NTY,NTY)	MAIN1730
174:	DO 41 I=2,N1Y	MAIN1740
175:	A2Y(I)=AY(1,1)*AY(NTY,I)-AY(NTY,1)*AY(1,I)	MAIN1750
176:	A1Y(I)=AY(1,I)+AY(1,NTY)*A2Y(I)/DENY	MAIN1760
177:	41 CONTINUE	MAIN1770
178:	DENZ=AZ(NTZ,1)*AZ(1,NTZ)-AZ(1,1)*AZ(NTZ,NTZ)	MAIN1780
179:	DO 441 I=2,N1Z	MAIN1790

```

180:      A2Z(I)=AZ(1,1)*AZ(NTZ,I)-AZ(NTZ,1)*AZ(1,I)      MAIN1800
181:      A1Z(I)=AZ(1,I)+AZ(1,NTZ)*A2Z(I)/DENZ             MAIN1810
182: 441 CONTINUE                                           MAIN1820
183: C                                                       MAIN1830
184: C      LOOP FOR CHANGING THE BOUNDARY POSITIONS        MAIN1840
185: C                                                       MAIN1850
186: 20 CONTINUE                                           MAIN1860
187:      VAR1Y=DABS(D1Y+BETAY-.5DC)                          MAIN1870
188:      VAR2Y=DABS(D2Y-1.)DC+.5DC+BETAY)                  MAIN1880
189:      VAR1Z=DABS(D1Z+BETAZ-SEL)                           MAIN1890
190:      VAR2Z=DABS(D2Z-1.)DC+SEL+BETAZ)                    MAIN1900
191:      WRITE(6,506) D1Y,D2Y,D1Z,D2Z                       MAIN1910
192: 5 6 FCPMAT(5(/),10X,'D1Y =',F10.7,5X,'D2Y =',F10.7,10X, MAIN1920
193: 1'D1Z =',F10.7,5X,'D2Z =',F10.7,1(/))                  MAIN1930
194:      DO 8 I=1,NTY                                         MAIN1940
195:      Y(I)=(D1Y+D2Y+2.D0*BETAY)*RTY(I)+.5DC-BETAY-D1Y   MAIN1950
196: P ACTY(I)=(2.D0*Y(I)-1.D0)*YMAX                         MAIN1960
197:      DO 888 I=1,NTZ                                       MAIN1970
198:      Z(I)=(D1Z+D2Z+2.D0*BETAZ)*RTZ(I)+SEL-BETAZ-D1Z    MAIN1980
199: 888 ACTZ(I)=Z(I)*H                                         MAIN1990
200:      RSEL=(BETAZ+D1Z)/(D1Z+D2Z+2.D0*BETAZ)              MAIN2000
201:      PYC=(BETAY+D1Y)/(D1Y+D2Y+2.D0*BETAY)              MAIN2010
202:      ARYC=(2.D0*0.5DC-1.D0)*YMAX                        MAIN2020
203: C                                                       MAIN2030
204: C      CALCULATION OF THE DIFFERENTIAL EQUATIONS CCEFFICIENTS MAIN2040
205: C                                                       MAIN2050
206:      CALL VELDIF(Z,H,UGR,UST,AM,U,V,ISTB,ALPHA,NTZ,AKYE,AKZE,CAKZE, MAIN2060
207: 1SEFL,1,US,DKN,DUN,HSKN,HGEC,AMM)                       MAIN2070
208:      DO 2500 L=2,N1Z                                       MAIN2080
209:      R1(L)=U(L)/XMAX                                       MAIN2090
210:      R2(L)=V(L)/2.D0/YMAX/(D1Y+D2Y+2.D0*BETAY)          MAIN2100
211:      R3(L)=CAKZE(L)/H/(D1Z+D2Z+2.D0*BETAZ)              MAIN2110
212:      R5(L)=AKYE(L)/4.D0/YMAX/YMAX/(D1Y+D2Y+2.D0*BETAY)**2 MAIN2120
213:      R6(L)=AKZE(L)/H/H/(D1Z+D2Z+2.D0*BETAZ)/(D1Z+D2Z+2.D0*BETAZ) MAIN2130
214: 2500 CONTINUE                                           MAIN2140
215:      DO 15 K=2,N1Y                                         MAIN2150

```

216:	DO 15 I=2,N1Y	MAIN2160
217:	AKY(K,I)=(-BY(K,1)*A1Y(I)/AY(1,1)+BY(K,I)+	MAIN2170
218:	1BY(K,NTY)*A2Y(I)/DFNY)	MAIN2180
219:	AVY(K,I)=(-AY(K,1)*A1Y(I)/AY(1,1)+AY(K,I)+	MAIN2190
220:	1AY(K,NTY)*A2Y(I)/DENY)	MAIN2200
221:	15 CONTINUE	MAIN2210
222:	DO 155 L=2,N1Z	MAIN2220
223:	DC 155 I=2,N1Z	MAIN2230
224:	AKZ(L,I)=(-BZ(L,1)*A1Z(I)/AZ(1,1)+BZ(L,I)+	MAIN2240
225:	1BZ(L,NTZ)*A2Z(I)/DFNZ)	MAIN2250
226:	DAKZ(L,I)=(-AZ(L,1)*A1Z(I)/AZ(1,1)+AZ(L,I)+	MAIN2260
227:	1AZ(L,NTZ)*A2Z(I)/DENZ)	MAIN2270
228:	155 CONTINUE	MAIN2280
229:	DO 10 J=1,NS	MAIN2290
230:	DC 10 I=1,NS	MAIN2300
231:	10 PW(J,I)=C.CDC	MAIN2310
232:	DC 113 K=1,NZ	MAIN2320
233:	DC 113 IJ=1,NY	MAIN2330
234:	JJ=IJ+(K-1)*NY	MAIN2340
235:	DC 112 J=1,NZ	MAIN2350
236:	I=IJ+(J-1)*NY	MAIN2360
237:	112 PW(JJ,I)=PW(JJ,I)+AKZ(K+1,J+1)*R6(K+1)/R1(K+1)+	MAIN2370
238:	1DAKZ(K+1,J+1)*R3(K+1)/R1(K+1)	MAIN2380
239:	DC 14 J=1,NY	MAIN2390
240:	I=J+(K-1)*NY	MAIN2400
241:	14 PW(JJ,I)=PW(JJ,I)+AKY(IJ+1,J+1)*R5(K+1)/R1(K+1)-	MAIN2410
242:	1AVY(IJ+1,J+1)*R2(K+1)/R1(K+1)	MAIN2420
243:	113 CONTINUE	MAIN2430
244:	C	MAIN2440
245:	C INTEGRATION USING DRKGS	MAIN2450
246:	C	MAIN2460
247:	1 CONTINUE	MAIN2470
248:	SUM=C.DC	MAIN2480
249:	KK=NDIM-1	MAIN2490
250:	DO 31 I=1,KK	MAIN2500
251:	PY(I)=1.DC/DFLOAT(NDIM)	MAIN2510

252:	31	SUM=SUM+DY(I)	MAIN2520
253:		DY(NDIM)=1.00-SUM	MAIN2530
254:		X^=PRMT(1)	MAIN2540
255:		DX^=DX	MAIN2550
256:		PRMT(2)=PRMT(1)+DX	MAIN2560
257:		PRMT(3)=DX	MAIN2570
258:		CALL DRKGS(PRMT,P,DY,NDIM,IHLF,FCT,AUX,PW)	MAIN2580
259:		X=PRMT(1)	MAIN2590
260:	65	IF(X.GT.1.0000) STOP	MAIN2600
261:		IF(X.GE..990-07) DX=3.00-07	MAIN2610
262:		IF(X.GE..990-06) DX=3.00-06	MAIN2620
263:		IF(X.GE..990-05) DX=1.00-05	MAIN2630
264:		IF(X.GE..990-04) DX=0.50-04	MAIN2640
265:		IF(X.GE..990-03) DX=0.250-03	MAIN2650
266:		IF(X.GE..990-02) DX=0.250-02	MAIN2660
267:		IF(X.GE..990-01) DX=0.100-01	MAIN2670
268:		IF(X.GE..499) DX=0.250-01	MAIN2680
269:		IF(X.GT.0.10-01) IICKY=1	MAIN2690
270:	C		MAIN2700
271:	C	TRANSFORMATION OF THE DRKGS RESULTS INTO A C(Y,Z) FORM	MAIN2710
272:	C		MAIN2720
273:		J=1	MAIN2730
274:		L1=1	MAIN2740
275:		L2=NY	MAIN2750
276:	81	DO 70 L=L1,L2	MAIN2760
277:		K=L-(J-1)*NY	MAIN2770
278:		KK=K+1	MAIN2780
279:		JJ=J+1	MAIN2790
280:		C(KK,JJ)=P(L)	MAIN2800
281:	70	CONTINUE	MAIN2810
282:		J=J+1	MAIN2820
283:		IF(J.GT.NZ) GO TO 82	MAIN2830
284:		L1=L2+1	MAIN2840
285:		L2=L2+NY	MAIN2850
286:		GO TO 81	MAIN2860
287:	82	CONTINUE	MAIN2870

```

288: C MAIN2880
289: C CALCULATION OF THE BOUNDARY CONCENTRATIONS MAIN2890
290: C MAIN2900
291: DO 83 I=1,NTZ MAIN2910
292: C(I,I)=0.CDC MAIN2920
293: 83 C(NTY,I)=0.CDC MAIN2930
294: DO 833 J=1,NTY MAIN2940
295: C(J,1)=0.CDC MAIN2950
296: 833 C(J,NTZ)=0.CDC MAIN2960
297: DO 84 L=2,N1Z MAIN2970
298: DO 84 I=2,N1Y MAIN2980
299: C(1,L)=C(1,L)-A1Y(I)*C(I,L)/AY(1,1) MAIN2990
300: 84 C(NTY,L)=C(NTY,L)+A2Y(I)*C(I,L)/DENY MAIN3000
301: DO 844 K=2,N1Y MAIN3010
302: DO 844 I=2,N1Z MAIN3020
303: C(K,1)=C(K,1)-A1Z(I)*C(K,I)/AZ(1,1) MAIN3030
304: 844 C(K,NTZ)=C(K,NTZ)+A2Z(I)*C(K,I)/DENZ MAIN3040
305: DO 85 I=2,N1Y MAIN3050
306: C(1,1)=C(1,1)-A1Y(I)*C(I,1)/AY(1,1) MAIN3060
307: C(NTY,1)=C(NTY,1)+A2Y(I)*C(I,1)/DENY MAIN3070
308: C(1,NTZ)=C(1,NTZ)-A1Y(I)*C(I,NTZ)/AY(1,1) MAIN3080
309: 85 C(NTY,NTZ)=C(NTY,NTZ)+A2Y(I)*C(I,NTZ)/DENY MAIN3090
310: C MAIN3100
311: C CALCULATION OF THE EFFECTIVE EMISSION HEIGHT CONCENTRATION MAIN3110
312: C MAIN3120
313: CALL INTRP(12,NTZ,RSFL,RTZ,FAZ,ZINTP) MAIN3130
314: DO 855 J=1,NTY MAIN3140
315: EHCO(J)=0.DC MAIN3150
316: DO 855 I=1,NTZ MAIN3160
317: 855 EHCO(J)=EHCO(J)+ZINTP(I)*C(J,I) MAIN3170
318: C MAIN3180
319: C CALCULATION OF THE CONCENTRATIONS AT Y=0 MAIN3190
320: C MAIN3200
321: CALL INTRP(12,NTY,RYC,RTY,FAY,YINTP) MAIN3210
322: DO 856 J=1,NTZ MAIN3220
323: CFCC(J)=0.DC MAIN3230

```

```

324:      DO 856 I=1,NTY                MAIN3240
325: 856 C=CO(J)=CECC(J)+YINTP(I)*C(I,J)  MAIN3250
326:      CCO1=C.DC                     MAIN3260
327:      CCO2=0.DC                     MAIN3270
328:      CCO3=0.DJ                     MAIN3280
329:      DO 857 I=1,NTY                MAIN3290
330:      CCO1=CCO1+YINTP(I)*EHCO(I)    MAIN3300
331: 857 CONTINUE                       MAIN3310
332:      C(Y=EHCO(1))                  MAIN3320
333:      C1Y=EHCO(NTY)                 MAIN3330
334: C                                   MAIN3340
335: C      CALCULATION OF THE MASS RATE  MAIN3350
336: C                                   MAIN3360
337:      Q=0.DC                          MAIN3370
338:      DO 47 I=2,N1Y                   MAIN3380
339:      DO 47 J=2,N1Z                   MAIN3390
340: 47 Q=Q+WY(I)*WZ(J)*C(I,J)*U(J)     MAIN3400
341:      G=2.DC*YMAX*(D1Y+D2Y+2.DC*BETAY)*H*(D1Z+D2Z+2.DC*BETAZ)*G  MAIN3410
342:      Q=1000.DC/60.DC*Q              MAIN3420
343:      ACTX=X*XMAX                     MAIN3430
344: C                                   MAIN3440
345: C      CALCULATION OF THE TRUE CENTERLINE CONCENTRATIONS  MAIN3450
346: C                                   MAIN3460
347:      RYC=(BETAY+D1Y+PV*ACTX/2.DC/YMAX)/(D1Y+D2Y+2.DC*BETAY)  MAIN3470
348:      DO 859 J=1,NTZ                 MAIN3480
349: 859 CECUY(J)=C.DC                   MAIN3490
350:      IF(RYC.GE.1.DDC) IST=1         MAIN3500
351:      CALL INTRF(12,NTY,RYC,RTY,FAY,YINTP)  MAIN3510
352:      DO 860 J=1,NTZ                 MAIN3520
353:      DO 860 I=1,NTY                 MAIN3530
354: 860 CECUY(J)=CECOY(J)+YINTP(I)*C(I,J)  MAIN3540
355:      APYC=PV*ACTX                   MAIN3550
356:      DO 858 I=1,NTZ                 MAIN3560
357:      CCO2=CCO2+ZINTP(I)*CECO(I)     MAIN3570
358:      CCO3=CCO3+ZINTP(I)*CECOY(I)    MAIN3580
359: 858 CONTINUE                       MAIN3590

```

360:	CZ=CFCOY(1)	MAIN3600
361:	C1Z=CFCOY(NTZ)	MAIN3610
362:	EPS=CCO3*RATIO	MAIN3620
363:	C	MAIN3630
364:	C	MAIN3640
365:	C TEST FOR THE PLUME SPREAD BY COMPARISON OF BOUNDARY	MAIN3650
366:	C CONCENTRATIONS WITH FPS (= C(TRUE CENTERLINE,EFFECTIVE	MAIN3660
367:	C EMISSION HEIGHT)*RATIO)	MAIN3670
368:	C - IF OK, PRINT RESULTS AND ADVANCE INTEGRATION (12)	MAIN3680
369:	C - IF NOT, GET NEW INITIAL CONDITION AND INTEGRATE AGAIN	MAIN3690
370:	C	MAIN3700
371:	IF(IOKYP.EQ.2.AND.IOKYM.FG.2) GO TO 12	MAIN3710
372:	IOKY=C	MAIN3720
373:	IOKZ=0	MAIN3730
374:	IF((COY).LT.EPS.AND.(C1Y).LT.EPS) IOKY=1	MAIN3740
375:	IF(VAR1Y.LT.1.CD-C8.AND.VAR2Y.LT.1.OD-C8) IOKY=1	MAIN3750
376:	IF(VAR1Y.LT.1.CD-C8.AND.(C1Y).LT.EPS) IOKY=1	MAIN3760
377:	IF(VAR2Y.LT.1.OD-C8.AND.(COY).LT.EPS) IOKY=1	MAIN3770
378:	IF(IOKY.EQ.1) GO TO 13	MAIN3780
379:	IF(D1Y.LT.0.5D0-BETAY-1.CD-C8.AND.(COY).GT.EPS)D1Y=D1Y+	MAIN3790
380:	1DD1Y*DMULY	MAIN3800
381:	IF(VAR2Y.GT.1.OD-C8.AND.(C1Y).GT.EPS) D2Y=C2Y+DD2Y*DMULY	MAIN3810
382:	IOKY=C	MAIN3820
383:	IF(IOKYP.EQ.1) IOKYP=2	MAIN3830
384:	IF(IOKYP.EG.0) IOKYP=1	MAIN3840
385:	13 CONTINUE	MAIN3850
386:	IF(IIOKY.EQ.0) GO TO 1333	MAIN3860
387:	IF(COY.GT.0.D0.AND.C1Y.GT.0.D0) GO TO 1333	MAIN3870
388:	IF((COY).LT.0.CD0)D1Y=D1Y-DD1Y*DMULY/2.5CD	MAIN3880
389:	IF((C1Y).LT.0.CD0) D2Y=D2Y-DD2Y*DMULY/2.5CD	MAIN3890
390:	IOKY=C	MAIN3900
391:	IF(IOKYM.EQ.1) IOKYM=2	MAIN3910
392:	IF(IOKYM.EQ.0) IOKYM=1	MAIN3920
393:	1333 CONTINUE	MAIN3930
394:	IF((COZ).LT.EPS.AND.(C1Z).LT.EPS) ICKZ=1	MAIN3940
395:	IF(VAR1Z.LT.1.CD-C8.AND.VAR2Z.LT.1.OD-C8) ICKZ=1	MAIN3950
396:	IF(VAR1Z.LT.1.CD-C8.AND.(C1Z).LT.EPS) IOKZ=1	MAIN3960

396:	IF(VAR2Z.LT.1.0D-08.AND.(CCZ).LT.EPS) ICKZ=1	MAIN3960
397:	IF(ICKY.EQ.1.AND.IOKZ.EQ.1) GO TO 12	MAIN3970
398:	IF(D1Z.LT.SEL-BETAZ-1.0D-08.AND.(C0Z).GT.EPS)D1Z=D1Z+	MAIN3980
399:	10D1Z*DMULZ	MAIN3990
400:	IF(VAR2Z.GT.1.0D-08.AND.(C1Z).GT.EPS) D2Z=D2Z+DD2Z*DMULZ	MAIN4000
401:	ICKZ=)	MAIN4010
402:	133 CONTINUE	MAIN4020
403:	IF(IOKY.EQ.1.AND.IOKZ.EQ.1) GO TO 12	MAIN4030
404:	IF(X.GE..99D-03) DMULY=2.0D	MAIN4040
405:	IF(X.GE..99D-02) DMULY=6.0D	MAIN4050
406:	IF(X.GE..99D-01) DMULY=10.0D	MAIN4060
407:	IF(X.GE..99D-03) DMULZ=4.0D	MAIN4070
408:	IF(X.GE..99D-02) DMULZ=12.0D	MAIN4080
409:	IF(X.GE..99D-01) DMULZ=16.0D	MAIN4090
410:	IF(0.5DC-BETAY-D1Y.LE.DD1Y*DMULY) DD1Y=(0.5DC-BETAY-D1Y)/DMULY	MAIN4100
411:	IF(1.0D-0.5DC-BETAY-D2Y.LE.DD2Y*DMULY)DD2Y=(1.0D-C.5DC-BETAY-D2Y)/	MAIN4110
412:	10DMULY	MAIN4120
413:	IF(SEL-BETAZ-D1Z.LE.DD1Z*DMULZ) DD1Z=(SEL-BETAZ-D1Z)/DMULZ	MAIN4130
414:	IF(1.0D-SEL-BETAZ-D2Z.LE.DD2Z*DMULZ)DD2Z=(1.0D-SEL-BETAZ-D2Z)/	MAIN4140
415:	10DMULZ	MAIN4150
416:	C	MAIN4160
417:	C CALCULATION OF NEW INITIAL CONDITION	MAIN4170
418:	C	MAIN4180
419:	X=XC	MAIN4190
420:	PRMT(1)=XC	MAIN4200
421:	DX=DX0	MAIN4210
422:	NCI=1	MAIN4220
423:	96 DO 92 I=1,NY	MAIN4230
424:	J=I+1	MAIN4240
425:	VIY=((D1Y+D2Y+2.0D*BETAY)*RTY(I+1)+C10Y-C1Y)/(D10Y+C20Y+	MAIN4250
426:	12.0D*BETAY)	MAIN4260
427:	IF(VIY.LT.1.0D0) GO TO 90	MAIN4270
428:	C(J,NCI)=C.0D0	MAIN4280
429:	GO TO 92	MAIN4290
430:	90 IF(VIY.GT.C.0D0) GO TO 95	MAIN4300
431:	C(J,NCI)=0.0D0	MAIN4310

```

432:      CO TO 92                                MAIN4320
433:      95 CALL INTRP(12,NTY,VIY,RTY,FAY,YINTP)  MAIN4330
434:      C(J,NCI)=CC(1,NCI)*YINTP(1)+CC(NTY,NCI)*YINTP(NTY)  MAIN4340
435:      DO 93 K=1,NY                             MAIN4350
436:      93 C(J,NCI)=C(J,NCI)+YINTP(K+1)*CC(K+1,NCI)  MAIN4360
437:      92 CONTINUE                               MAIN4370
438:      NCI=NCI+1                                MAIN4380
439:      IF(NCI.GT.NTZ) GO TO 955                 MAIN4390
440:      GO TO 96                                  MAIN4400
441:      955 NCI=1                                  MAIN4410
442:      1000 DO 42 I=1,NZ                         MAIN4420
443:      J=NCI+(I-1)*NY                           MAIN4430
444:      VIZ=((D1Z+D2Z+2.00*BETAZ)*RTZ(I+1)+D10Z-C1Z)/(D10Z+D20Z+
445:      12.000*BETAZ)                             MAIN4440
446:      IF(VIZ.LT.1.000) GO TO 40                MAIN4450
447:      P(J)=C.CDC                                MAIN4460
448:      GO TO 42                                  MAIN4470
449:      40 IF(VIZ.GT.0.000) GO TO 45              MAIN4480
450:      P(J)=C.CDC                                MAIN4490
451:      GO TO 42                                  MAIN4500
452:      45 CALL INTRP(12,NTZ,VIZ,RTZ,FAZ,ZINTP)  MAIN4510
453:      P(J)=C(NCI+1,1)*ZINTP(1)+C(NCI+1,NTZ)*ZINTP(NTZ)  MAIN4520
454:      DO 43 K=1,NZ                             MAIN4530
455:      43 P(J)=P(J)+ZINTP(K+1)*C(NCI+1,K+1)    MAIN4540
456:      42 CONTINUE                               MAIN4550
457:      NCI=NCI+1                                MAIN4560
458:      IF(NCI.GT.NY) GO TO 20                   MAIN4570
459:      GO TO 1000                                MAIN4580
460:      C                                          MAIN4590
461:      C      PRINT AND STORE THE RESULTS        MAIN4600
462:      C                                          MAIN4610
463:      12 CONTINUE                               MAIN4620
464:      IOKYP=0                                    MAIN4630
465:      IOKYM=0                                    MAIN4640
466:      D10Y=D1Y                                   MAIN4650
467:      D20Y=D2Y                                   MAIN4660

```

```

468:      D1CZ=D1Z      MAIN468C
469:      D2CZ=D2Z      MAIN469C
470:      DO 66 I=1,NTY  MAIN470C
471:      EHCO(I)=1000.DO*EHCO(I)  MAIN471C
472:      DO 66 J=1,NTZ  MAIN472C
473:      IF(I.EQ.1) CECCO(J)=CFCCO(J)*1000.DO  MAIN473C
474:      IF(I.EQ.1) CECCY(J)=CECCOY(J)*1000.DO  MAIN474C
475:      CC(I,J)=C(I,J)  MAIN475C
476:      66 C(I,J)=C(I,J)*1000.DO  MAIN476C
477:      CCO1=1000.DO*CCO1  MAIN477C
478:      CCO3=1000.DO*CCO3  MAIN478C
479:      WRITE(6,500) ACTX,Q,IHLF  MAIN479C
480:      500 FORMAT(2(/),20X,'X =',F12.3,20X,'Q =',F10.2,10X,'IHLF =',15,/)  MAIN480C
481:      WRITE(6,2000)  MAIN481C
482:      2000 FORMAT(2(/))  MAIN482C
483:      WRITE(6,352) (ACTY(I),I=1,NTYH),ARYC  MAIN483C
484:      352 FORMAT(1X,132('*')/1X,'* Z/Y *',10F12.2,' *')  MAIN484C
485:      WRITE(6,650)  MAIN485C
486:      68 CONTINUE  MAIN486C
487:      I=NTZ  MAIN487C
488:      502 CONTINUE  MAIN488C
489:      WRITE(6,300) ACTZ(I),(C(J,I),J=1,NTYH),CECC(I)  MAIN489C
490:      300 FORMAT(1X,'*',F7.2,1X,'*',10F12.5,' *')  MAIN490C
491:      I=I-1  MAIN491C
492:      IF(I.EQ.0) GO TO 501  MAIN492C
493:      GO TO 502  MAIN493C
494:      501 CONTINUE  MAIN494C
495:      WRITE(6,650)  MAIN495C
496:      650 FORMAT(1X,132('*'))  MAIN496C
497:      WRITE(6,300) HSEL,(EHCC(I),I=1,NTYH),CCO1  MAIN497C
498:      WRITE(6,2000)  MAIN498C
499:      WRITE(6,352) (ACTY(I),I=NTYH1,NTY),ARYC  MAIN499C
500:      WRITE(6,650)  MAIN500C
501:      668 CONTINUE  MAIN501C
502:      I=NTZ  MAIN502C
503:      5502 CONTINUE  MAIN503C

```

504:	WRITE(6,300) ACTZ(I),(C(J,I),J=NTYH1,NTY),CECOY(I)	MAIN5040
505:	I=I-1	MAIN5050
506:	IF(I.EQ.0) GO TO 5501	MAIN5060
507:	GO TO 5502	MAIN5070
508:	5501 CONTINUE	MAIN5080
509:	WRITE(6,650)	MAIN5090
510:	WRITE(6,300) HSEL,(EHCC(I),I=NTYH1,NTY),CCC3	MAIN5100
511:	IF(IST.EQ.1) STOP	MAIN5110
512:	GO TO 1	MAIN5120
513:	900 CONTINUE	MAIN5130
514:	END	MAIN5140

```

1:      SUBROUTINE DRKGS(PRMT,Y,DERY,NDIM,IHLF,FCT,AUX,PW)      DRKG 10
2:      C                                                    DRKG 20
3:      C                                                    DRKG 30
4:      C THIS SUBROUTINE SOLVES A SYSTEM OF FIRST ORDER ORDINARY DIFFERENTIAL DRKG 40
5:      C EQUATIONS WITH GIVEN INITIAL CONDITIONS              DRKG 50
6:      C                                                    DRKG 60
7:      C                                                    DRKG 70
8:      C PRMT      - AN INPUT OUTPUT VECTOR WITH DIMENSION GREATER OR DRKG 80
9:      C              EQUAL TO 5                               DRKG 90
10:     C PRMT(1)   - LOWER BOUND OF THE INTERVAL              DRKG 100
11:     C PRMT(2)   - UPPER BOUND OF THE INTERVAL             DRKG 110
12:     C PRMT(3)   - INITIAL INCREMENT OF THE INDEPENDENT VARIABLE DRKG 120
13:     C PRMT(4)   - UPPER ERROR BOUND                       DRKG 130
14:     C PRMT(5)   - NO INPUT PARAMETER. IT IS 0 UNLESS THE USER WANTS TO DRKG 140
15:     C              TERMINATE RKGS AT ANY OUTPUT POINT     DRKG 150
16:     C DERY      - INPUT VECTOR OF ERROR WEIGHTS. LATERON IS THE VECTOR DRKG 160
17:     C              OF DERIVATIVES                          DRKG 170
18:     C NDIM      - THE NUMBER OF EQUATIONS IN THE SYSTEM   DRKG 180
19:     C IHLF      - THE NUMBER OF BISECTIONS OF THE INITIAL INCREMENT DRKG 190
20:     C AUX       - AN AUXILIARY STORAGE ARRAY (8 ROWS AND NDIM COLUMNS) DRKG 200
21:     C                                                    DRKG 210
22:     C                                                    DRKG 220
23:     C      IMPLICIT REAL*8(A-H,C-Z)                        DRKG 230
24:     C      DIMENSION Y(1),DERY(1),AUX(8,1),A(4),B(4),C(4),PRMT(1), DRKG 240
25:     C      1PW(NDIM,NDIM)                                  DRKG 250
26:     C      DO 1 I=1,NDIM                                    DRKG 260
27:     C      1 AUX(8,I)=DERY(I)/15.D0                         DRKG 270
28:     C      X=PRMT(1)                                        DRKG 280
29:     C      XEND=PRMT(2)                                     DRKG 290
30:     C      H=PRMT(3)                                       DRKG 300
31:     C      PRMT(5)=0.D0                                     DRKG 310
32:     C      CALL FCT(Y,NDIM,DERY,PW)                        DRKG 320
33:     C                                                    DRKG 330
34:     C FRROR TEST                                          DRKG 340
35:     C                                                    DRKG 350

```

36:	IF(H*(XEND-X))36,37,2	DRKG 360
37:	C	DRKG 370
38:	C PREPARATIONS FOR RUNGE-KLITA METHCD	DRKG 380
39:	C	DRKG 390
40:	2 A(1)=.5D0	DRKG 400
41:	A(2)=.29289321881345248D0	DRKG 410
42:	A(3)=1.7071067811865475D0	DRKG 420
43:	A(4)=.166666666666666667D0	DRKG 430
44:	B(1)=2.D0	DRKG 440
45:	B(2)=1.D0	DRKG 450
46:	B(3)=1.D0	DRKG 460
47:	B(4)=2.D0	DRKG 470
48:	C(1)=.5D0	DRKG 480
49:	C(2)=.29289321881345248D0	DRKG 490
50:	C(3)=1.7071067811865475D0	DRKG 500
51:	C(4)=.5D0	DRKG 510
52:	C	DRKG 520
53:	C PREPARATIONS OF FIRST RUNGE-KUTTA STEP	DRKG 530
54:	C	DRKG 540
55:	DO 3 I=1,NDIM	DRKG 550
56:	AUX(1,I)=Y(I)	DRKG 560
57:	AUX(2,I)=DERY(I)	DRKG 570
58:	AUX(3,I)=C.D0	DRKG 580
59:	3 AUX(6,I)=C.D0	DRKG 590
60:	IREC=0	DRKG 600
61:	H=H+H	DRKG 610
62:	IHLF=-1	DRKG 620
63:	ISTEP=0	DRKG 630
64:	IEND=0	DRKG 640
65:	C	DRKG 650
66:	C START OF A RUNGE-KUTTA STEP	DRKG 660
67:	C	DRKG 670
68:	4 IF((X+H-XEND)*H)7,6,5	DRKG 680
69:	5 F=XEND-X	DRKG 690
70:	6 IEND=1	DRKG 700
71:	C	DRKG 710

72:	C	RECORDING OF INITIAL VALUES OF THIS STEP	DRKG 720
73:	C		DRKG 730
74:		7 CONTINUE	DRKG 740
75:		IF(PRMT(5))40,8,40	DRKG 750
76:		8 ITEST=0	DRKG 760
77:		9 ISTEP=ISTEP+1	DRKG 770
78:	C		DRKG 780
79:	C	START OF INNERMOST RUNGE-KUTTA LCCP	DRKG 790
80:	C		DRKG 800
81:		J=1	DRKG 810
82:		10 AJ=A(J)	DRKG 820
83:		BJ=B(J)	DRKG 830
84:		CJ=C(J)	DRKG 840
85:		DO 11 I=1,NDIM	DRKG 850
86:		R1=H*DERY(I)	DRKG 860
87:		R2=AJ*(R1-BJ*AUX(6,I))	DRKG 870
88:		Y(I)=Y(I)+R2	DRKG 880
89:		R2=R2+R2+R2	DRKG 890
90:		11 AUX(6,I)=AUX(6,I)+R2-CJ*R1	DRKG 900
91:		IF(J-4)12,15,15	DRKG 910
92:		12 J=J+1	DRKG 920
93:		IF(J-3)13,14,13	DRKG 930
94:		13 X=X+.500*H	DRKG 940
95:		14 CALL FCT(Y,NDIM,DERY,PW)	DRKG 950
96:		GOTO 10	DRKG 960
97:	C		DRKG 970
98:	C	TEST OF ACCURACY	DRKG 980
99:	C		DRKG 990
100:		15 IF(ITEST)16,16,20	DRKG1000
101:	C		DRKG1010
102:	C	IN CASE ITEST=0 THERE IS NO POSSIBILITY FOR TESTING OF ACCURACY	DRKG1020
103:	C		DRKG1030
104:		16 DO 17 I=1,NDIM	DRKG1040
105:		17 AUX(4,I)=Y(I)	DRKG1050
106:		ITEST=1	DRKG1060
107:		ISTEP=ISTEP+ISTEP-2	DRKG1070

108:	18	IHLF=IHLF+1	DRKG1080
109:		X=X-F	DRKG1090
110:		F=.507*H	DRKG1100
111:		DO 19 I=1,NDIM	DRKG1110
112:		Y(I)=AUX(1,I)	DRKG1120
113:		DERY(I)=AUX(2,I)	DRKG1130
114:	19	AUX(6,I)=AUX(3,I)	DRKG1140
115:		GOTO 9	DRKG1150
116:	C		DRKG1160
117:	C	IN CASE ITEST=1 TESTING OF ACCURACY IS POSSIBLE	DRKG1170
118:	C		DRKG1180
119:	20	IMOD=ISTEP/2	DRKG1190
120:		IF(ISTEP-IMOD-IMOD)21,23,21	DRKG1200
121:	21	CALL FCT(Y,NDIM,DERY,PW)	DRKG1210
122:		DO 22 I=1,NDIM	DRKG1220
123:		AUX(5,I)=Y(I)	DRKG1230
124:	22	AUX(7,I)=DERY(I)	DRKG1240
125:		GOTO 9	DRKG1250
126:	C		DRKG1260
127:	C	COMPUTATION OF TEST VALUE DELT	DRKG1270
128:	C		DRKG1280
129:	23	DELT=0.D0	DRKG1290
130:		DO 24 I=1,NDIM	DRKG1300
131:	24	DELT=DELT+AUX(8,I)*DABS(AUX(4,I)-Y(I))	DRKG1310
132:		IF(DELT-PRMT(4))28,28,25	DRKG1320
133:	C		DRKG1330
134:	C	ERRPCR IS TOO GREAT	DRKG1340
135:	C		DRKG1350
136:	25	IF(IHLF-10)26,36,36	DRKG1360
137:	26	DO 27 I=1,NDIM	DRKG1370
138:	27	AUX(4,I)=AUX(5,I)	DRKG1380
139:		ISTEP=ISTEP+ISTEP-4	DRKG1390
140:		X=X-F	DRKG1400
141:		IEND=C	DRKG1410
142:		GOTO 18	DRKG1420
143:	C		DRKG1430

144:	C	RFSULT VALUES ARE GOOD	CRKG1440
145:	C		CRKG1450
146:		28 CALL FCT(Y,NDIM,DERY,PW)	CRKG1460
147:		DO 29 I=1,NDIM	CRKG1470
148:		AUX(1,I)=Y(I)	CRKG1480
149:		AUX(2,I)=DERY(I)	CRKG1490
150:		AUX(3,I)=ALX(6,I)	CRKG1500
151:		Y(I)=AUX(5,I)	CRKG1510
152:		29 DERY(I)=ALX(7,I)	CRKG1520
153:		IF(PRMT(5))40,30,40	CRKG1530
154:		30 DO 31 I=1,NDIM	CRKG1540
155:		Y(I)=AUX(1,I)	CRKG1550
156:		31 DERY(I)=ALX(2,I)	CRKG1560
157:		IREF=IHLF	CRKG1570
158:		IF(IEND)32,32,39	CRKG1580
159:	C		CRKG1590
160:	C	INCREMENT GETS DOUBLED	CRKG1600
161:	C		CRKG1610
162:		32 IHLF=IHLF-1	CRKG1620
163:		ISTEP=ISTEP/2	CRKG1630
164:		H=H+H	CRKG1640
165:		IF(IHLF)4,33,33	CRKG1650
166:		33 IMOD=ISTEP/2	CRKG1660
167:		IF(ISTEP-IMOD-IMOD)4,34,4	CRKG1670
168:		34 IF(DFLT-.0200*PRMT(4))35,35,4	CRKG1680
169:		35 IHLF=IHLF-1	CRKG1690
170:		ISTEP=ISTEP/2	CRKG1700
171:		H=H+H	CRKG1710
172:		GOTO 4	CRKG1720
173:	C		CRKG1730
174:	C	RETURNS TO CALLING PROGRAM	CRKG1740
175:	C		CRKG1750
176:		36 IHLF=11	CRKG1760
177:		CALL FCT(Y,NDIM,DERY,PW)	CRKG1770
178:		GOTO 39	CRKG1780
179:		37 IHLF=12	CRKG1790

```
180:      GOTD 39
181:      38 IHLF=13
182:      39 CONTINUE
183:      PRMT(1)=X
184:      50 FORMAT(2(/),20X,'X =',F16.12,10X,'IHLF =',I5)
185:      40 RETURN
186:      END
```

```
DRKG1800
DRKG1810
DRKG1820
DRKG1830
DRKG1840
DRKG1850
DRKG1860
```

1:	SUBROUTINE FCT(YP,M,DY,PW)	FCT	10
2:	C	FCT	20
3:	C	FCT	30
4:	C THIS SUBROUTINE COMPUTES THE DERIVATIVES (RIGHT HAND SIDES)	FCT	40
5:	C OF THE SYSTEM TO GIVEN VALUES OF YP(CONCENTRATION)	FCT	50
6:	C	FCT	60
7:	C	FCT	70
8:	IMPLICIT REAL*8(A-H,O-Z)	FCT	80
9:	DIMENSION YP(M),DY(M),PW(M,M)	FCT	90
10:	DO 15 J=1,M	FCT	100
11:	DY(J)=0.000	FCT	110
12:	DO 10 I=1,M	FCT	120
13:	10 DY(J)=DY(J)+PW(J,I)*YP(I)	FCT	130
14:	15 CONTINUE	FCT	140
15:	RETURN	FCT	150
16:	END	FCT	160

```

1:      SUBROUTINE VELDIF(XZ,H,UGR,UST,AM,U,V,ISTB,ALPHA,N3,AKY,AKZ,DAKZ, VELD 10
2:      ISFL,IND,US,DKN,DUN,HSKN,HGEO,AMM) VELD 20
3:      C VELD 30
4:      C VELD 40
5:      C THIS SUBROUTINE CALCULATES THE VELOCITY AND TURBULENT VELD 50
6:      C DIFFUSIVITY VECTORS (TWO-DIMENSIONS) AS FUNCTIONS OF VELD 60
7:      C ELEVATION AND STABILITY CLASS VELD 70
8:      C VELD 80
9:      C VELD 90
10:     IMPLICIT REAL*8(A-H,O-Z) VELD 100
11:     DIMENSION XZ(12),AKY(12),AKZ(12),DAKZ(12),CCEFK(6),DKN(6), VELD 110
12:     ITDFKN(6),DUN(6),TDFUN(6),L(12),V(12),HGEO(6) VELD 120
13:     DATA CCEFK/570.D0,555.D0,540.D0,222.D0,0.D0,-70.500/ VELD 130
14:     IF(IND.NE.0) GO TO 5 VELD 140
15:     US=UST*(1.D0-DFXP(-SFL*H/AM)*DCOS(SEL*H/AM)) VELD 150
16:     RETURN VELD 160
17:     5 CONTINUE VELD 170
18:     TDFKN(ISTB)=DKN(ISTB)/H VELD 180
19:     U(1)=UGR VELD 190
20:     PV=DEXP(-DKN(ISTB)/AM)*DSIN(DKN(ISTB)/AM)/ VELD 200
21:     1(1.D0-DEXP(-DKN(ISTB)/AM)*DCOS(DKN(ISTB)/AM)) VELD 210
22:     U1=UST*(1.D0-DEXP(-DKN(ISTB)/AM)*DCOS(DKN(ISTB)/AM))/ VELD 220
23:     1(DKN(ISTB)/DUN(ISTB))*AMM VELD 230
24:     V(1)=-PV*L(1) VELD 240
25:     TDFUN(ISTB)=HGEO(ISTB)/H VELD 250
26:     DO 25 L=2,N3 VELD 260
27:     L(L)=UST*(1.D0-DEXP(-XZ(L)*H/AM)*DCOS(XZ(L)*H/AM)) VELD 270
28:     IF(XZ(L).LE.TDFKN(ISTB)) L(L)=U1*(XZ(L)*H/DUN(ISTB))*AMM VELD 280
29:     IF(XZ(L).LT.TDFUN(ISTB)) V(L)=-UST*DEXP(-XZ(L)*H/AM)* VELD 290
30:     1DSIN(XZ(L)*H/AM) VELD 300
31:     IF(XZ(L).GE.TDFUN(ISTB)) V(L)=0.D0 VELD 310
32:     IF(XZ(L).LT.TDFKN(ISTB)) V(L)=-PV*U(L) VELD 320
33:     25 CONTINUE VELD 330
34:     IF(ISTB.GE.5) GO TO 10 VELD 340
35:     IF(DKN(ISTB).GT.1.D-CR) GO TO 20 VELD 350

```

36:	DO 4 L=2,N3	VELD 360
37:	AKZ(L)=COEFK(ISTR)+90.D0	VELD 370
38:	DAKZ(L)=0.D0	VELD 380
39:	4 AKY(L)=ALPHA*AKZ(L)	VELD 390
40:	RETURN	VELD 400
41:	20 CONTINUE	VELD 410
42:	TDSKN=1.D0-100.D0/H	VELD 420
43:	IF(H.LE.HSKN) TDSKN=1.D0	VELD 430
44:	DO 2 L=2,N3	VELD 440
45:	IF(XZ(L)-TDFKN(ISTR)) 11,12,12	VELD 450
46:	11 AKZ(L)=COEFK(ISTB)*XZ(L)/TDFKN(ISTB)+90.D0	VELD 460
47:	DAKZ(L)=CCEFK(ISTR)/DKN(ISTR)	VELD 470
48:	GO TO 16	VELD 480
49:	12 IF(XZ(L)-TDSKN) 13,13,14	VELD 490
50:	13 AKZ(L)=COEFK(ISTR)+90.D0	VELD 500
51:	DAKZ(L)=0.D0	VELD 510
52:	GO TO 15	VELD 520
53:	14 AKZ(L)=COEFK(ISTR)*H*(1.D0-XZ(L))/100.D0+90.D0	VELD 530
54:	DAKZ(L)=-CCEFK(ISTR)/100.D0	VELD 540
55:	15 CONTINUE	VELD 550
56:	16 AKY(L)=ALPHA*(COEFK(ISTB)+90.D0)	VELD 560
57:	2 CONTINUE	VELD 570
58:	GO TO 50	VELD 580
59:	10 CONTINUE	VELD 590
60:	DO 3 L=2,N3	VELD 600
61:	AKZ(L)=CCEFK(ISTB)+90.D0	VELD 610
62:	DAKZ(L)=0.D0	VELD 620
63:	3 AKY(L)=ALPHA*AKZ(L)	VELD 630
64:	50 CONTINUE	VELD 640
65:	RETURN	VELD 650
66:	END	VELD 660

C  
C  
C  
C  
C  
C

INPUT DATA REQUIRED

10	10	4					
4000.00+00		500.00+00	4000.00+00	8.90000+00			0.0
687.220+00		322.490+00	30.00+00	60.0000+00			0.20
50.00+00	50.00+00	50.00+00	50.00+00	50.00+00	50.00+00		
10.00+00	10.00+00	10.00+00	10.00+00	10.00+00	10.00+00		
147.350+00	145.670+00	143.970+00	1101.310+00	1544.140+00	253.280+00		
.00+00		0.10-06	0.10-06	1.0000-07			
.28610-02		.28610-02	0.10-01	0.0120-01			
.28610-12		.28610-02	0.120-02				
0.00+00		0.10-06	0.250-02	0.250-02			
.25000-02		.25000-02	1500.00+00	0.140+00			

APPENDIX B

NOMENCLATURE

a	Constant in equation (3.14)
$A_{ij}$	Element of the discretizational matrix of first derivatives
$B_{ij}$	Element of the discretizational matrix of second derivatives
C	Mean concentration, $\text{mg}/\text{m}^3$
$C_a$	Mean concentration obtained by an analytical solution
$C_c$	Mean concentration calculated by the present work
$C_i$	Mean concentration at the i-th interior orthogonal collocation point - two-dimensional models
$C_o$	Equivalent mean concentration at the source
$C_{k\ell}$	Mean concentration at the interior orthogonal collocation point $(\eta_k, \zeta_\ell)$ - three-dimensional models
e	Absolute error defined by equation (3.1), %
$E_{ij}$	Elements of the collocation matrix
f	Coriolis parameter, $\text{sec}^{-1}$
H	Effective emission height, m
$k_1$	Reaction rate constant, $\text{min}^{-1}$
K	Turbulent diffusivity, $\text{m}^2/\text{sec}$
$K_1$	Turbulent diffusivity at an elevation $z_1$
m	Exponent in power-law form for the mean wind velocity profile
n	Exponent in power-law form for the turbulent diffusivity profile
N	Number of interior orthogonal collocation points.

$p$	Atmospheric pressure
$Q$	Source strength, kg/sec unless otherwise specified
$Q_x$	Mass rate through $y$ - $z$ plane at $x$ =constant, gm/sec unless otherwise specified
$r$	Parameter in equation (2.9)
$r$	Mathematical parameter that represents the ratio of boundary to centerline concentration
$R$	Rate of generation of species
$s$	Parameter in equation (2.9)
$t$	Time, sec
$u$	Mean wind velocity in the $x$ -direction, m/sec unless otherwise specified
$u_1$	Mean wind velocity at an elevation $z_1$
$u_{10}$	Mean wind velocity at 10 meters
$\underline{U}$	Eigenvectors of matrix $E$
$\underline{U}^{-1}$	Eigenrows of matrix $E$
$v$	Mean wind velocity in the $y$ -direction, m/sec unless otherwise specified
$w$	Mean wind velocity in the $z$ -direction, m/sec unless otherwise specified
$W$	Quadrature weights
$x$	Cartesian coordinate in mean wind direction, m unless otherwise specified
$x_{\max}$	Maximum distance in the $x$ -direction, m
$y$	Cartesian coordinate in lateral direction, m
$y_{\max}$	Maximum distance in the $y$ -direction, m

$z$	Cartesian coordinate in vertical direction, m
$z_{\max}$	Maximum height above terrain (in some cases refers to the elevation of the inversion layer), m
$z_1$	Reference height, m

### Greek Symbols

$\alpha$	Angle between geostrophic velocity and surface boundary layer velocity, °
$\beta$	Mathematical parameter that represents a source dimension
$\Gamma$	Gamma function
$\delta$	Mathematical parameter used for spatial variable transformations
$\delta_{ij}$	Kronecker delta function
$\Delta$	Knee height for the vertical turbulent diffusivity profile, m
$\epsilon$	Upper error bound in "DRKGS"
$\zeta$	Dimensionless spatial variable in the z-direction
$\eta$	Dimensionless spatial variable in the y-direction
$\underline{\underline{\Lambda}}$	Eigenvalues of matrix E
$\xi$	Dimensionless spatial variable in the x-direction
$\rho$	Density
$\sigma$	Standard deviation
$\tau$	Eddy stresses
$\phi$	Geostrophical latitude, °
$\psi$	Variable used in Figure 4.6. Represents ground-level concentration

Superscripts

- i Initial value profile for the concentration
- \* Refers to dimensionless spatial variables

Subscripts

- G Refers to geostrophic flow
- i Index in collocation equations
- k Represents the y-direction in collocation equations
- ℓ Represents the z-direction in collocation equations
- x Refers to x coordinate direction
- y Refers to y coordinate direction
- z Refers to z coordinate direction
- Denotes a vector quantity
- = Refers to a matrix